The FOLD-and-THRUST BELTS of the SOUTHERN CENTRAL ANDES

A

FIELD-EXCURSION

TO THE **MENDOZA & SAN JUAN** PROVINCES

IN **NW ARGENTINA**

2nd - 8th MARCH 2017

BY

LAURA GIAMBIAGI, STELLA MOREIRAS, MANFRED STRECKER

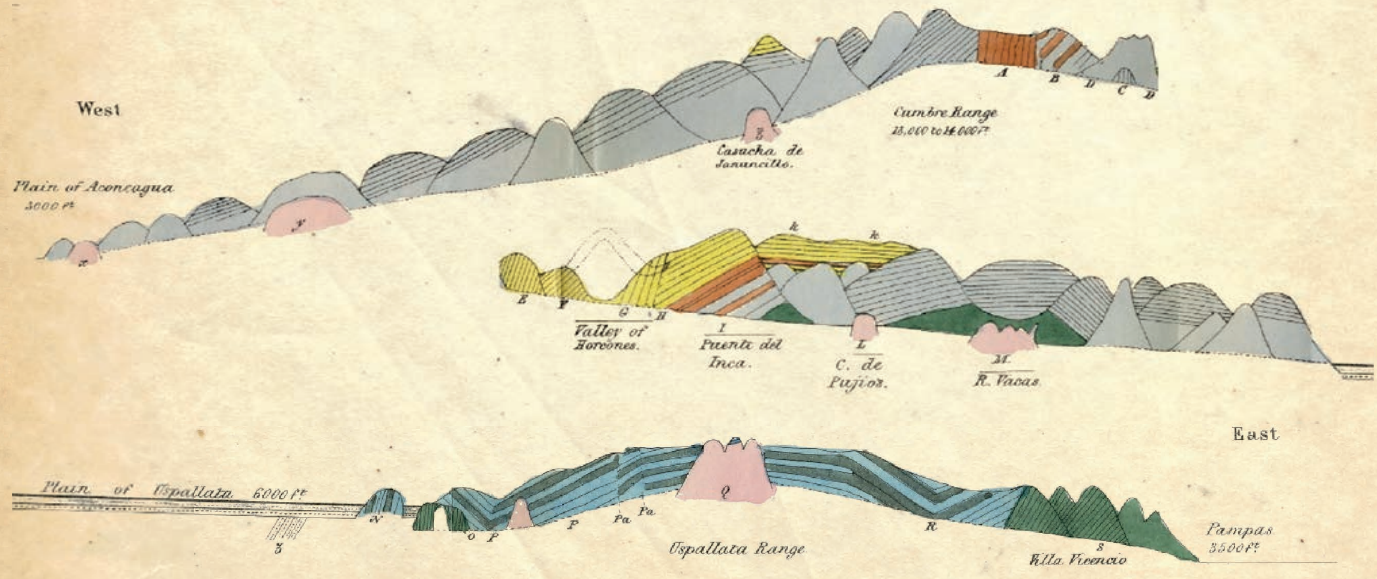

STRATEGY - INTERNATIONAL RESEARCH TRAINING GROUP - IGK 2018

CONICET - CONSEJO NACIONAL DE INVESTIGACIONES CIENTÍFICAS Y TÉCNICAS

Fig. 2 - Deformed rift-deposits of the Triassic Barreal Group at the Cerro el Alcázar site near the town of Barreal at the eastern margin of the Calingasta Basin. (Photograph by H. Wichura)

Itinerary

- Day 1 - Thu. 2-03-2017: Mendoza - Uspallata (Precordillera/Frontal Cordillera)
- Day 2 - Fri. 3-03-2017: Uspallata - Las Cuevas - Uspallata (Frontal & Main Cordillera)
- Day 3 - Sat. 4-03-2017: Uspallata - Calingasta - Rodeo (Uspallata/Calingasta/Iglesia Basin)
- Day 4 - Sun. 5-03-2017: Rodeo - Jáchal - Rodeo (Iglesia Basin/Precordillera)
- Day 5 - Mon. 6-03-2017: Rodeo - San Juan and Part I "Show & Tell Event"
- Day 6 - Tue. 7-03-2017: Transfer to Mendoza and Part II "Show & Tell Event"

This field-excursion guide has in part been adapted from the following sources:

Ramos, V., Giambiagi, L., Godoy, E., Tunik, M and Bechis, F. (2010) Sedimentation and tectonics across the Andes. In: del Papa, C. & Astini, R. (Eds.), Field Excursion Guidebook, 18th International Sedimentological Congress, Mendoza, Argentina, FE-B1, pp. 1- 43.

Moreiras, S.M. (2010) Geomorphological evolution of the Mendoza River Valley In: del Papa, C & Astini, R (Eds.), Field Excursion Guidebook, 18th International Sedimentological Congress, Mendoza, Argentina, FE-B2, pp. 1-21

Fig. 1 - Front cover illustration: Sketch-section of the Cumbre or Uspallata pass (Darwin, 1846).

Field-school outline

This field trip provides the opportunity to examine the sedimentary and tectonic evolution of the Southern Central Andes, in one of its most classic sections. We will examine an active thrust front with progressive deformation and growth strata, distal and proximal synorogenic deposits, and provenance and source analyses in order to reconstruct the uplift history of the Andes. A second objective will be the examination of the Triassic rift sedimentation and tectonics, with special emphasis in the tectonic inversion of the region. The third and final objective will be to examine the platform retroarc deposits of Mesozoic age, facies changes across the different thrust sheets and the interfingering with the volcanic arc products.

The route as chosen will show the different structural styles of the Precordillera thrust front, the Cordilleras Frontal and Principal as indicated on the field trip map (Fig. 3).

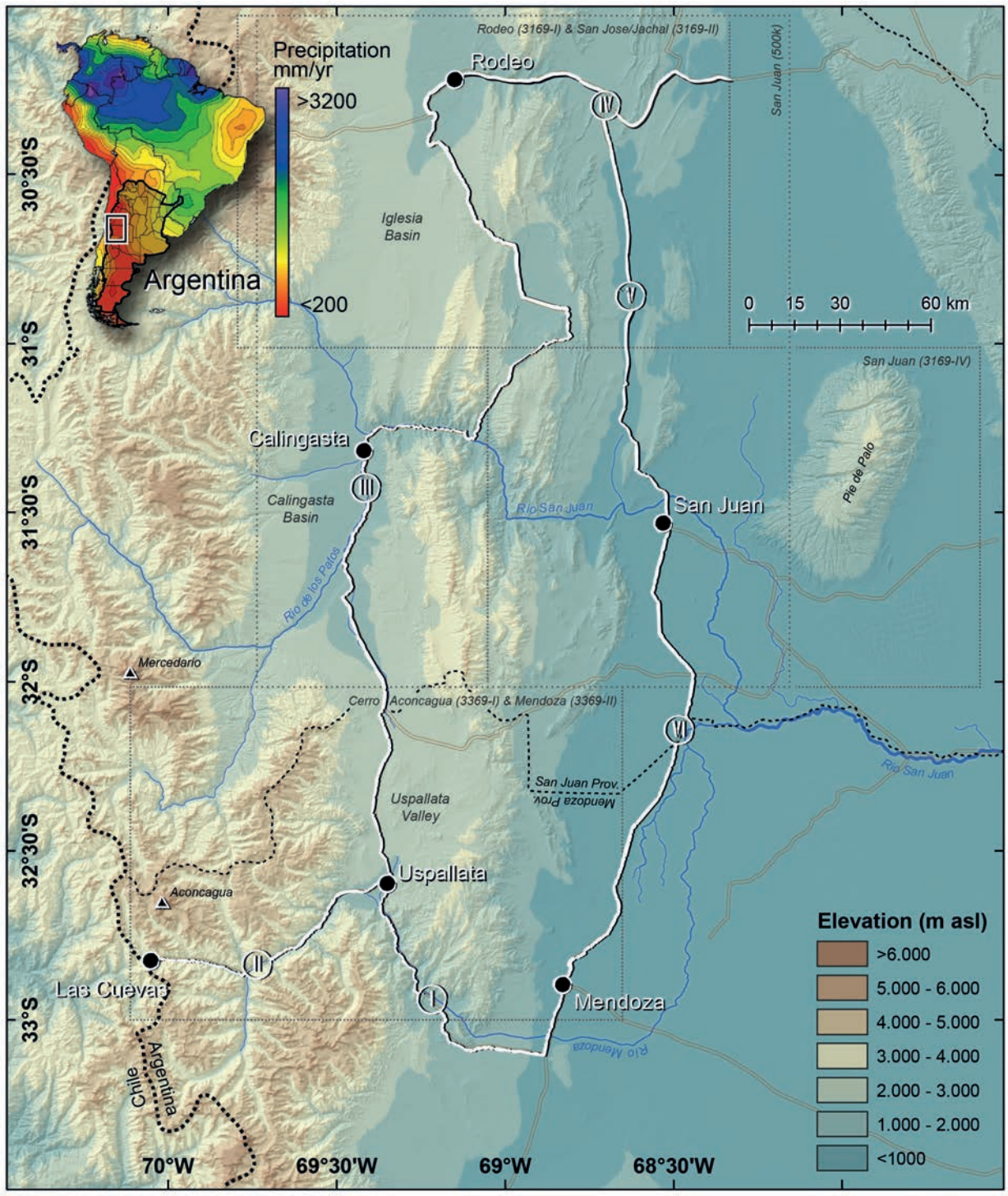

Fig. 3 - Digital elevation map of the southernmost Central Andes in NW Argentina. Numbers on field-trip route correspond with date and itinerary. Dashed rectangles outline the limits of geological maps attached in this field guide. Inset figure show the annual rainfall distribution in South America (Liebmann & Allured, 2005).

Fig. 4 - Tectonic and geodynamic scenario of South America. Note the correlation of oceanic ridges, flat slab segments and the formation of inland topographies within the distal foreland. From Davila & Lithgow-Bertelloni (2013).

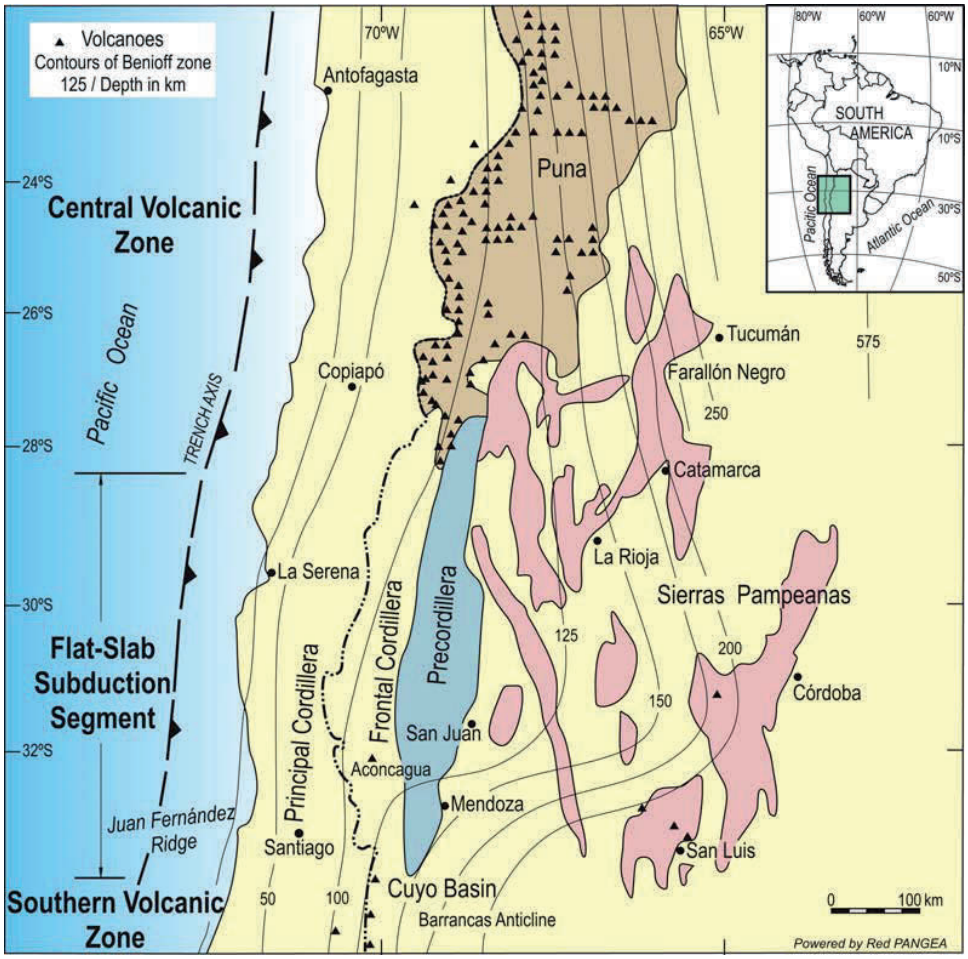

Fig. 5 - Pampean flat-slab segment with indication of isobaths to the Nazca oceanic plate based on Cahill & Isacks (1992), main basement uplifts of Sierras Pampeanas (Jordan et al. 1989), and location of the Precordillera fold and thrust belt (Ramos et al. 2002). For more information see Ramos & Folguera (2009).

Brief review of the history of geologic exploration and research

The geologic understanding of the Central Andes started with the pioneering explorations of Charles Darwin in 1835, who was the first to describe the marine Mesozoic deposits deformed by faults (see front cover image), both along the present road that crosses the High Andes as well as across the pass further south. We are going to have the opportunity to examine the profile described by Darwin, and the mountain shelters where he stayed crossing the main range.

Several German naturalists were sent by the Academia Nacional de Ciencias and the Museo de La Plata, to geologically explore the High Andes of San Juan and Mendoza. According to the early observations of German Burmeister in 1857-1858, the structure outlined by Stelzner (1873), and the descriptions of Wherli & Burckhardt (1898), the Andes was a relatively simple mountain belt, which lacked the thrusts and overthrusts known in other mountain belts at that time. Later in 1906 and 1907, Walter Schiller, a young geologist and mountain climber working in the Argentine Geological Survey conducted the first reconnaissance of the region. As a result of his work many structural complexities and important thrusting were recognized (Schiller, 1907, 1912).

At the same time, the Precordillera was also explored and its stratigraphy, structural geology and mineral resources was established making this one of the best known regions at that time (e.g., Stelzner, 1885; Bodenbender, 1902; Stappenbeck, 1910; Keidel, 1921; Bracaccini, 1946). Over the last decades, many studies have provided a large volume of information on different aspects of the sedimentology, structure and geologic evolution of this part of the Central Andes (reviewed in Caminos, 2000).

Major geological provinces

This segment of the Central Andes (see Fig. 4) has been divided into a series of morphostructural units or geological provinces based on structural styles, geologic evolution, and morphological expression (Fig. 5-7).

Sierras Pampeanas

The Sierras Pampeanas are characterized by a series of crystalline basement blocks of Precambrian- Early Paleozoic age, which were uplifted and tilted during Neogene-Quaternary Andean compression (González Bonorino, 1950) in association with an episode of shallow subduction (Jordan et al., 1983 a,b; Kay et al., 1987; Ramos et al., 2002). The resulting structures closely resemble those of the Laramide region in North America (Jordan & Allmendinger, 1986).

The basement is composed of metamorphic and igneous rocks, which correspond to two distinct orogenic cycles. The oldest Brasiliano or Pampean cycle is preserved along the eastern Sierras Pampeanas, and both its metamorphic facies as well as the related igneous rocks define a north-south trending belt of Late Proterozoic - Early Cambrian age (600-520 Ma). The younger cycle is characterized by outcrops along the western Sierras Pampeanas, which define the Famatinian orogen, an Early Paleozoic magmatic belt that reached its magmatic climax between 490 and 460 Ma (reviewed in Pankhurst & Rapela, 1998; Ramos, 2004).

This metamorphic basement was partially covered by continental deposits from the Late Paleozoic Paganzo Group and Tertiary synorogenic deposits in alluvial and fluvial facies related to the uplift of the Sierras Pampeanas. Triassic and Cretaceous continental sequences were additionally deposited along rift basins developed in the E and W margins of the Sierras Pampeanas.

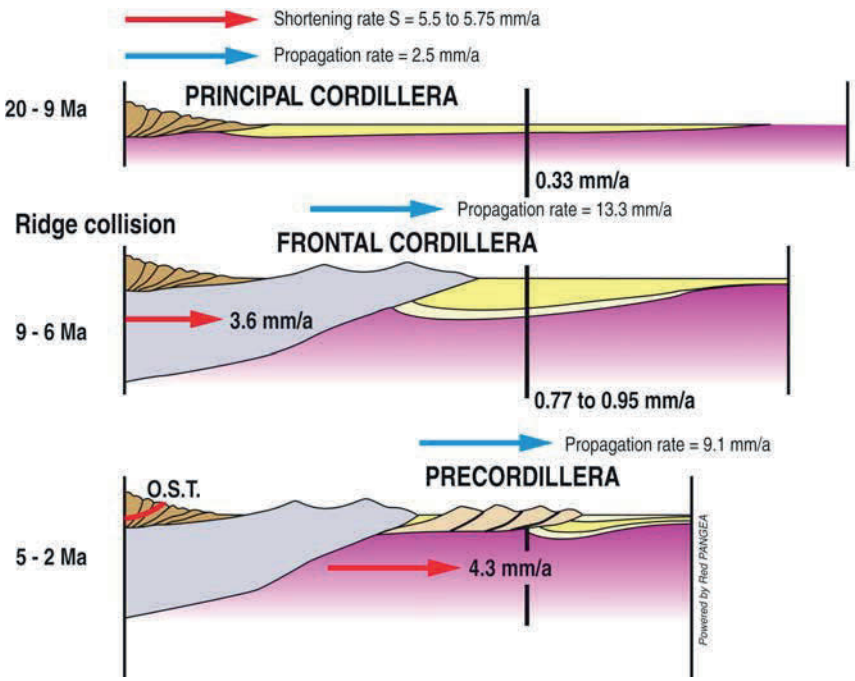

Fig. 6 - The Aconcagua fold and thrust belt in the Central Andes at 32°S latitude with variations on shortening and propagation rates through time (after Ramos et al. 1996b and Hilley et al. 2004) and the subsidence rates in the foreland basin after Irigoyen et al. (2002). From Ramos & Folguera (2009).

Precordillera

The Precordillera is an Andean fold-and-thrust belt with a typical thin-skinned structure developed in an early Paleozoic carbonate platform. The western edge of the Precordillera coincides with a longitudinal depression known as the Iglesia-Calingasta-Uspallata valley. This tectonic trough is similar to the Canadian Rocky Mountain trench as the present morphology is controlled by the old Paleozoic continental margin (Price, 1981; Baldis et al., 1984).

The Early Paleozoic history is represented by a carbonate platform of Early Cambrian to Middle Ordovician age. A detailed biostratigraphic zonation has been defined in these highly fossiliferous deposits (see review of Benedetto et al., 1999). Clastic marine Middle to Upper Ordovician rocks cover the platform deposits in the eastern and central sectors, while slope and oceanic facies occur to the west. This Early Paleozoic continental margin is unconformably covered by foreland basin deposits of Silurian to Devonian age. A major deformation, known as the Chanic orogeny, affected these Early Paleozoic rocks in the Mid-Late Devonian.

The previous slope facies were covered by continental Early Carboniferous alluvial deposits in the western Precordillera. Late Paleozoic rocks correspond mainly to littoral marine facies in the western Precordillera and to continental fluvial to alluvial deposits in the central and eastern Precordillera. Paganzo Group rocks overlap the eastern Precordillera.

In well known localities such as Barreal and Rinconada, among others, excellent outcrops of Gondwana glacial deposits are preserved in both marine and continental facies (Keidel, 1921; Du Toit, 1927). Synorogenic Tertiary deposits permit the reconstruction of the Precordillera thrust sequence, which began about 18 Ma ago in the northwest and continues until the present in the eastern side.

Cordillera Frontal

The Cordillera Frontal is composed of units that formed during the Gondwanide orogeny in the Late Paleozoic to Early Mesozoic. These units result from Andean type subduction, followed by generalized extension. Most of the rocks of this province are Late Paleozoic- Triassic andesitic to silicic magmatic rocks of the Choiyoi Group (Caminos, 1979). During the Andean deformation the Cordillera Frontal behaved as a rigid block, as shown by the presence of thick-skinned thrusts (Ramos et al., 1996 a,b). Volcanic activity started in the Middle Carboniferous with subduction related andesites, dacites and rhyolites. A subsequent period of generalized extension from Middle Permian up Early Triassic times resulted in the thick pile of Choiyoi rhyolites, and associated granites (Kay et al., 1989; Llambías & Sato, 1990). These volcanic rocks, which reach thickness of up to 2-4 km along the Río Mendoza valley, unconformably overlie the older rocks. Deformation of the Carboniferous- Early Permian rocks occurred in the middle Permian San Rafael orogenic phase (Ramos, 1988a).

The boundary between the Cordillera Frontal and the Precordillera was the locus of Triassic rifting associated with ≤2 km synrift deposits, and scattered alkaline basalts (Ramos & Kay, 1991).

Cordillera Principal

The Cordillera Principal, or Main Andes, was the locus of the Andean orogeny during latest Mesozoic and Cenozoic times. Jurassic and Cretaceous marine deposits were deformed in different styles depending on the extent of basement involvement in the deformation. In this sector thin-skinned structures such as the Aconcagua fold-and-thrust belt developed (Yrigoyen, 1976; Ramos et al., 1996a,b). A thick sequence of marine Mesozoic deposits unconformably overlies the Carboniferous flysch and the Choiyoi volcanics of the Cordillera Frontal. Several sedimentary cycles are recognized from the Early Jurassic to the Early Cretaceous (Groeber, 1946). These cycles begin with black shales, sandstones, and limestones and terminate with thick gypsum levels and continental red beds. Abundant ammonites permitted a biostratigraphic zonation of these deposits (Aguirre Urreta & Rawson, 1997).

Along the continental divide these sedimentary sequences interfinger with volcanic and pyroclastic rocks of Late Jurassic-Early Cretaceous age. The volcanic pile which can be up to 6 km thick in the Chilean side has a burial metamorphism typical of that developed in a high thermal gradient during active subsidence (Levi et al., 1982). These volcanic sequences also occur along a western inner arc developed in the Cordillera de la Costa. An intra-arc basin between the two arcs is filled with shallow marine and continental Mesozoic deposits north of this section (Charrier, 1973; Ramos et al., 1996a,b), which shift to an Eocene to Oligocene age southward.

Most of the Early and Middle Mesozoic was dominated by an

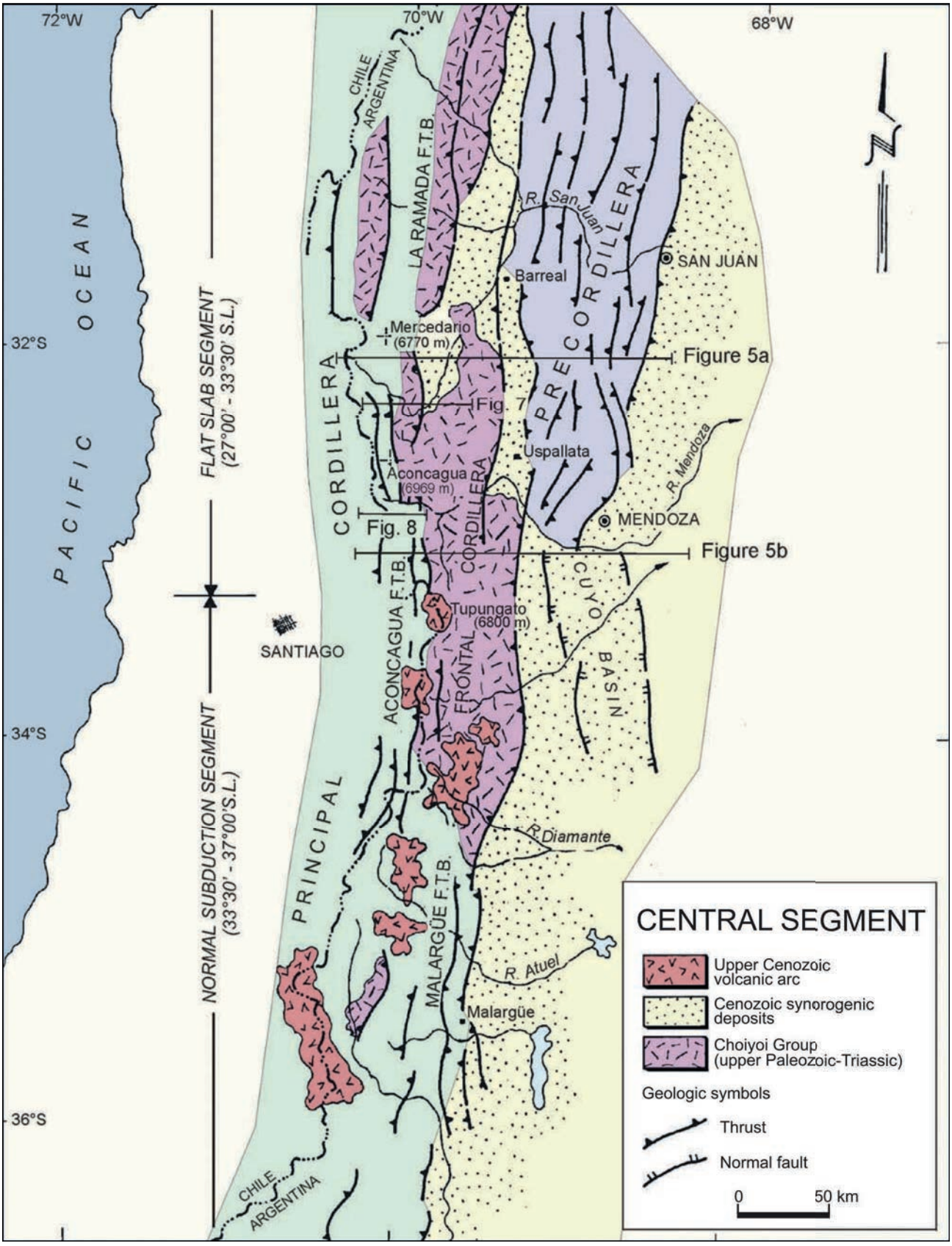

Fig. 7 - Regional structural units of the southern central Andes, with locations of the different crustal and structural cross sections of the central segment. In the Principal Cordillera the La Ramada, Aconcagua, and Malargüe belts are indicated (Based on Ramos et al., 1996).

extensional regime closely linked to a negative trench roll-back velocity associated to the early stages of the South Atlantic opening (Ramos, 1999). Later, onset of the main drift phase in the Atlantic induced a positive overriding velocity to the South American Plate during the middle Cretaceous and the tectonic regime changed to the present Andean compressional stage. A series of volcanic arcs shifted from the Cordillera de la Costa in the Jurassic to the Cordillera Principal during the Neogene (Ramos, 1988a). The volcanic and volcaniclastic rocks interbedded with alluvial-fan facies record shallowing of the subduction zone during the Neogene until the magmatic activity ceased in Sierra del Morro, 750 km away from the trench (Kay & Mpodozis, 2002). Glacial deposits from four different glaciations are widespread in the main valleys, representing alpine type glaciations during Pliocene and Quaternary times.

Cordillera de La Costa

Along the present continental margin, a series of Late Paleozoic metamorphic rock are preserved which represent pieces of an accretionary prism that developed in the Late Paleozoic (Hervé et al., 2000). Emplaced in this metamorphic basement, are a series of magmatic belts of Permian, Jurassic and Cretaceous age. Most of this region is suspected to have significant latitudinal displacements (Forsythe et al., 1986; Mpodozis & Ramos, 1990). On the eastern flank of the Cordillera de la Costa, the Mesozoic marine sequences developed west of the Mesozoic volcanic rocks interfinger with volcanic rocks and are associated with Manto-type copper deposits.

Modern plate tectonic setting

This segment of the Central Andes between 28-33°S has a distinctive plate tectonic setting. The present convergence rate between the subducted Nazca plate and the South American plate averages about 9 cm per year (Fig. 4). Earthquake hypocenter locations delineate a Benioff zone that is gently dipping to the east, defining a shallow subduction zone (Fig. 5) (Cahill & Isacks, 1992; Pardo et al., 2002).

This flat subduction segment is characterized by an almost flat section at about 100 kilometers depth, and it is flanked to the north and south by steeper segments that dip about 30°E. A corresponding tectonic segmentation exists in the plate above the Benioff zone. The most obvious and consistent correlation is between Quaternary volcanism and the dip of the subducted slab. Quaternary volcanism is absent in the subhorizontal segment.

The development of the Sierras Pampeanas geological province is controlled by the flat subduction. Present tectonic shortening is principally concentrated along a narrow belt between this province and the Precordillera. Intraplate earthquake nests have been found in the basement of the eastern Precordillera and the western Sierras Pampeanas, in close coincidence with the superficial neotectonic activity. Focal mechanisms indicate east-west contraction with minor to no strike-slip components (Chinn & Isacks, 1983; Pardo et al. 2002).

The origin of this flat subduction segment has been attributed to the approach and subduction of aseismic ridges at the Pacific continental margin (Pilger, 1981; Yañez et al. 2001); to changes in the age of the subducted oceanic crust (Wortel, 1984), and to the differential shortening of a previously weakened hot continental crust (Isacks, 1988; Cahill & Isacks, 1992). See recent review in Ramos et al. (2002).

Terrane history

The existence of oceanic rocks separating the Cordillera Frontal from Precordillera has attracted the attention of geologists since the early work of Borrello (1969). These oceanic rocks have been interpreted as indicating a suture between different continental terranes (Ramos et al., 1984, 1986), consequently, several other sutures have been identified (Ramos, 1984, 1988a,b; Mpodozis & Ramos, 1990, Astini et al., 1995, 1996).

The first report of Borrello (1963) of North American olenellid trilobites from Precordillera of west central Argentina, in Villicum near San Juan, gave rise to assume a connections between Laurentia and Gondwana. The first attempt to explain the presence of these *olenellids* in South America was made by Ross (1975), who explained it as larval transfer by oceanic currents. The location of this fauna, known outside of Laurentia, was intriguing mainly because it was only known in the ancestral North American craton that also included *olenellid* fauna of the northwestern British Isles (Peach et al., 1907).

Several years later, the striking coincidence in the subsidence curves of the Appalachians carbonates and the Precordillera carbonate platform, induced Bond et al. (1984) to suggest that both regions were conjugate margins and shared a common rift-drift transition. The shared carbonate platformal history and faunal provinciality between the Precordillera and the Laurentian margin of the Appalachians led Ramos et al. (1986), to propose that Precordillera was a far travelled terrane derived from northern Appalachians. This proposal was refined by Mpodozis & Ramos (1990), and Astini et al. (1995, 1996), within the tectonic framework of the early Paleozoic basement of the Andes.

Two different models have been proposed to explain the accretion of the Precordillera to the protomargin of Gondwana. According to the first one, an independent microcontinent or microplate, detached from Laurentia during early Cambrian time, collided against Gondwana during middle to late Ordovician time (Ramos et al., 1986; Benedetto & Astini, 1993; Astini et al., 1995, 1996). The second model favors a continent to continent collision between Laurentia and Gondwana during early to middle Ordovician time from 487 to 467 Ma. Subsequently, during the late Ordovician the detachment of the two continents left behind the Precordillera terrane on the Gondwanan side, with the opening of an ocean on the western side of Precordillera (Dalla Salda et al. 1992 a,b; Dalziel, 1992, 1993, 1997; Dalziel et al., 1994, 1996).

Both proposals required an active early Paleozoic margin in the Sierras Pampeanas, and explained the magmatism and the Ordovician deformation known as the Ocloyic event as result of a collisional orogeny (Ramos, 1986; Dalla Salda et al., 1992 a,b).

The microcontinent hypothesis required a second early Paleozoic accretion to close the ocean that bounded the western Precordillera. The accretion of the Chilenia microcontinent produced a second foreland basin and a shifting of the magmatic activity to the Pacific margin (Ramos et al., 1984). This collision occurred either in late Devonian time (Ramos et al., 1986) or as proposed by Astini (1996) during the early Devonian. Sedimentologic studies of these foreland basins and geochronologic data of peak metamorphism and associated deformation suggest an early Devonian age for the beginning of accretion.

The challenging pre-Pangea SWEAT reconstruction of the late Proterozoic continents proposed by Moores (1991), complemented by Dalziels' 1991 Laurentian end run, provided a context for the transfer of the Precordillera. See recent reviews by Thomas & Astini (1999, 2003).

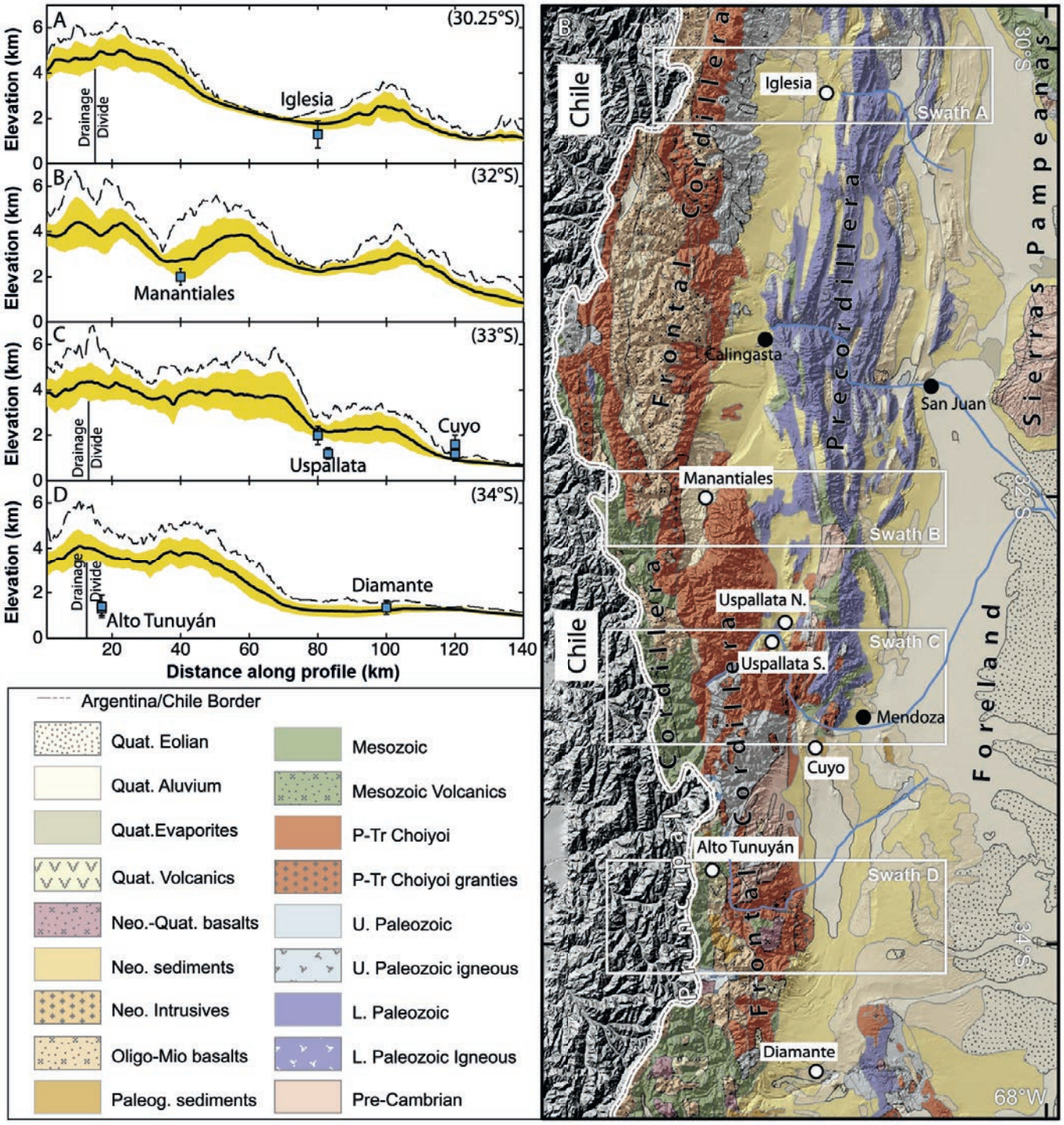

Fig. 8 - Simplified geology of the southern Central Andes from the 1:3,000,000 geologic map of Argentina showing the major geologic provinces and elevation swath profile positions (white boxes) shown in the upper left panel. (Upper left panel) Calculated middle to late Miocene paleoelevations and their 2-sigma uncertainties plotted with swath profiles of the modern topography and the 1-sigma deviation from the mean topography calculated in each swath. Modified after Hoke et al. (2014).

Andean tectonics

The Cenozoic sedimentary history records the eastward migration of the orogenic front. Thick sequences of continental deposits (Santa María Conglomerates of Schiller, 1912) unconformably overlie the Mesozoic rocks in the Cordillera Principal. The angular unconformity is clearly seen east of Cerro Aconcagua and west of Cerro Penitentes. Those conglomeratic deposits are interpreted as alluvial fan sediments interfingered with the volcanics of the Farellones Formation (25 to 10 Ma at this latitude, Munizaga & Vicente, 1982). A minimun age of 8.6 Ma was obtained in the continental deposits based on K/Ar dating of pyroclastic rocks interbedded in the uppermost section of the Santa María Conglomerates (Ramos et al., 1996 b). The Neogene deposits further east of the High Cordillera are represented by distal fluvial facies partially synchronous with the Santa María Conglomerate and the volcanism of the Farellones Formation. The Neogene extra Andean sequences at these latitudes (30-33°S) contain several tuff layers, which attest to the cordilleran volcanic activity at that time. An unconformity separates the La Pilona beds exposed in the Uspallata valley and the Cacheuta area from older Neogene beds. This unconformity was produced during the Late Miocene event that folded and thrusted the Santa María Conglomerates and Farellones volcanics about 10-8 Ma ago (Ramos et al., 1996 a,b) and was also responsible for deformation in the Cordillera

Frontal. The Late Miocene and Pliocene deposits of the Uspallata and Cacheuta regions were folded and thrusted at that time with the subsequent deposition of the alluvial fan deposits of the Mogotes Formation during the Plio-Pleistocene.

Therefore, the Neogene sedimentary facies show a migration of the coarse alluvial fan facies from (a) the inner area of Cerro Penitentes in the High Andes (20-10 Ma), to (b) the Uspallata valley and Cacheuta (10-5 Ma), and to (c) the outer foothills of Mendoza city (2 Ma and the Holocene active front). Even the Plio-Pleistocene fanglomerates of the Mogotes Formation cropping out west of Mendoza city (Cerro La Gloria) and other younger alluvial fans have been deformed by neotectonic activity in the Mendoza region.

The seismic sections of the plains located eastward of the Precordillera clearly show that the present orogenic front is composed of a set of imbricated thrusts. This structural style was corroborated by drilling, and it has somewhat similar characteristics to the previous fronts. The thrust front in the eastern side of the Precordillera is still active. Intense compressive deformation as seen in Sierra de Las Peñas (see Cortés, 1990) and as inferred from earthquake focal mechanisms and escarpments on the alluvial fans, is continuing today. The Andean structure of the Central Andes is the result of a combination of several tectonic mechanisms.

There is a striking coincidence between the increase of plate motion rates, the cessation of magmatism, and the compressive deformation at the orogenic fronts. Most of the Oligocene was quiescent with extension (Godoy et al., 1999), coincident with the volcanic rifting west of the Cordillera Principal. This extension ended at about 20 Ma north of the section of this field excursion, when volcanic activity of the Farellones Formation started (Munizaga & Vicente, 1982). These interrelated tectonic features demonstrate that change in the geometry of the Benioff zone followed:

a) Eastward migration of the subduction related magmatic foci from a position about 180 km from the trench at app. 25 Ma, to 700 km away from the trench at 2 Ma up to the Central Sierras Pampeanas in the latest Pliocene (Ramos et al., 1991, Mpodozis & Kay, 2002).
b) Geochemical characteristics support thickening of the continental crust, between 18 Ma and the present, related to tectonic stacking of the Andean Cordillera (Kay et al., 1991).
c) Eastward shifting of the orogenic deformation during the last 20 Ma: 275 km from the trench at 20-10 Ma, 325 km at 10-5 Ma, and 365 km at 2 Ma. This implies an average propagation rate of 2.5 mm/a of the orogenic front since the last 20 Ma, although the shifting was probably episodic.

The causes of the change in the Benioff zone geometry and segmentation are probably complex and multifacetic:

a) The break up of the Farellones plate into the Cocos and Nazca plates, which occurred at 25 Ma, starts a period of higher convergence rates (Handschumacher, 1976). This age coincides with the initiation of Farellones magmatism and is a milestone in the geodynamic evolution of the area.
b) The increase in plate convergence from 25-26 Ma up to 10 Ma (defined by Pilger, 1984; Pardo Casas and Molnar, 1987) when the present deceleration began.
c) Several authors have explained the present segmentation of the subducted Nazca plate as controlled by the collision of aseismic ridges (Pilger, 1981). In his interpretation the buoyancy effects produced by subduction of those ridges, combined with the younger age of the subducted slab, would contribute to lower the subduction angle. The effects of the Juan Fernandez hot spot trace subduction began about 15 Ma ago according to Pilger (1984). At the present latitudes evidence of shallowing of the subduction zone shows a similar trend of southward migration, which can be correlated with the southward shifting of the Juan Fernandez ridge collision along the trench (von Huene et al., 1997; Yañez et al., 2001).

Although south of the region of flat subduction the slab is younger and shows a higher thermal gradient, its present angle of subduction is about 30° (Isacks et al., 1982). Isacks' model (1988) indicates that the present dip of the different slab segments is controlled by the upper plate width of previously weakened zone. This zone is related to the size of the asthenosphere wedge between the oceanic and the continental plates. A greater amount of shortening occurred in the central segment because the weakened area was the widest, as indicated by the extension of the magmatic activity in the Puna Altiplano. In the analysed segment (30-31°S) a relatively narrow weakened zone along the overriding of the Nazca plate by the South American plate is associated with relatively minor shortening.

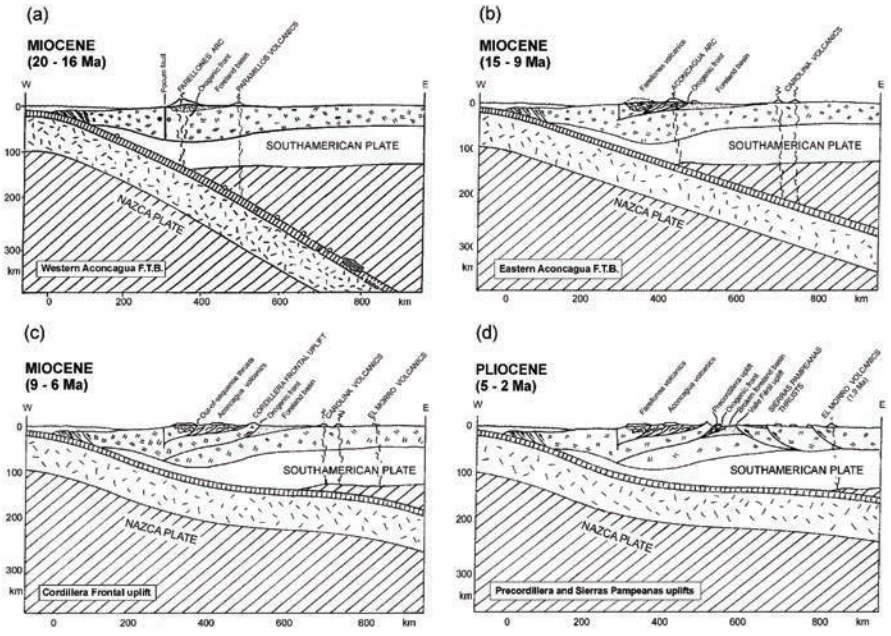

Fig. 9 - Late Cenozoic stages of Andean evolution associated with the shallowing of Nazca plate subduction. Geometries of the Wadati-Benioff zone are constrained by the location of the volcanic front. (a) Normal subduction prior to Juan Fernandez Ridge collision; (b) initial slab flattening related to the beginning of ridge collision at 11 Ma; (c) maximum deformation, thrust front propagation, and arc migration during shallowing of the subduction zone; and d) last arc magmatic activity prior to present-day cessation of magmatism. From Ramos et al. (2002).

Present-day climatic setting

The Andes constitute a major orographic barrier to atmospheric circulation, which (including precipitation amounts) is dominated by the westerlies in austral winter and by the subtropical high-pressure belt in austral summer (Bluestein, 1993). The central part of Chile is semiarid (~400 mm/a; Falvey & Garreaud, 2007), whereas in central-western Argentina, climate conditions progress from arid (<200 mm/a) in the northwest to semiarid in the southeast (200–300 mm/a) (Hoffmann, 1992).

During austral winter, the subtropical Pacific anticyclone weakens and is displaced northward, enhancing westerly flow across the Andes, producing a precipitation maximum over the western slopes (Saavedra & Foppiano, 1992). Little of this Pacific moisture reaches the E Andean flanks. In austral summer, interaction of semi-permanent low pressure in Argentina, and the subtropical South Atlantic anti-cyclone, generates a northeasterly flow over central regions of Argentina and a net moisture transport from the Atlantic and southern Brazil (Barros et al., 1996). River discharge on both flanks of the Andes is strongly correlated with the amount of snowpack and exhibits remarkably similar interannual variability, highlighting the existence of a clear regional hydrologic signal between 31-37°S (Fig. 10; Masiokas et al., 2006).

The transition between easterly and westerly winds has large annual and interannual variation with an average position of ~32°S. The average position appears to have been stable since the Last Glacial Maximum (Haselton et al., 2002). Climatic studies in our area emphasize the strong effect of the Andes in altering climate across adjacent lowlands on both sides of the range (Ereño & Hoffmann, 1978; Viale & Nuñez, 2011). South of 30°S, Pacific-sourced moisture is mainly discharged on the western flank of the Andes during austral winter. Spillover moisture from the west crosses the range and accounts for nearly all precipitation at elevations >2,400 m and is nearly absent at the foot of the mountains (Fig. 11B). Such an effect has been documented previously in river and rainfall in the Patagonian Andes (e.g., Smith & Evans, 2007; Stern & Blisniuk, 2002). Likewise, Atlantic-sourced moisture, largely from the low-level Andean jet (Fig. 10), condenses and precipitates on the eastern flank and foothills of the southern central Andes as summer convective storms. Only under certain atmospheric conditions, such as low-level high-pressure moving along eastward over central Argentina or a midlevel trough just west of the Andes, does Atlantic-derived moisture penetrate into the core and western flanks of the range (Fig 11C).

As a consequence of the southward migration of storm tracks, summer precipitation on the lowlands of Chile and the western flank of the Andes between 32.5 and 35.5 is minor (<50 mm). In contrast, winter precipitation reaches 300–400 mm in the lowlands of Chile, increases to 700–800 mm in valleys over the windward slope of the range, and sharply decreases east of the crest. Precipitation amount decreases from 200–300 mm in river valleys immediately east of the crest to less than 50 mm in Uspallata Valley and adjacent low lands of Argentina. On the eastern flank of the Frontal Cordillera, the Precordillera, and in the adjacent lowlands of Argentina, the average summer precipitation regime of 150–200 mm is typically produced by orogenic-synoptic convective storms, which are linked to northerly and easterly low-level winds that carry moisture from the Atlantic and Amazon Basin.

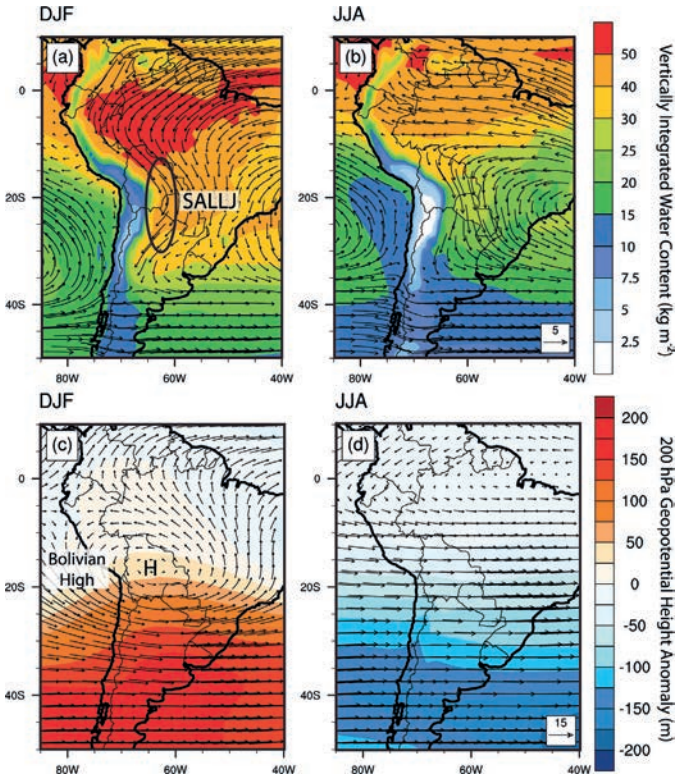

Fig. 10 - Seasonal climatology for South America from ERA-Interim reanalysis data (Dee et al., 2011). Climatological (1979–2013) mean 850 hPa winds (vectors, m/s) overlying vertically integrated column water (kg/m2) for (a) austral summer (DJF) and (b) winter (JJA). Climatological (1979–2013) mean upper level (200 hPa) winds overlying anomalous 200 hPa geopotential height relative to the zonal average for (c) DJF and (d) JJA. Major features of DJF large-scale circulation drive increased moisture convergence to the central Andes like the South American Low-Level Jet and the Bolivian High. From Fiorella et al. (2015).

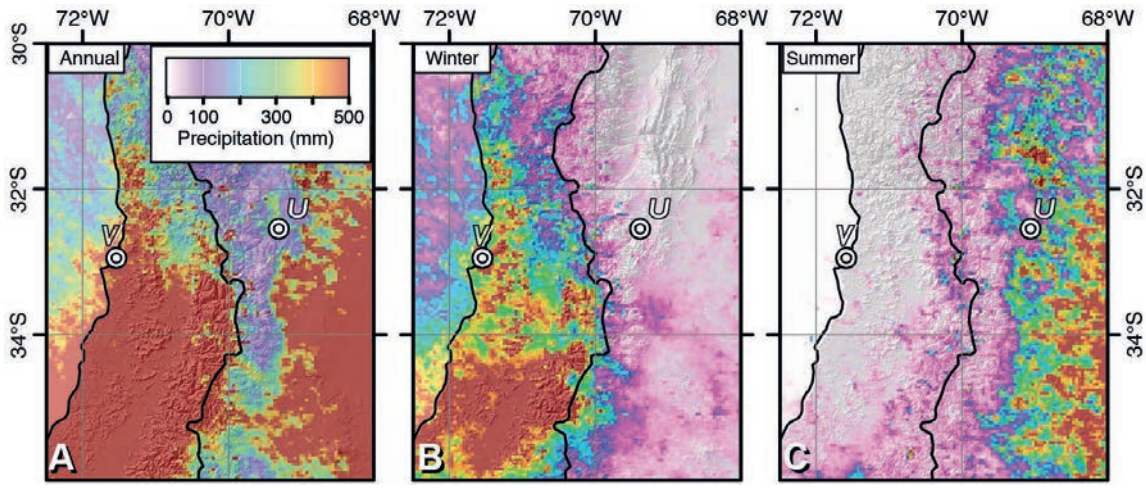

Fig. 11 - (a) annual, (b) winter, and (c) summer precipitation derived from using TRMM (Bookhagen & Strecker, 2008) over a 12-year period from 1998 to 2009. V - Valparaiso; U - Uspallata. From Hoke et al. (2013).

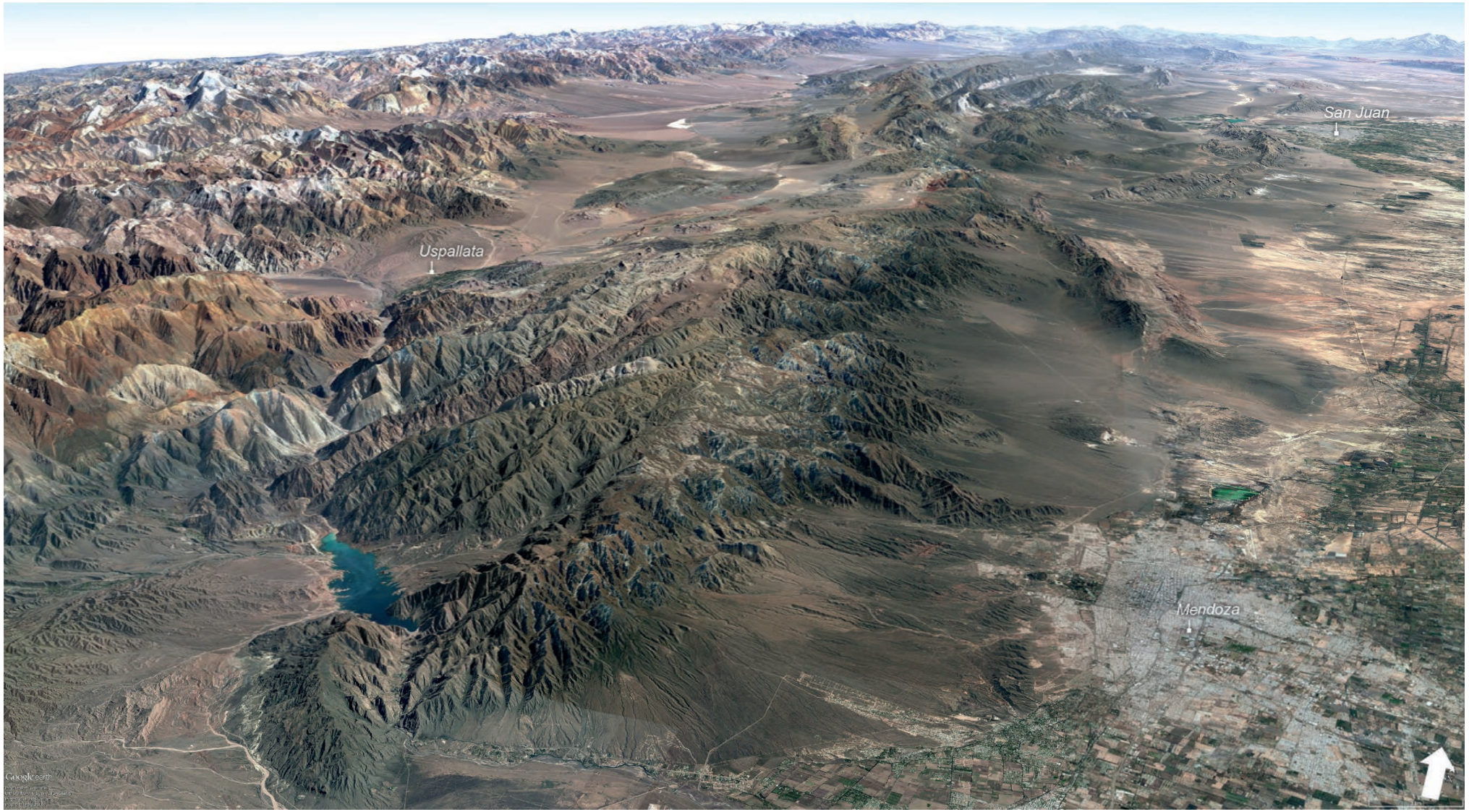

Fig. 12 - Overview of the southern Precordillera (Google Earth)

Day 1.

Stop 1.1 Cerro de la Gloria: active deformation of the Precordillera thrust front (32.8886°S; 68.8885°W)

At our first stop, at the eastern foothills of the Precordillera in the outskirts of Mendoza city, an introduction to the upcoming field trip will be given.

Drive along the thrust front of the Precordillera

The field trip begins in the city of Mendoza, which is built along the trace of the Cerro La Cal fault. The fault scarp can be seen across Las Heras Avenue, a few meters west where it intersects Perú Street. The railroad seen here was built along the fault scarp, a few years after the 1861 earthquake that destroyed the city of Mendoza. Leaving Mendoza, highway 7 to Chile runs parallel to the orogenic front, which is defined at these latitudes by an imbricate fan of thrust sheets with neotectonic activity that deformed and uplifted a complex system of terraces.

Drive across the southern end of the Precordillera

The road continues to the west and north. Along the northern side is the Sierra de Cacheuta, which limits the southernmost part the Precordillera range. The general south-plunging structure in this region is related to the southern boundary of the flat-slab segment. To the south, the Precordillera disappears and is replaced by the mildly structurally inverted Triassic Cuyo rift basin. The Sierra de Cacheuta is composed of Devonian sedimentary rocks that are intruded by Carboniferous to Early Permian diorites and granites. These sedimentary rocks, known as the Villavicencio Formation, correspond to gray- and greenwackes and mudstones with typical turbiditic arrangement. The sandstones show normal gradation with erosive base and tool marks and grade into mudstones. These deposits contain vegetal remains and trace fossils assigned to *Nereites* ichnofacies (Baldis & Peralta, 1999).

The sequence is unconformably overlain by Permo-Triassic Choiyoi volcanic rocks and Triassic rift deposits. Sedimentary sequences related to the passive eastern side of the Triassic rift can be seen on both sides of the road. These rocks are principally black shale that formed in the sag stage of the Triassic rift. They have an onlap relation with the Permo-Triassic Choiyoi volcanic rocks. Covering the Triassic sediments are the synorogenic deposits of the Miocene Marino Formation (14 to 9 Ma), which is associated with the main uplift of the Main Cordillera at these latitudes.

The road continues west and crosses the Río Blanco valley, which coincides with an inverted normal fault that puts Triassic sediments over Miocene deposits. Further west, the thick sequence of black shales is again the continental lacustrine deposits of the Triassic Cacheuta Formation, which is the main source rock for petroleum in the prolific Cuyo Basin.

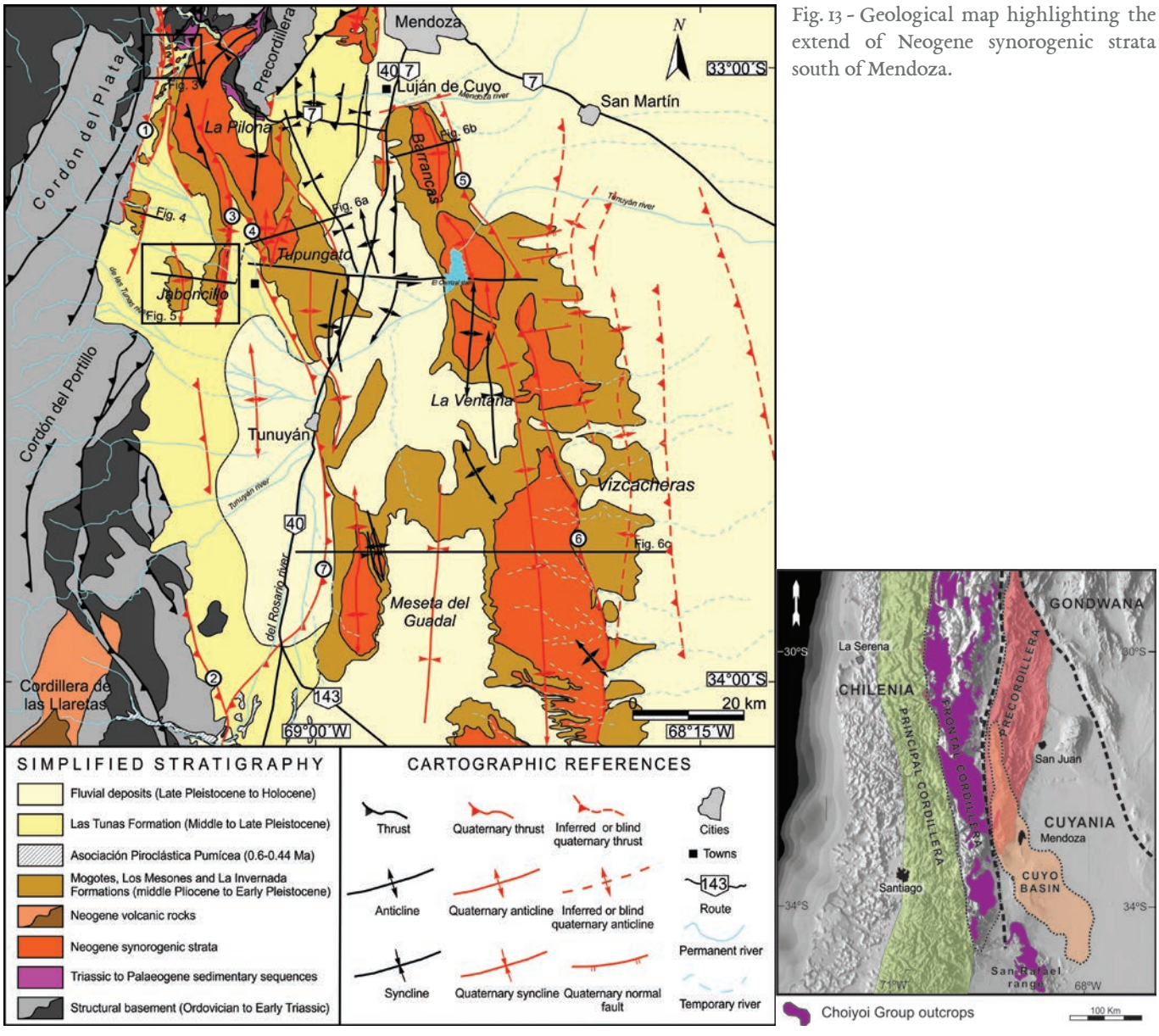

Fig. 13 - Geological map highlighting the extend of Neogene synorogenic strata south of Mendoza.

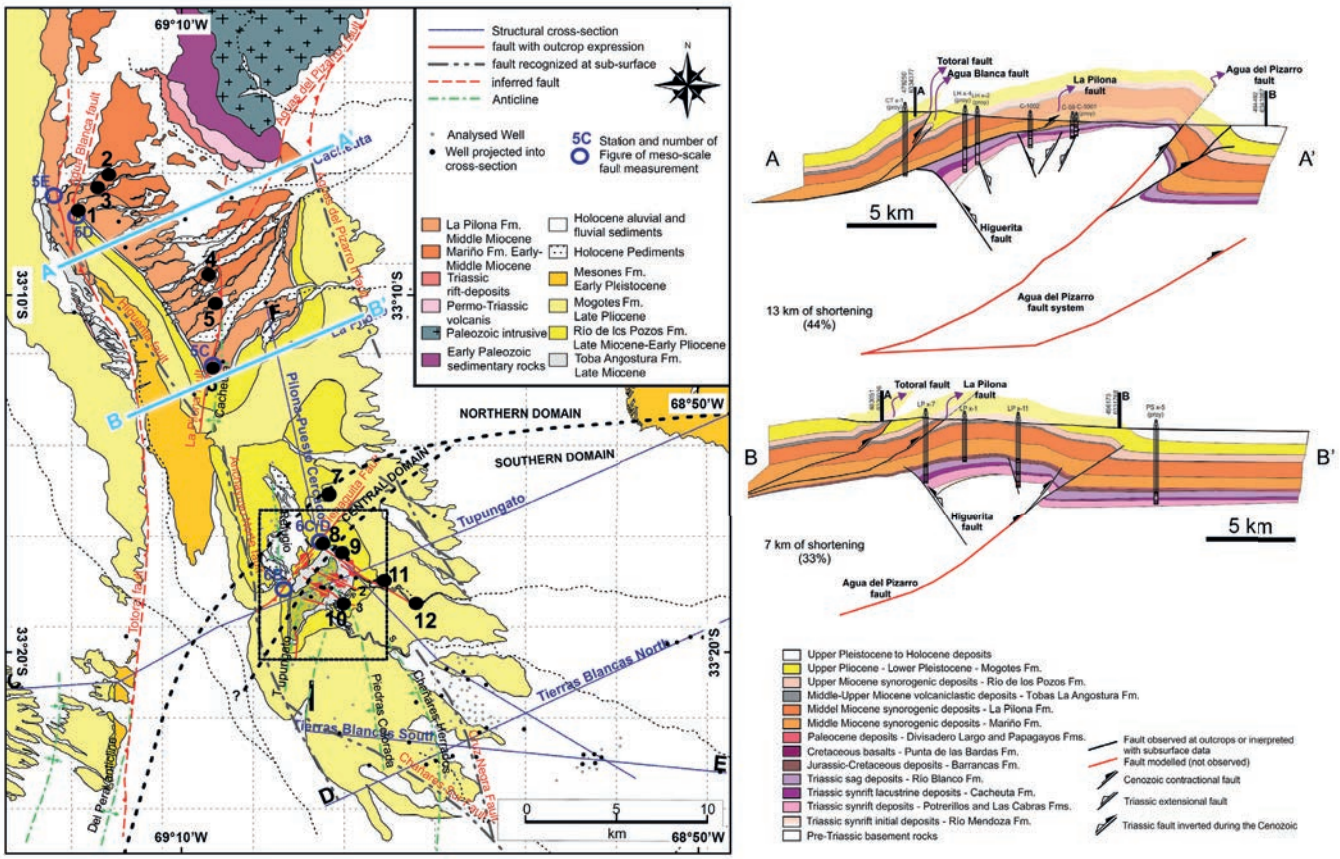

Fig. 14 - Geological map of the Neogene Cacheuta sub-basin located to the south of Mendoza (left). Structural profiles across the Cacheuta sub-basin, revealing the inversion of Triassic normal faults.

Stop 1.2 Inversion of the Triassic Cuyo basin and Neogene Cacheuta basin (33.0648°S; 69.1594°W)

Upper Cenozoic clastic deposits occur in the Santa María basin, between the Cordilleras Principal and Frontal, the Uspallata basin, between Cordillera Frontal and Precordillera, and in the Cacheuta basin (Figs 13 & 14). During the uplift of the Cordillera Principal, these three basins were connected and received sediments from the volcanic-arc and the Mesozoic units of the cordilleras de la Costa and Principal. The foreland basin was broken by the uplift of the Cordillera Frontal, separating the proximal deposits cropping out in the Santa María basin from the distal deposits of the Cacheuta basin.

Distal deposits

Between 3,000 and 4,000 m of synorogenic deposits unconformably overlay the Triassic and Paleogene rocks in the Cuyo basin. The oldest unit, the Mariño Formation, comprises 50 m of conglomerate and sandstone beds with predominance of volcanic clasts recording alluvial and fluvial setting, 180 m thick of cross-bedded sandstones of eolian origin, and 800 m of alluvial sandstones and conglomerates derived from the Cordillera Principal.

The La Pilona Formation unconformably overlies the Mariño Formation. It consists of 800 m of sandstones and conglomerates recording fluvial deposition. A regionally extensive ash-rich unit within the synorogenic deposits (Tobas Angostura Formation) unconformably overlies La Pilona Formation and consists of tuffs, sandstones and conglomerates (Irigoyen et al., 2000). This unit is overlaid by the Río de los Pozos Formation, which consists of mudstones, sandstones and conglomerates. Provenance studies indicate the Cordón del Plata as a source area for this unit (Irigoyen, 1997; Chiaramonte et al., 2000). The Pliocene-Pleistocene Mogotes Formation consists of boulder conglomerates interbedded with mudstones, sandstones and tuffaceous horizons, representing proximal alluvial-fan facies. The source area of this unit corresponds to both Cordillera Frontal and Precordillera.

Magnetostratigraphy carried out by Irigoyen et al. (2000), in the area between 33° 00' and 33° 20'S, calibrated by ^{40}Ar-^{39}Ar dating of interbedded air-fall deposits, indicates an age of 15.7 Ma for the base of the Mariño Formation and 12.2 Ma for the top. Deposition of the La Pilona Formation started at or slightly before 11.7 Ma and continued to 9 Ma in the Cacheuta-Tupungato area (33° to 33°20'S; Irigoyen et al., 2000) . In the same area, the same authors dated the deposition of the Tobas Angostura Formation between 8.9 and 8.7 Ma and deposition of the Río de los Pozos Formation between 8.7 and 5.8 Ma.

Proximal deposits

Synorogenic proximal facies correspond to the Santa María Conglomerates, firstly described by Schiller (1912) and Gonzalez Bonorino (1950), which will be seen at the stop at Cerro Penitentes. The upper part of this peak is formed by remnants of horizontal beds of conglomerates, lying unconformably on Mesozoic rocks. They are composed of conglomerates with unclear lamination. The size of the clasts varies from fine sand to boulders of 25 to 30 cm, being the volcanic rock fragments the most common ones. The conglomerates were deposited in the Santa Maria foreland basin during the Early to Middle Miocene on a high-energy alluvial fan environment (Pérez & Ramos, 1996).

Neogene synorogenic deposits provide time constraints on the evolution of the Andes and indicate regional along-strike change in style and timing of deformation. North of 33°S significant deformation has occurred between 12 to 9 Ma with the uplift of the Cordillera del Tigre in the Cordillera Frontal, as indicated by paleocurrent data from the La Pilona Formation (Irigoyen, 1997).

South of 33°30'S the foreland basin continued to receive sediments from the Cordillera Principal (Giambiagi et al., 2003) . Therefore, it has been suggested that Cordillera del Tigre was uplifted first and then the Cordón del Plata and Cordon del Portillo followed between 9 and 6 Ma (Giambiagi et al., 2003). The last ranges to be uplifted were the southern part of the Cordón del Portillo, the Cordillera de las Llaretas and Precordillera, as registered by clast provenance of the Rio de los Pozos and Mogotes Formations.

Drive-by geology: Cordón del Plata, Rock glaciers & Neotectonics

This rather short trip provides a panoramic view (left) of the Cordón del Plata mountain range (Cordillera Frontal), where the Río Blanco is fed by a number of large rock glaciers. Early studies in this region determined at least four Quaternary glaciations in this region (Wayne & Corte, 1983). Later however, the genesis of these chaotic deposits was reconsidered to have been derived from debris flows (rather than being moraines) that were emplaced in the piedmont region of the Cordillera Frontal. These Quaternary alluvial fans overlie Pleistocene terraces of the Río Mendoza and are affected by the Carrera-Fault System (CFS) that was responsible for the Plio-Pleistocene uplift of the Cordillera Frontal (Polanski, 1962, 1963; Cortés, 1993; Irigoyen, 1997, Irigoyen et al., 2000; Giambiagi et al., 2003). Evidence of neotectonic activity in the eastern sector of this fault system is documented by offset Quaternary alluvial fans along the Río Blanco and by steeply-dipping reverse faults that juxtapose Tertiary deposits with the Quaternary levels (Cortés et al., 1999; Fauqué et al., 2000; Folguera et al., 2001; Casa, 2005; García, 2004; García et al., 2005). More evidence for Quaternary activity of these faults comes from the clustering of several rock avalanches in the northern sector of the Cordón del Plata (Cortés et al., 1999; Fauqué et al., 2000; Moreiras, 2006a; 2006b).

Fig. 15 - Triassic rift basins of central-western Argentina and the main subbasins. From Stipanicic & Marsicano (2002).

Stop 1.3 Triassic Cuyo basin (32.9355°S; 69.2165°W)

The overlap of Triassic rift basins in southern South America with the Permo-Triassic Choiyoi granite-rhyolite province suggests a generic relation in an extensional regime (Figs 13 & 15). The Choiyoi rocks are crustal melts that formed in a trans-tensional setting (Giambiagi & Martínez, 2008) in association with extensive basaltic underplating during a period of relatively slow motion of the Gondwana supercontinent over the underlying mantle. The Cuyo rift basin developed slightly east of the main Choiyoi magmatic belt and is partially coeval with the termination of the acidic magmatism.

The margins of the Triassic basins follow first order tectonic boundaries with the hanging-walls following the suture zones of terranes that were accreted during the Paleozoic. Opposing polarities of half-grabens developed a local trans-tensional regime with transfer zones linking rift segments. Brittle faulting that took place during the rift stage allowed basaltic magmas to penetrate the cooling, refractory crust (Ramos & Kay, 1991).

The Cuyo basin is located to the east of an extensive sequence of Ordovician oceanic mafic magmatic rocks that mark the boundary between the Cuyania terrane which includes the Precordillera, and the Chilenia terrane to the west. These terranes were most likely sutured together in the Late Devonian to the Early Carboniferous (Ramos et al., 1986). The western margin of the Cuyo basin parallels the proposed terrane suture for more than 700 kilometers along the boundary of the upper plate. The Ischigualasto and the Beazley basins further east have a similar setting; in that they developed on the eastern side of the Cuyania terranes near its Late Ordovician to Early Silurian suture with the Pampia terrane, which incorporates the Sierras Pampeanas east of the Pie de Palo range (see Ramos, 2004).

Middle Triassic (235 Ma) alkaline basalts interfinger with late synrift deposits. Relatively low degrees of melting (4-5 %) in the mantle are suggested for the basalts, consistent with the comparatively narrow width of the Cuyo basin and their eruption during the last stages of Choiyoi magmatism (Ramos & Kay, 1991). No evidence of volcanic activity is found in the Cuyo rift during most of the Late Triassic, as this period was dominated by a generalized subsidence related to the thermal decay and sedimentary loading that characterizes sag phases. The upper crust became more brittle as silicic magmatism terminated allowing brittle fracturing of the upper crust to create a pathway for relatively primitive basaltic magmas to reach the surface. The basalts could represent a late phase in the stationary supercontinent-related heating of the upper mantle. Subsequently, the Middle Jurassic Andean arc developed to the west contemporaneous with generalized backarc rifting associated with the early opening of the South Atlantic. Arc volcanism is mainly concentrated on the western slope of the Main Andes.

The synrift deposits of the Triassic Río Mendoza Formation fanglomerates are separated by a strong angular unconformity from the Early Paleozoic rocks of the Villavicencio Formation, and the volcanics of the Choiyoi Group. The conglomerates of the Río Mendoza Formation are composed by thick tabular and lenticular bodies of volcaniclastic, poorly mature conglomerates and agglomerates with a generalized fining upward stacking pattern They represent the alluvial fan deposits that form the basal synrift

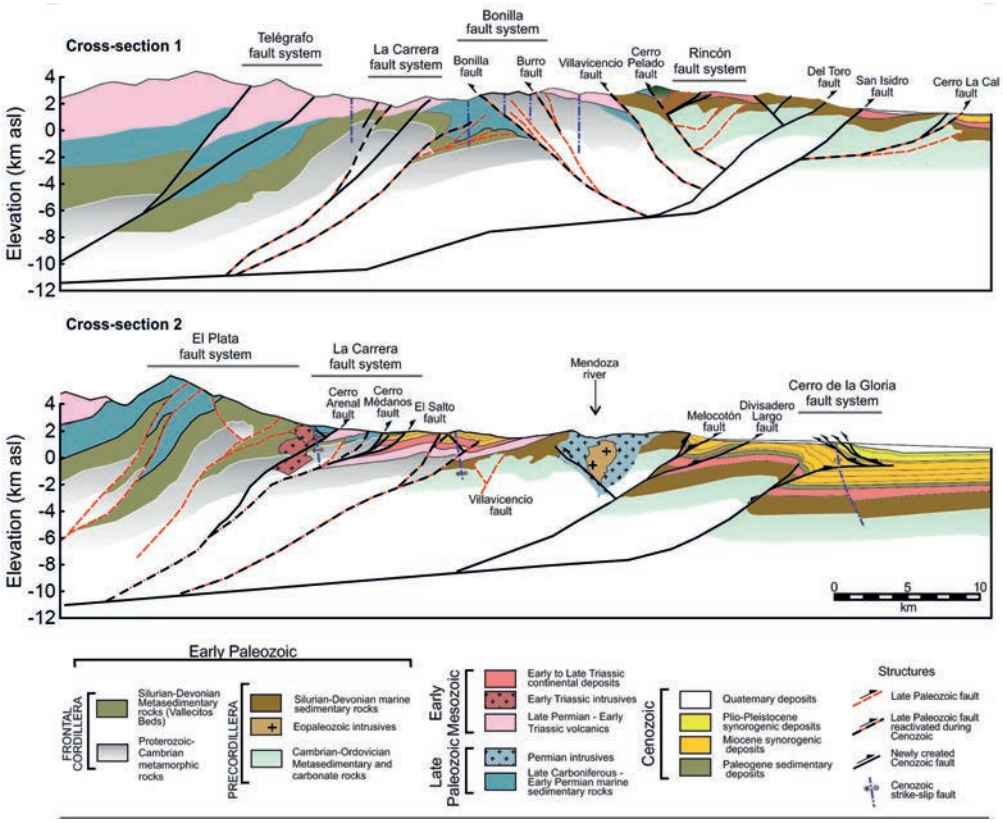

Fig. 16 - Balanced cross-sections 1 and 2 (for locations see geological map of the southern Precordillera in the attachment), showing the relationship between Andean (black lines), Permo-Triassic (blue lines) and late Paleozoic Gondwanan (red lines) and Chanic (green lines) structures. Modified from Giambiagi et al. (2014).

sequence of the Cuyo rift. The overlying Cerro de Las Cabras Formation is made up of two sections, the lower one is a mud-rich one with intercalated lenticular bodies of conglomerates and pebbly sandstones. The upper section is a fine-grained succession composed of multicolored mudstones, tuffs and pyroclastic siltstones (Spalletti, et al., 2005, 2008).

Above these units, the rest of the sequence of the Triassic rift deposits in the Uspallata Group can be seen. The Potrerillos Formation is the thickest Triassic unit and is characterized by cyclic alternations of gravel-, sand- and mud-rich intervals suggesting fluvial deposition. These formations constitute the first cycle of the Triassic rift sequence. These deposits are followed by a succession of lacustrine black shales of the Cacheuta Formation that indicates the synrift climax phase. The Triassic succession ends with the red beds of the Rio Blanco Formation representing the sag phase. The black shales of the Chacheuta Formation are the most important source rock of the oil fields of the Cuyo basin, southeast of the city of Mendoza. Concomitant of the Triassic synrift continental sedimentation and volcanism, WNW to NNW extensional faults developed, with fault-slip data indicating a NE stretching direction (Giambiagi et al., 2010).

Stop 1.4 Complex relationship between Frontal Cordillera and Precordillera thrust faults (32.8765°S; 69.2661°W)

The Las Carreras fault seen at this stop is the northern continuation of the Cordón del Plata thrust front (Fig. 16). In this location, the Permian Guido Granite is thrust over Ordovician (?) low-grade metamorphic rocks and the Choiyoi volcanic rocks. The fault was responsible for the late Miocene uplift of the Cordillera Frontal and was active during late Miocene and early Pliocene times, as inferred from the synorogenic Tertiary deposits east of the Cordón del Plata just to the south (Ramos, 1993).

The volcanic rocks of the Choiyoi Group seen in this region can be separated into two sections. The lower section, which can be seen at km 1107 along highway 7, is formed by andesitic volcanic rocks that represent the pre-Choiyoi stage of subduction related magmatism. The upper sequence is dominated by rhyolites.

Drive-by geology: Tigre Dormido landslide (32.773°S 69.319°W)

The Tigre Dormido (TD) landslide was generated at the eastern slopes of the Cerro Minero (3,813 m asl) and descended through the Quebrada La Soltero into the Río Mendoza. Remnants of this event are found along the valley walls and the Río Mendoza indicating a total volume of ~1.7 km³ (Fig. 17). A resulting landslide-dammed lake had a volume of ~1.6 km³ (Di Tommaso & Fauqué, 2005). Associated lake deposits have only been preserved in a strongly eroded 10-m thick sequence of reddish silt and clay. The monomictic TD deposit is composed of rhyolites. Its characteristic yellow color and some lamination with black layers of manganese oxide are mainly due to hydrothermal alteration in the source area.

The TD landslide deposit can be correlated with two glacial outwash deposits from the Punta de Vacas and Uspallata glaciations (Moreiras, 2006a; 2010a). Since the Uspallata outwash onlaps onto parts of the TD-rock avalanche and associated lake deposits, the rock avalanche must be older than the outwash. As the Uspallata glaciation was assigned an at least Early to Middle Pleistocene age (Espizúa & Bigazzi, 1998), the TD-rock avalanche must have occurred before or during this time period. Thus, OSL-ages of ~10±3 ka, obtained from the lake sediments, must be an underestimation of the real age. In situ cosmogenic nuclide exposure ages of landslide boulders, however, also reveal relatively young ages for the landslide of ~47±4 ka (Fauqué et al. 2008d). New OSL-dating of the lacustrine sediments confirms a late Pleistocene age (~44±4 ka, Moreiras et al., 2015).

Drive across the Cordillera Frontal

Route 7 continues west into the Cordillera Frontal, which is the locus of the Late Paleozoic tectonic activity that has been called the Gondwanian orogeny since the early work of Du Toit (1927). The Frontal Cordillera contains the early Permian subduction-related magmatic rocks as well as the subsequent widespread

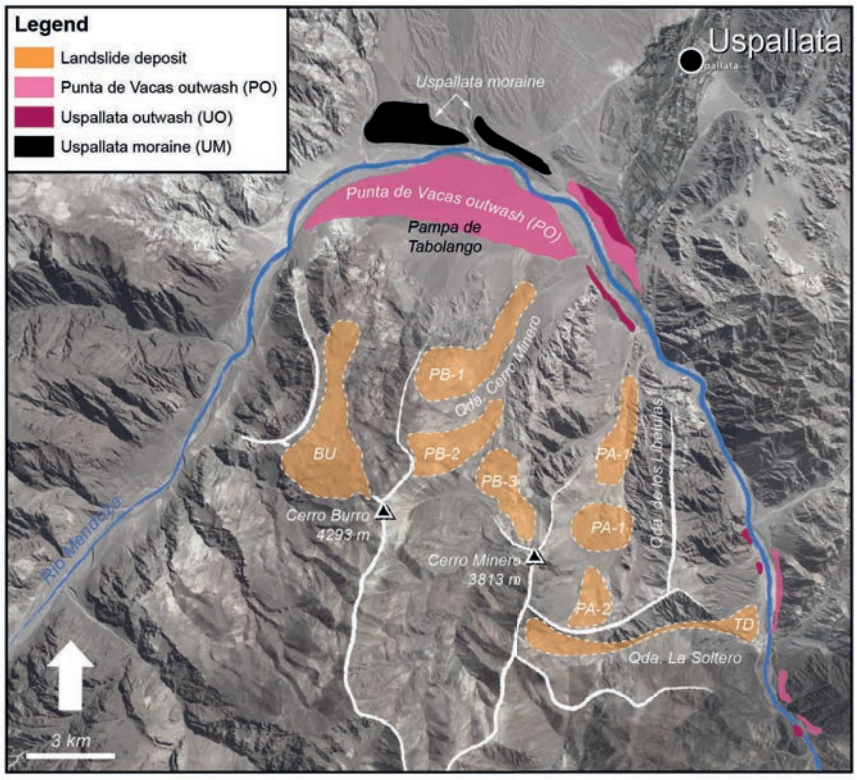

Fig. 17 - Large landslides in the Uspallata region: (a) Tigre Dormido (TD); (b) Placetas Amarillas 1 (PA-1); (c) Placetas Amarillas 2 (PA-2), c-Piedras Blancas 1 (PB-1); (d) Piedras Blancas 2 (PB-2); (e) Piedras Blancas 3 (PB-3), and (f) Burro (BU) (after Fauqué et al., 2000, 2001). Pleistocene drifts identified in the area are the Uspallata terminal moraine (UM), Uspallata outwash (UO), and Punta de Vacas outwash (PO) (after Espizúa, 1993; Moreiras, 2003, 2004b).

Permo-Triassic rhyolitic magmatic rocks known as the Choiyoi Province (Kay et al., 1989).

These Late Paleozoic-Triassic batholiths and associated acidic volcanic rocks record the history of an important period of crustal growth on the margin of western Gondwana. These events follow a period of Middle to Late Paleozoic subduction that culminated with uplift and crustal thickening, followed by extensional collapse of the orogen associated with extensive melting of the crust (Mpodozis & Kay, 1992). The formation of the Choiyoi province has been associated with a relatively stable period in the history of Gondwana during which underplated mantle basalts caused extensive crustal melting. There is no evidence for subduction of oceanic crust beneath the Cordillera Frontal during this time. There are syn-extensional faults in the Choiyoi group sequences. These events are related to the final assembly of the Gondwana continent and the first stages of its fragmentation.

Late Paleozoic subduction of the Protopacific Ocean along the new western border of Gondwana resulted in formation of the wide accretionary prism that is now exposed along the Chilean coast and the plutonic and volcanic rocks known as the pre-Choiyoi assemblage (Kay et al., 1989; Mpodozis & Kay, 1990) in the Cordillera Frontal. Synchronous intra-arc and back-arc sedimentary basins forming in both Argentina and Chile were filled by several thousand meters of Devonian (?) to Lower Permian marine and continental sediments (Caminos, 1979; Polanski, 1970). The Late Permian to Triassic history of the Cordillera Frontal region is dominated by the extensive Choiyoi graniterhyolite province whose formation precedes and in part overlaps the development of Triassic rift basins just to the east (Ramos & Kay, 1991).

The Choiyoi province extends for more than 2500 km from Collaguasi (22°S) in northern Chile to the Neuquén Basin and northern Patagonian Andes near 400S (Mpodozis & Kay, 1990). Particularly extensive sequences of rhyolitic ignimbrites (Cortes, 1985) and granitic batholiths occur (e.g., Colangtiil and San Guillermo batholiths; Llambias & Sato, 1990) occur in the San Rafael block in Argentina to the south (34°S) and in the Cordillera Frontal (29°-33°S; Caminos, 1979). Volcanic calderas are still recognizable in some places.

A major lower Permian compressional deformation is recognized in the Cordillera Frontal where a pronounced unconformity separates folded and faulted Devonian and Carboniferous sediments from undeformed Middle to Upper Permian Choiyoi volcanic sequence. This deformational phase known as the San Rafael (Polanski, 1970) was also recognized as a period of low magmatic activity in western Argentina (Perez & Ramos, 1990). Further east, in the Carboniferous Paganzo basin, in the modern Precordillera and Sierras Pampeanas, no deformation is observed. At that time, a change occurs from deposition of active rifting of synrift facies to sag facies.

One possible explanation for compressional deformation and crustal thickening is that oblique collision of an exotic terrane occurred along the coast at this time. This scenario is consistent with the work of Rapalini (1989) who used paleomagnetic evidence to suggest that pre-mid Permian rocks in Argentina are rotated as a consequence of oblique plate motion along the Pacific margin. Late Permian rocks are not rotated. The orientation and intensity of the mylonitic and cataclastic zones in the granitoids are also most easily explained by oblique motion (Mpodozis & Kay, 1990). Collision could also explain the apparent end of subduction related magmatism. An alternative explanation was presented by Martínez et al. (2006), who related the San Rafael deformation and the cessation of arc related magmatism to a period of flat-subduction.

Between stops 3 and 4, post tectonic granitoids such as the Guido Granite can be seen in the western part of Precordillera. These granites were emplaced during the Late Paleozoic. They have an Early Permian age and could be subduction-related granitoids similar to the ones described in Chile further north (Mpodozis & Kay, 1990). Mafic dikes were emplaced during the late episodes of crystallization.

The post-collisional granites and rhyolites typical of the Choiyoi province show chemical characteristics consistent with an ongm by crustal melting with heat provided by basaltic underplating. The Choiyoi province is only one of the granite-rhyolite provinces that formed along the western border of Gondwana from

the Upper Paleozoic to the Lower Jurassic (see Mpodozis & Kay, 1990). Others include the "Mitu" province between Peru and Bolivia, the Choiyoi province discussed here, the Chon Aike province in Patagonia, the Antarctica Peninsula and Ellsworth-Witmore in Antarctica, and the New England fold belt in Australia. The combined outcrops form a belt of more than 10,000 km, developed along the Pacific margin of Gondwana, preceding its rupture and dispersal. In most of these regions, Late Paleozoic calc-alkaline arc-related plutons are deformed and uplifted. These events are followed by the intrusion of high levels hypersilicic rhyolites and granites ranging in age from Upper Permian to Lower Jurassic. In all cases, these events represent the final amalgamation of Gondwana, the extensional collapse of compressional regimes and the initial stages of breakup of the supercontinent. The tectonic processes occurring are those associated with subduction, terrane collision, and extension. The large amounts of granite and rhyolite generated are the results of the focusing of these events during a short period of time, associated with the formation and break-up of a supercontinent.

Day 2.

Drive into the Cordillera Principal: The High Andes

The Cordillera Principal or High Andes starts west of Punta de Vacas. Here the Gondwana evolutionary stage of the Cordillera is heavily overprinted by Mesozoic and Cenozoic events. The Mesozoic to Cenozoic evolution is characterized by two stages: (1) the Jurassic to Early Cretaceous intra-arc development of a carbonatic sedimentary basin that is intermittently interrupted by volcanic activity; and (2) the formation of a Cenozoic fold and thrust belt (Figs 18 & 19). Neogene deformation and contraction started in Chile in the Paleogene at these latitudes with an extensional stage during the Oligocene (Godoy et al., 1999). The structures seen in the Aconcagua fold and thrust belt on the Argentine side of the Cordillera are mainly early Miocene to late Miocene in age.

One of the outstanding features of the first stage is the development of many Mesozoic marine sequences that were controlled by transgressions and regressions from the Pacific side. Those sequences are grouped into four sedimentary cycles, which are separated by regional first order unconformities. These sequences are clearly depicted in the Neuquén basin further to the south, where a well developed Liassic to Cenomanian marine retroarc basin developed behind the magmatic arc in the eastern foothills of the Cordillera. The Neuquén basin is linked to the north with the Aconcagua basin which we are seeing here.

The Aconcagua Basin has a different paleogeography with a larger participation of volcanic rocks, but similar middle Jurassic to Cretaceous stratigraphic cycles. There are interesting parallels between the evolution of the basin and the magmatic arc history (Ramos, 1985a,b). The main periods of regional unconformities in the foreland are coincident periods when the magmatic arc migrated eastward. The intermittent nature of the magmatic activity, as well as the spatial variation of the volcanic front in the Andes, are closely related to changes in plate motion controlled by variations in the spreading velocities of the Pacific and Atlantic oceanic ridges. Removal of the continental margin by forearc subduction erosion can also be related to the migration of the arc volcanic fronts. Such processes seem to be associated with the shallowing of the subduction zone at this latitude and just to the south in the last 10 Ma (see Kay et al., 2005).

Most of the Chilean and the westernmost Argentine Mesozoic basins of the Cordillera Principal are intra-arc basins controlled by the development of two distinctive arcs: an inner more active arc along the Cordillera de la Costa of Chile concentrates the main andesitic activity and an outer arc produces rock suites that are mainly of andesitic to bimodal composition. Several authors have proposed an extensional regime in the arc massif region mainly during the Early Cretaceous, which was responsible for the intra-arc basin development. This process has been envisaged as an intra continental spreading which has controlled the rapid subsidence of the volcanic pile where burial metamorphism closely followed extrusion (Levi & Aguirre, 1981). This extensional regime in the arc has been attributed to a negative trench roll-back velocity prior to the opening of the South Atlantic Ocean of the Western Gondwana plate. The opening of the South Atlantic Ocean in the Neocomian (~ 125 Ma) changed the absolute motion of South America to a positive trench roll-back velocity and to a compressive regime in the arc (Ramos, 1999).

The intermittent activity of the outer arc is closely related to periods of sea level lowstands in both the intra arc and the retro-arc basins. These local sea level changes have been partially correlated with the world-wide eustatic onlap cycles. The intra-arc basins were active until Early Barremian times when an important eastward migration of the main magmatic arc occurred, together with a low stand period in the retro-arc and intra-arc basins and the development of a single and expanded central arc. The retro-arc easternmost basin was exclusively continental from this time on, and the Pacific sea no longer reached the eastern side of the cordillera. This important paleogeographic change is closely linked with the beginning active spreading in the South Atlantic. Soon after the opening of the South Atlantic a new increase in plate motion started a compressive regime, which eliminated the intra-arc basins and the arc front moved toward the foreland. This second step is recognized in these latitudes at about 110 Ma when the Cristo Redentor and the Juncal Formations were deposited. The eastward expansion of the magmatic arc could be related to a decrease in the subduction angle of the slab, coeval with a higher convergence rate, combined by the tectonic erosion at the subduction zone.

The maximum sea floor spreading rate at the Pacific and the South Atlantic spreading centers was reached in the Late Cretaceous (ca. 80 Ma). A positive trench roll-back velocity at this time may be responsible for the development of a fold and thrust belt on the eastern flank of the Andean orogen. At the same time, a foreland basin formed at the leading edge of the deformational front in response to tectonic loading in the adjacent thrust belt. At the final stage of compression, several granitoid stocks were emplaced in the arc massif.

Stop 2.1 Uspallata Neogene basin (32.6193°S; 69.4359°W)

The southern end of the Calingasta-Uspallata valley is seen at this stop. At these latitudes, the Cordillera Frontal is thrust over the Precordillera. A series of imbricate thrust put Choiyoi volcanic rocks repeatedly on top of Miocene continental foreland basin strata.

Quaternary evolution

South of Río Mendoza, the Pampa de Tabolango (plain) merges with the Punta de Vacas outwash plain. The northern side is characterized by the Uspallata terminal moraine and its outwash deposits. Both are partially submerged in alluvial fan deposits, which have been grouped into the San Alberto Formation (Cortés, 1993). At the northern tip of the Cordón del Plata, multiple large-scale landslides were generated. Among them is the Piedras Blancas rock avalanche (PB) that likely initiated as a rota-

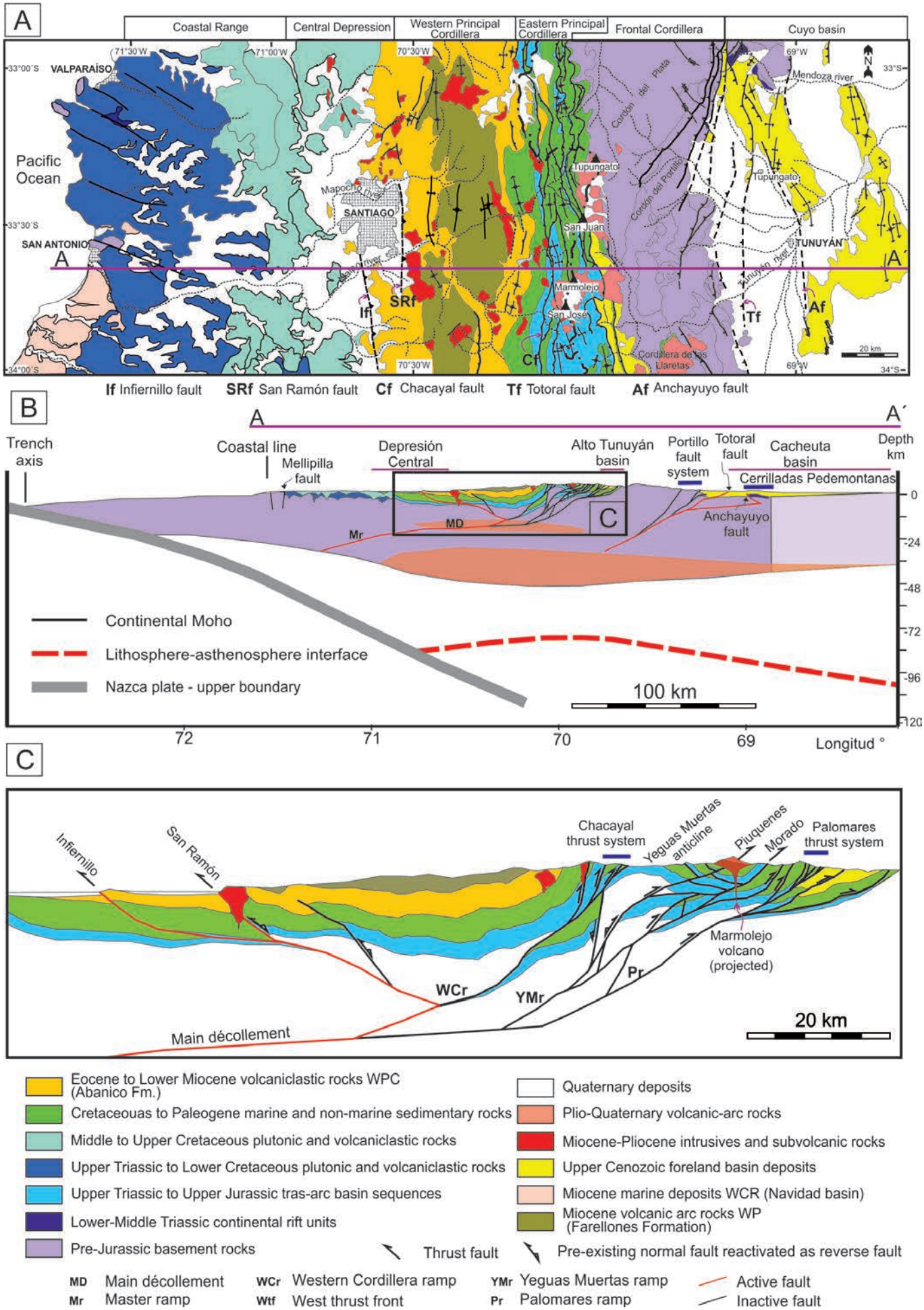

Fig. 18 - (A) Geological map across the Andes at 33.5°S; (B,C) Regional and detailed structural cross sections.

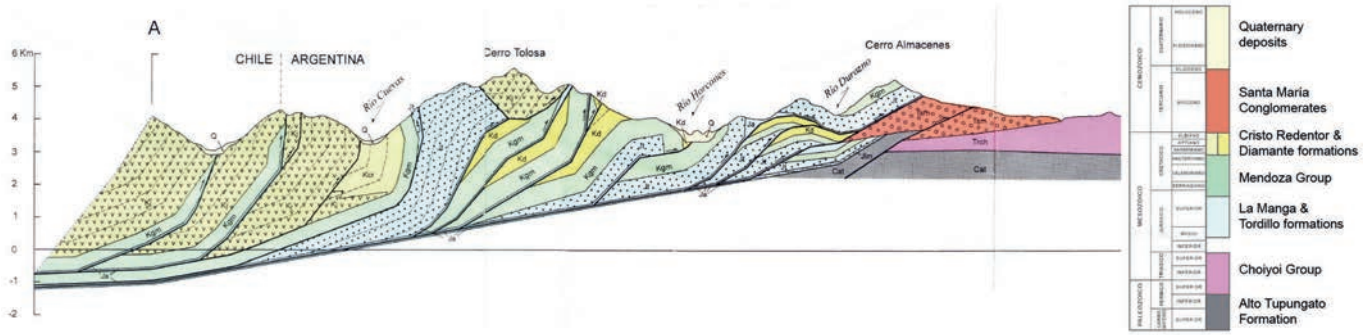

Fig. 19 - Structural cross section through the Cordillera Principal at ca. 32.75°S latitude.

tional slide and then evolved into a large debris flow. Rock masses moved ca. 10 km northward, descending ~2,000 m into the Pampa de Tabolango. This event moved ~0.9 km³ of debris and subsequently covered an area of ~7.5 km². Earlier landslides in this sector exist, but are hard to trace. The PB landslide did dam a lake, as is evidenced by a 30-m thick sequence of sands, silts, and clays in the Quebrada Cerro Minero, with an areal extent of ~0.75 km² with a maximum lake level at 2,677 m (the present-day local base level of the Río Mendoza at this location is about 1,750 m). Fossilized mammal teeth from the lake sediments (*Hippidion devillei*, Cerdeño et al, 2008) suggest a Late Pliocene to Late Pleistocene age (Alberti & Prado, 2004).

Similar to the TD landslide, the PB landslide is covered by volcanic ash-bearing alluvial fans. Tephrochronological results suggest a temporal correlation with samples of the middle ash level found in the area (Moreiras, 2010a). This landslide event has been assigned a Latest Pleistocene age, as a carbonate-cemented breccia found in a block was dated to 15 ka BP (AMS14C, Fauqué et al., 2001). Later, CRN-dating suggested an age of ca. 109 – 208 ka (Fauqué et al. 2008d). According to more recent CRN ages, the occurrence of at least three isolated events separated by a certain amount of time is plausible (Moreiras et al., 2015). More recently, the middle ash layer was radiometrically dated ($^{40}Ar/^{39}Ar$), which gave an age of 350 ± 80 ka. The date suggests that, as the PA-1 rock avalanche is older than this ash level, the maximum age for the PA-1 rock avalanche should be Middle Pleistocene (Moreiras et al., 2006).

At the northern tip of the Cordón del Plata, the Carrera-Fault System (CFS) comprises two major steeply westward dipping faults, juxtaposing intrusives and volcanic rocks with tertiary sediments: (a) the Placetas Amarillas fault; and (b) the Piedras Blancas fault (Cortes, 1993). Clustering of rock avalanches is linked to neotectonic activity of these faults (e.g. Moreiras, 2010a). Epicenters of shallow crustal earthquakes with M>3.5 show a certain alignment with the CFS evidencing younger reactivations.

Stop 2.2 Permo-triassic extensional structures (32.7882°S; 69.6456°W, 2230 m)

This stop provides a good example of the Gondwanian tectonics. A normal fault pusts in contact the western facies of the Carboniferour deposits with the pyroclastic sequences of the Choiyoi Group. Along the fault trace a rhyolitic dike of Late Triassic age intruded, probably related to extensional movement of the fault. The well stratified pyroclastic deposits of the Choiyoi Group have been dated in 235-238 Ma by K-Ar (Pérez & Ramos, 1996), indicating a Middle Triassic age.

The angular unconformity that separated the Late Carboniferous-Early Permian marine deposts from the Choiyoi Group volcaniclastic deposits represents the San Rafael compressional phase of Middle Permian age.

Stop 2.3 Aconcagua frontal thrusts and Santa Maria basin (32.8408°S; 69.8415°W)

This stop shows the thrust front of the Miocene Aconcagua fold and thrust belt. Middle to Late Jurassic limestones (La Manga Formation) thrust over thick early to middle Miocene Santa Maria conglomerates that in turn unconformably overlie marine and continental Jurassic strata. The east-verging Penitentes thrust dips at 5° to 22° to the west. The effects of erosion have led to the near formation of a klippe on the top of Cerro Visera further east. A thin blanket of Choiyoi volcanic rocks unconformably overlying Carboniferous deposits and Permian granitoids, where Late Permian - Early Triassic extensional faults are preserved.

The La Manga Formation is a calcareous unit of 50 to 60 m on the Aconcagua area where three sections can be differentiated. The siliciclastic lower section is made of irregular massive sandstones or with cross stratification. They are covered by bindstones and rudstones but massive mudstones, wackestones and packstones with oyster, ammonites and equinoderms outline on the middle section. The section ends with thick corallineous floatstones overlaid by oolitic packstones and grainstones brecciated probably due to kastic phenomena.

The La Manga Formation represents the onset of the sedimentary infill of this basin their basal facies overlied the pre-Jurassic basement and lately evolved to marine deposits, mainly carbonatic ones. The siliciclastic facies has been interpreted as belonging to a fluvial system coming from the east that passes into a calcareous platform. The development of several prograding sequences is interrupted by an important sea level fall registered by the exposure of the platform (Lo Forte, 1992). The Auquilco Formation is reflecting the important marine restriction related to the sea level fall. This unit is made of laminar and nodular anhydrite with red sandstones and micritic mudstones subordinated. The interpreted sedimentary environment is a shallow and hypersaline body related to clastic continental deposits to the continent that is rep laced by red and green sandstones of the Tordillo Formation (Lo Forte, 1999). The sedimentary environment of this unit is related to the interaction of the volcanic arc and the continental environment where braided rivers and sheet flood deposits are related to volcanic flows and lahars (Sanguinetti & Cegarra, 1991) . Isotopes analysis indicates the absence of significant contribution of continental waters or hydrothermal solutions for the gypsum in the study area (Lo Forte et al 2005).

The next sedimentary cycle, known as Mendoza Group (Weaver 1931), begins with an important sea level rise during the lower Tithonian. It is represented in the Aconcagua area by the deposition of the dark shales of the Vaca Muerta Formation and it evolved into the Quintuco Formation with platform related facies (Aguirre Urreta & Lo Forte, 1999). These black shales are seen over the red sandstones of the fluvial system or over the evaporites of the hypersaline lake and laterally pass to volcanic and clastic

sediments near the active volcanic arc and also to a calcareous platform. A series of marine restricted and fluvial environment is installed due to a new sea level fall known as the Mulichinco Formation. The Mendoza Group ends with the deposition of the Agrio Formation representing the greater expansion of the valanginian-hauterivian sea on the Aconcagua basin.

Stop 2.4 Aconcagua FTB (32.8248°S; 69.9107°W)

This is the most classic section of the High Andes. Compare the evolution of the knowledge since Darwin with the present interpretation (Fig. 1 and 19). The section shows the autochthon, which is composed of Carboniferous hornfels, thin pyroclastic deposits of Choiyoi Group and Jurassic limestones and conglomerates of proximal facies and small outcrops of marine Early Cretaceous; the first thrust plate, which is composed of Middle to Late Jurassic marine and continental deposits and Early Cretaceous continental to transitional marine deposits; and the second thrust plate, which has Late Jurassic gypsum at the base and Titho-Neocomian continental and marine strata above. All these sequences are intruded by thick Miocene (15 Ma) trachytic dikes. Cretaceous basaltic and andesitic lenses that are interbedded in the sequence in the first thrust sheet become more abundant in the westernmost thrust sheets (Ramos, 1985a,b).

The Puente del Inca is a natural bridge formed during the last deglaciation, probably in the Late Pleistocene, as an ice bridge associated with an avalanche. The presence of thermal springs, controlled by the Penitentes thrust, cemented with sulphates and carbonates and an intense biogenic precipitation of the avalanche deposits (travertine-cemented landslide debris), leading the way to the present bridge (Ramos, 1993).

Stop 2.5 Aconcagua from Horcones (32.8111°S; 69.9424°W)

At this stop, there is a magnificent view of the Pared Sur (south wall) of the Aconcagua (6,967 m asl., Fig. 20). The wall is formed by volcanic and breccia flows of andesitic composition of the Aconcagua Volcanic Complex (15 to 8.9 Ma, Ramos & Yrigoyen, 1987, Godoy et al., 1988; Kay et al., 1991). On the western side of the valley, there is an imbrication of Jurassic continental red beds and Early Cretaceous limestones. On the eastern side, the diapiric effects of the Late Jurassic gypsum of the Auquilco Formation produced the complex structure of Cerro Panta. To the south, the fault imbrications are visible from the second to the fourth thrust sheets repeating the different Titho-Neocomian units.

Stop 2.6 Cretaceous arc and back arc basin (32.814°S; 70.0499°W)

This stop shows that the westernmost thrust sheets are dominated by volcanic and volcaniclastic rocks derived from the volcanic arc. These Early Cretaceous (Neocomian) rocks have Valanginian (137 to 132 Ma) ammonites, which corroborate the Neocomian age of the sequence. The thrusts formed an imbricate fan with the western and older thrusts rotated 25° to vertical and almost overturned.

In the northern margin, the Neocomian limestones override Late Jurassic-Early Cretaceous red beds. The thickness of these continental and volcaniclastic deposits exceeds several times the normal thickness of these units, indicating their proximity to the volcanic arc. A large rock avalanche was produced from one of the volcaniclastic members of the Mesozoic deposits.

Optional history stop

Depending on the time available and the weather an optional stop is to visit a colonial shelter built in 1765. The Spanish Royal Mail constructed those shelters to enable crossing the Andes during the winter. At that time, Spaniards were at war with the British Empire, which reduced the likelihood of a safe passage through the Strait of Magellan.

Day 3.

Optional stop - Darwin Triassic forest (32.4843°S; 69.1239°W)

This is the classic locality where in 1835 Darwin found the first fossil floras of southern South America (Brea et al., 2009). He reported a fossil forest with vertical silicified stems of "*Araucarites*"

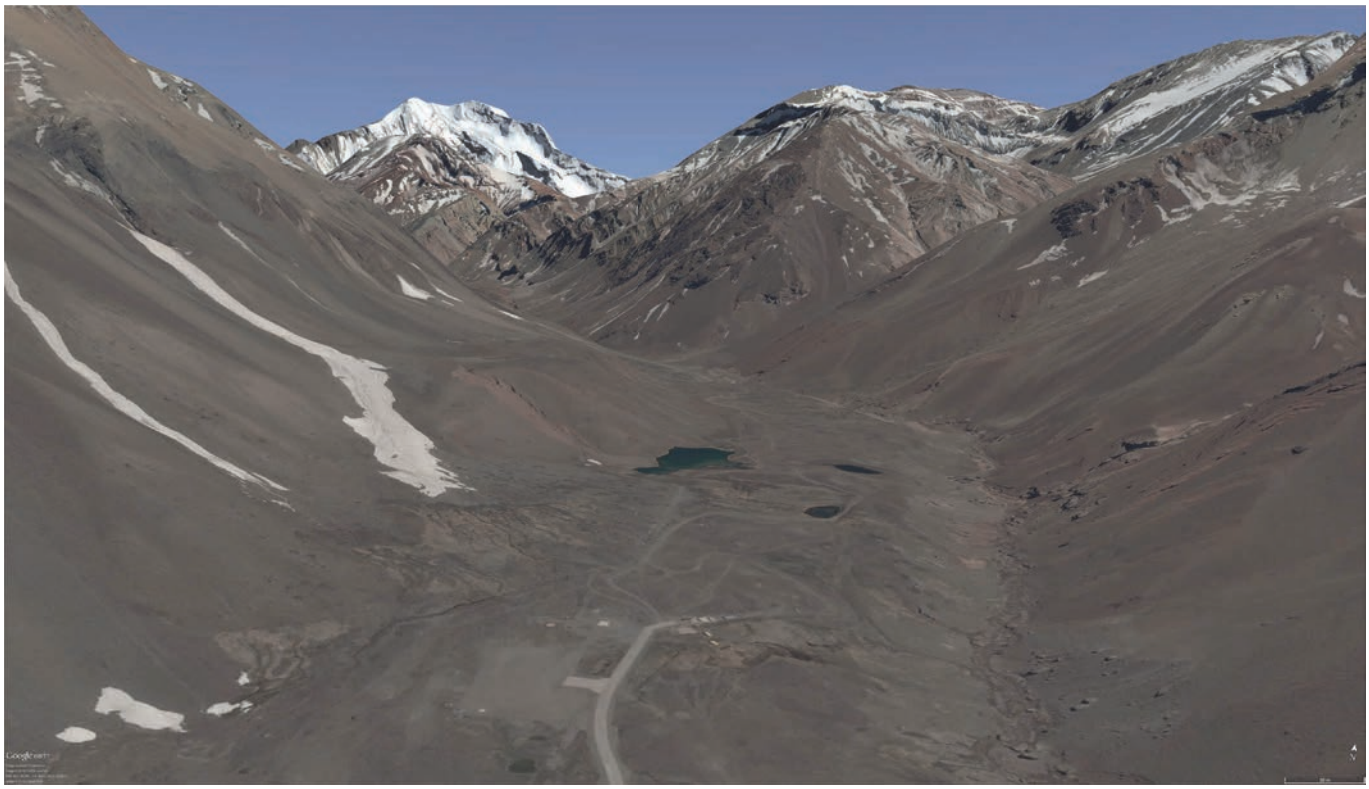

Fig. 20 - 3D-view of the Cerro Aconcagua at Horcones (Google Earth).

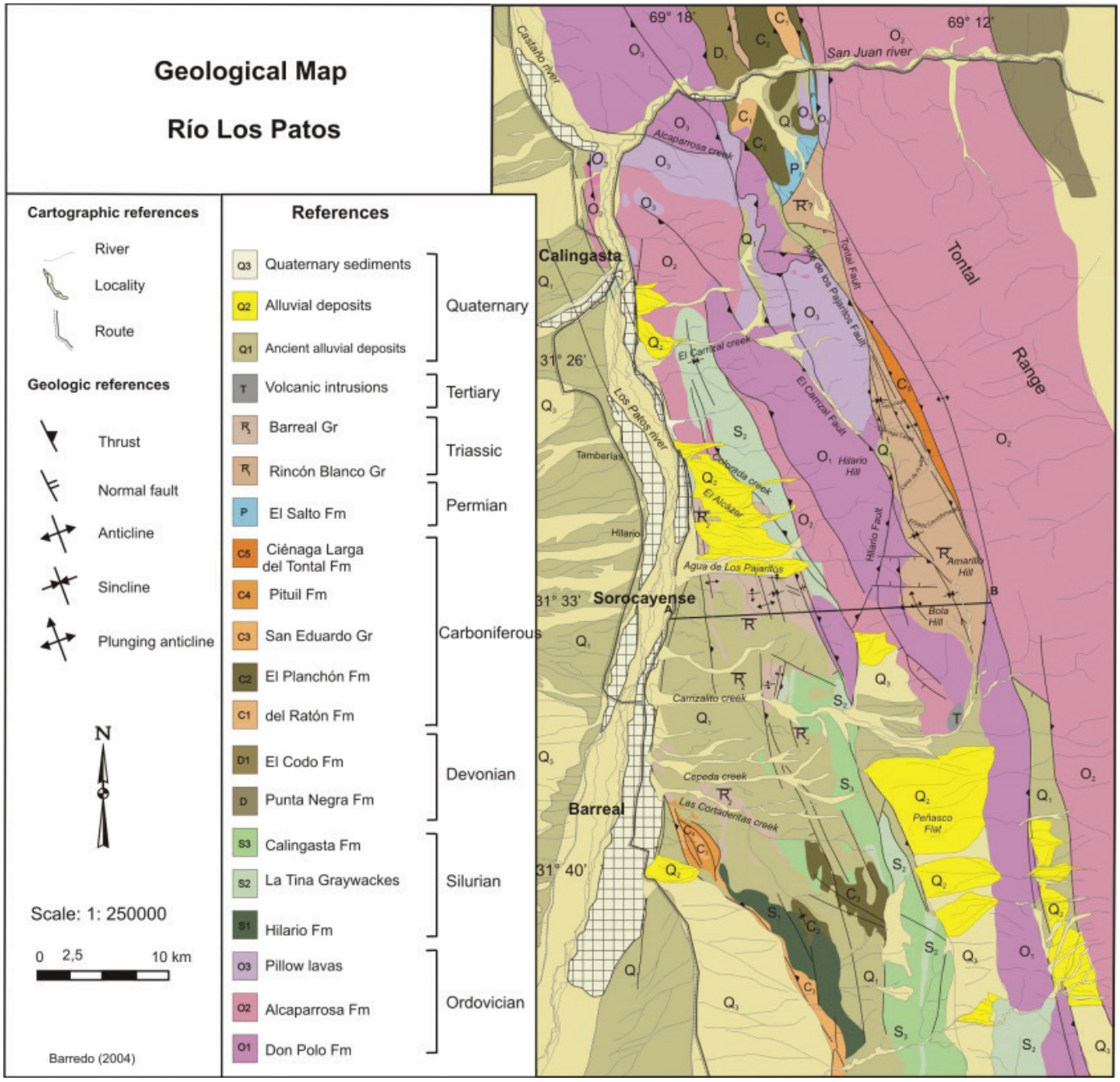

Fig. 21 - Geological map of the Calingasta-Barreal region (Barredo, 2004).

in life position near the Agua de la Zorra locality. Electronic microscopic studies performed by Brea (1997) confirms that the trunks belong to *Araucarioxylon*. At this locality, Darwin wondered about the processes that would cause the burial of the conifer trunks, which he considered had happened in a marine sedimentary environment. Now, it is interpreted that the forest was buried by pyroclastic flows in a Triassic rift depocenter (Poma et al., 2009). Synchronous alkaline basalts of Agua de la Zorra have been dated to 235 Ma.

Stop 3.1 Río Blanco Triassic rift (31.4778°S; 69.3949°W)

This stop is located 17 km north of Barreal, near the locality of Hilario. It coincides with a small outcrop of Triassic deposits characterized by tuffs, reworked tuffs, siltstones and fine-grained, lacustrine and fluvial sandstones deposited in a rift-related depocenter (Figs 2 & 21). The active margin is located to the east and it is characterized by coarse conglomerates and red sandstones.

The Precordillera fold-and-thrust belt.

The Cenozoic Precordillera is a fold-and-thrust belt east of the main Andean Cordillera (Fig. 22). The best analogy for the tectonic setting of the Precordillera (thin-skinned) and its neighboring reverse-fault bounded basement ranges of the Sierras Pampeanas (thick-skinned) in a similar geodynamic context, is the early Tertiary Wyoming-Colorado fold-and-thrust belt in the western US. The Precordillera and the Sierras Pampeanas are still actively deforming and uplifting and display numerous geomorphic and structural features related to active tectonism. In the area of the town of San Juan the Precordillera borders the Tulum Valley, which in turn is flanked by the actively deforming Sierra Pie de Palo basement uplift to the east. The Tulum Valley is filled with several kilometers of Miocene to Recent sediments derived from the uplift of the Precordillera and the High Andes; in contrast, the Iglesias Basin to the west of the Precordillera is a large-scale intermontane piggy-back basin which records repeated episodes

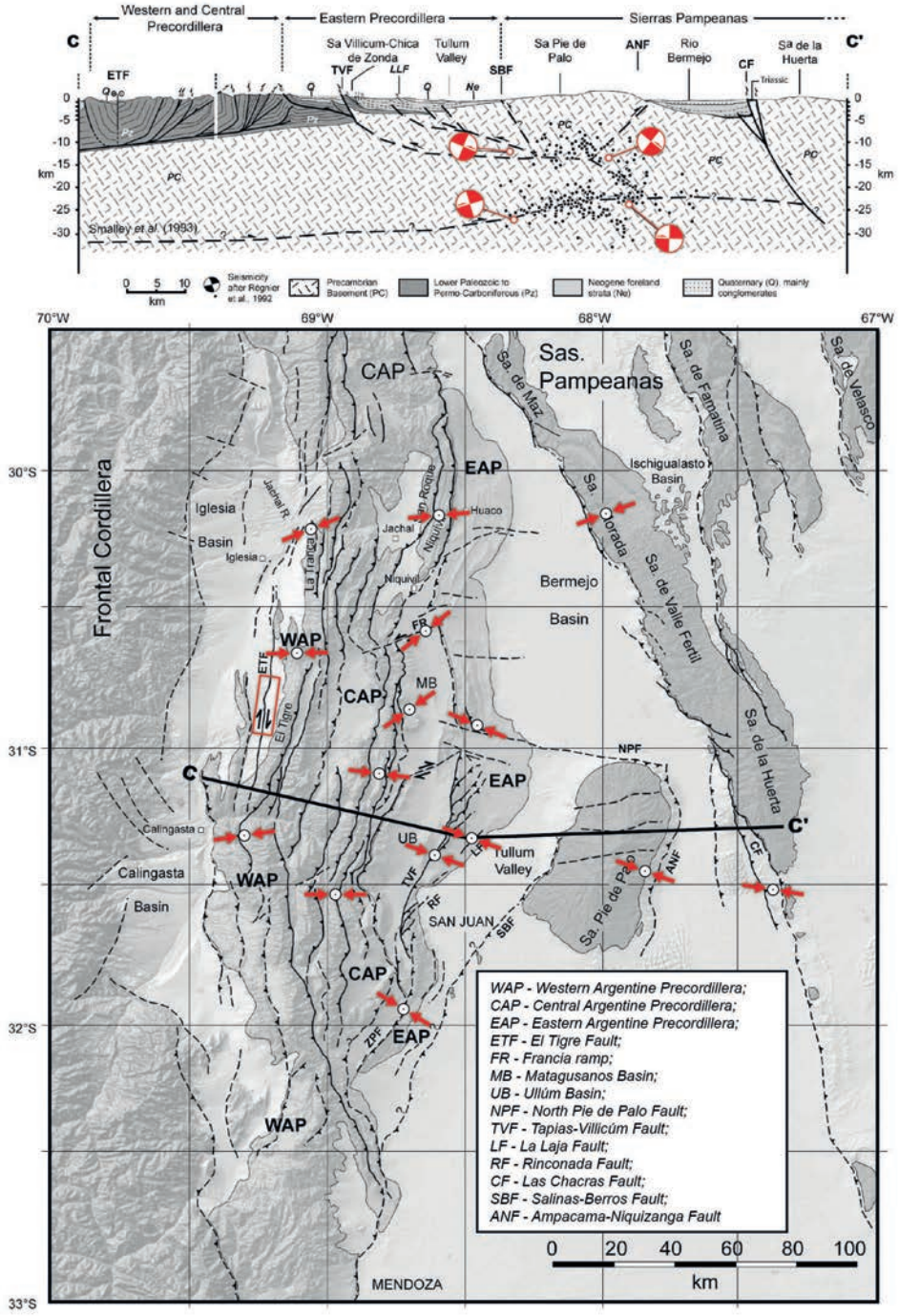

Fig. 22 - Shaded relief map of the Argentine Precordillera and western Sierras Pampeanas showing main structural sub-provinces and major regional structures (dotted lines refer to either inferred or buried faults). Arrows show compressional directions from inversion results of fault kinematic data (Siame et al. 2005). (top) Schematic regional cross-section (CC′) at about 31°30′S with seismicity after Régnier et al. (1992).

of thrusting and strike-slip faulting and superposed basin-filling and excavation episodes.

Geodynamic background

The flat subduction associated with the region of the Precordillera and the Sierras Pampeanas has been inferred to be closely linked to the subduction of the Juan Fernández Ridge, which, because of a "dog-leg" shape in its now subducted trace, moved southward along the South American plate margin from 22 to 10 Ma. However, since 10 Ma the segment entering the trench is nearly parallel to the convergence direction, resulting in a stable configuration since then (Yañez et al., 2002). The link between ridge subduction and the flat geometry appears to be supported by anomalously high frequency of seismicity in the subducted plate aligned with the ridge (Pardo et al., 2002; Gans et al., 2011). Progressive enrichment of arc magmatic rocks indicates that the main phase of shallowing of the subducted plate occurred between 10 and 5 Ma (Kay & Abbruzzi, 1996), in broad agreement with the history of subduction of the Juan Fernández Ridge. Seafloor magnetic lineations, global plate circuits, and GPS geodesy has revealed that the convergence rate at the Chilean plate boundary has decreased by a factor of 2 in the past 15 m.y. (Pardo-Casas & Molnar, 1987; Somoza, 1998; Angermann et al., 1999; Kendrick et al., 2003). Currently, convergence is ~63 mm/yr toward 079.5° at the latitude of the Precordillera. This convergence produces GPS measurable displacements of ~10 mm/yr with respect to stable South America in the central Precordillera, which is thought to be due to elastic deformation from a combination of locking of the interplate subduction zone and locking of the Precordillera décollement (Brooks et al., 2003).

Tectonic and structural setting

The Precordillera thrust belt is built on a foundation of a Paleozoic terrane, Cuyania, accreted to South America prior to the start of the Jurassic to present Andean orogeny (Ramos et al., 1986, 2002; Ramos, 2008). The central part of the Precordillera

has a layered sequence of Cambrian to Permian strata dominated by the Cambrian–Ordovician San Juan Limestone found at the base of many of the thrust plates. The remainder of the succession is composed of siliciclastic rocks. Several low-angle unconformities within the Paleozoic section occur throughout the belt, and pre-Andean deformation becomes increasingly important to the west. In the westernmost part of the Precordillera, the Ordovician changes facies to slope and basinal flysch with pillow basalts and ultramafic rocks that signal the allochthonous boundary between the Cuyania and Chilenia terranes (Ramos et al., 1986). South of ~31°S, the Precordillera is influenced by the location of Triassic grabens (Ramos & Kay, 1991). To the east , the eastern sector of the Precordillera is composed of thick-skinned, west-verging structures. These structures are akin to the neighboring Sierras Pampeanas (Ortíz & Zambrano, 1981; Zapata & Allmendinger, 1996b). Deep crustal seismicity beneath the eastern Precordillera confirms its thick-skinned nature (Smalley et al., 1993). To the west, the Iglesia Basin (Fig. 22) has several structures with significant strike-slip components, including the well-known El Tigre fault (Bastías & Bastías, 1987; Siame et al., 1997, 2002) and local features visible on seismic reflection data that resemble flower structures (Alvarez-Marrón et al., 2006). However, strike-slip faulting is not significant farther east. Importantly, thrust timing in the Precordillera established by Jordan et al. (1993, 2001) shows that the Precordillera thrust belt initiated between 21 and 19 Ma with progressive eastward migration of the thrust front through time.

The Precordillera comprises four structural regions (Fig. 22):

1) Villlicum-Zonda-Pedernal (eastern Precordillera). This part of the range extends along a NNE strike for >200 km. Thrusts dip to the east and probably involve basement units. Principal exposed units are Cambrian/Lower Ordovician in age.
2) Matagusanos Valley (intermontane Ullum-Zonda Valley). This valley is bounded on the east by the west-verging Zonda thrust and the easternmost, east-verging thrust of the central Precordillera on the west. The valley hosts approximately 6 km of Cenozoic strata that overlie Cambrian-Ordovician limestones. To the north the west-dipping Precordillera thrusts encounter east-dipping basement thrusts of the Sierra Pampeanas.
3) Central thrust region (central Precordillera). Thrust faults in the central region dip to the west and involve Ordovician to Carboniferous strata. Miocene volcanic and sedimentary rocks are also present and deformed, and help to constrain the age of the thrusting.
4) Western thrust region (western Precordillera). The thrust faults in the western Precordillera generally dip to the west. Lower Paleozoic outcrops are dominated by deeper water facies (shales). Permian and Triassic units are also involved in the deformation. Pillow lavas and other volcanic rocks occur in the Paleozoic sequence.

Geology of the Calingasta - Iglesia Basin

The Iglesia Basin developed between the Frontal Cordillera (western margin) and the Precordillera thin-skinned thrust belt (eastern margin). Translated passively on top of the westernmost ("Las Trancas") thrust sheet (see below), the Iglesia Basin is classified as the wedge-top component to the more extensive Bermejo foredeep depozone (Fig. 22) preserved on the eastern side of the Precordillera (Allmendinger et al. 1990). Interpretation of basin-scale 2D seismic profiles suggests the presence of at least eleven

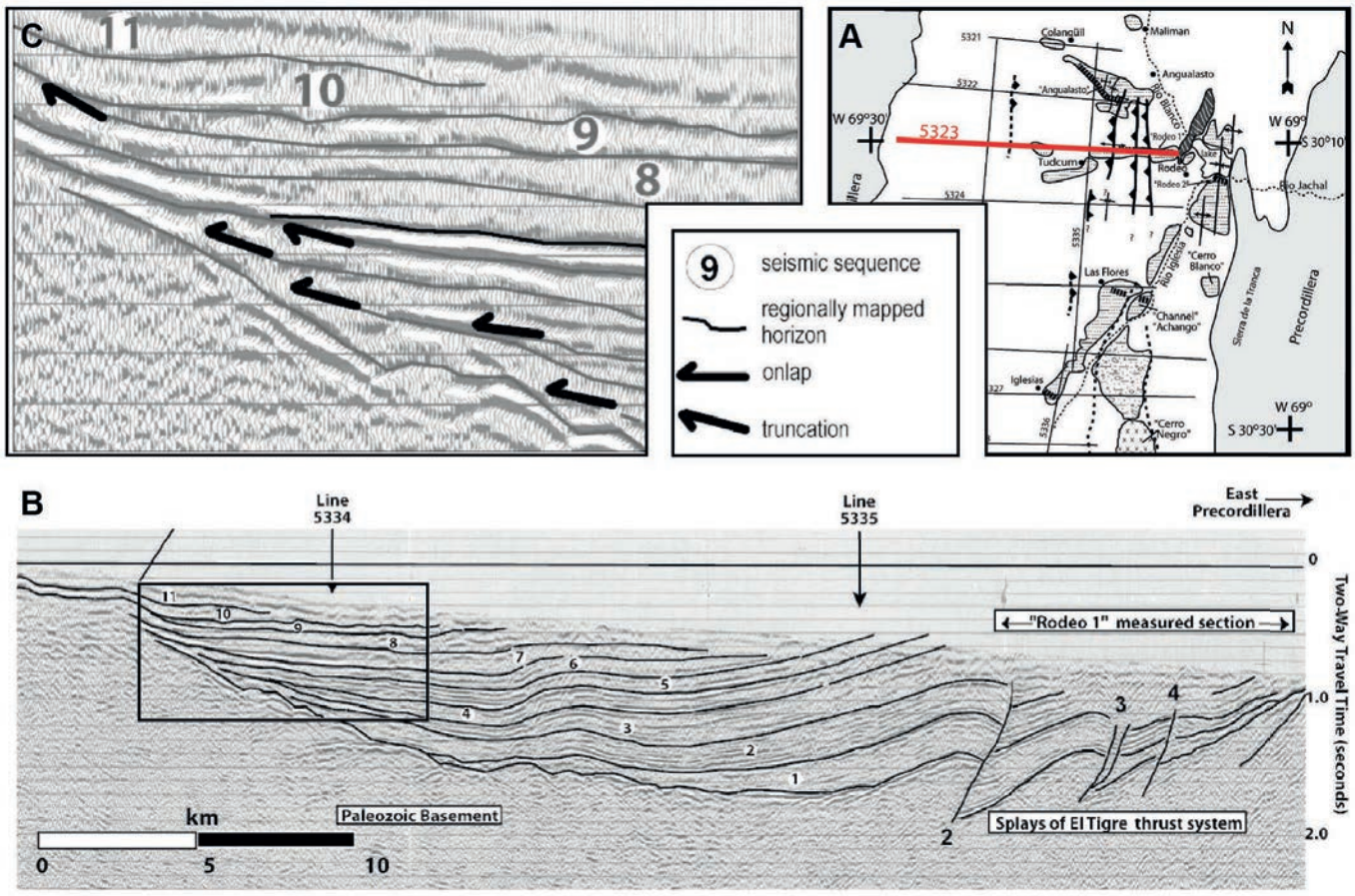

Fig. 23 - E-W reflection seismic profile immediately N of Rodeo (see inset, line 5323) depicting the nature of seismic sequence boundaries and intrabasinal thrusting in the Tertiary Iglesia basin fill. Numbers depict sequences referred to below (Ruskin & Jordan, 2007).

stratigraphic sequences defined by reflector geometries (onlap, toplap, and truncation) within 3.5 km thickness of the mainly fluvial Mio–Pliocene Iglesia Group (Beer et al. 1990; Jordan et al., 1994).

Because the eastern half of the basin fill is gently inclined, the seismic sequences identified by Beer et al. (1990) are exposed as surface outcrops (Fig. 23), permitting radiometric and magnetostratigraphic dating of surface strata to constrain the ages of the seismic sequences. To the W of the town of Rodeo the full duration of sequence deposition was approximately between 20.2 to 4.3 Ma (Jordan et al. 1997). Overall, the sequence constitutes a terrestrial fining-upward succession punctuated by depositional hiatuses of varied outcrop expression.

Overall basin geometry, a north-trending lens reaching 3.5 km in the basin center, was controlled by vertical motions on both tectonically controlled margins as well as out-of-sequence intrabasinal thrusting. It has been suggested that the intra-basinal deformation is dominated by blind thrust faults related to the El Tigre fault system (26°–36°S, 69°10'W; Figs 22 and 24), which offset the strata at depth and divide the basin into at least six north-trending structural sub-basins. The stratigraphic sequences are brought to surface levels by fault-propagation folds, some exhibiting growth-strata relations in the subsurface. The prevalence of folds over faults facilitates tracing units among discontinuous outcrops and from seismic to outcrop. The basin broadened (in east to west dimension) during deposition of the lower seven sequences, followed by restriction of the youngest four sequences to the westernmost structural sub-basin. Some sequence boundaries correspond to enhanced rotation along their western margin, associated with Tertiary uplift of the Frontal Cordillera. Most exposures are confined to longitudinal belts parallel to the structural trend and in axial positions, although well-exposed sections have also been measured and dated along the eastern margin.

Stop 3.2 El Tigre fault (30°52'13.33"S, 69°13'21.66"W) (Fig. 24)

This stop coincides with the intercept between the Provincial Road 425 and the NNE-striking El Tigre Fault. The area coincides with a stepover between two fault strands and the formation of sag ponds (Fig. 24).

The El Tigre Fault is a 120-km-long right-lateral strike-slip fault in the Calingasta-Iglesia Valley, which comprises at least seven rupture segments that terminate in restraining and releasing stepovers; the trace of the fault manifests itself by numerous geomorphic features (alluvial-fan and stream offsets, pressure ridges, sag ponds) and surface disruptions, which provides unambiguous evidence for Quaternary tectonic activity along this structure (Siame et al. 1997; Costa et al. 2000). The El Tigre Fault geometry and segmentation are closely coupled with the overall trend of the Precordillera. For example, slight variations in strike of the different sectors of the Precordillera are parallel to the El Tigre Fault geometry and its discontinuities (Siame et al. 1997): the southern termination of the El Tigre Fault coincides with the Precordillera where it bends from N160°E to N10°E in the vicinity of the Río San Juan. In the north, the El Tigre Fault steps westward and forms a horsetail-termination, which again coincides with another change in orientation of the Precordillera. Siame et al. (1997) therefore suggested that the El Tigre Fault is a crustal-scale fault, which is intimately related to the structures of the Precordillera fold-and-thrust belt. This interpretation is supported by the intra-basinal thrusts in the Rodeo area in the northern part of the valley, where E-verging thrusts in the Calingasta-Iglesia piggy-back basin have been interpreted to be rooted in the El Tigre fault plane (Beer et al., 1990). Thus, the Precordillera appears to be a transpressive system and the kinematics of the El Tigre Fault is compatible with a

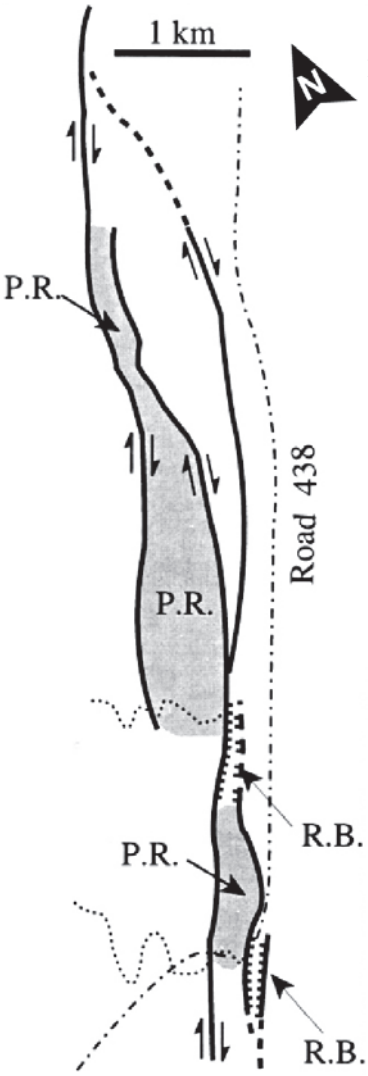

Fig. 24 - Schematic interpretation of the El Tigre Fault near our stop showing a complex stopover area with alternating releasing and restraining areas respectively expressed by releasing basins or sag ponds (R.B.) and pressure ridges (P.R.). From Siame et al. (1997). For orientation see Fig. 22.

system of partitioned deformation comprised of a dextral strike-slip component, while the thrusts in the Precordillera and the adjacent reverse faults of the Sierras Pampeanas should accommodate N110°E-oriented shortening (Fig. 22). This direction corresponds to the orientation of the σ_1-axes computed from both focal mechanism (present-day) and fault kinematic (geologic) datasets from the Precordillera and the westernmost Sierras Pampeanas (Siame et al., 2006).

Especially the southern sector of the fault is geomorphically very well expressed due to the offset of extensive alluvial fan levels that are younger than 0.7 Ma (Siame et al., 1997; Fazzito et al., 2013). Here, the fault trace is also characterized by an east-facing steep slope, generally flanked by sag ponds on the eastern foot of the scarp, while beheaded streams characterize the sectors to the west of the fault (see on Page 25). These geomorphic markers provide good evidence for right-lateral displacements, with a maximum offset of 260 ± 20 m accrued during the Late Quaternary (Siame et al., 2006). Cosmic ray exposure dating of the abandoned fan surfaces allowed constraining a horizontal slip-rate for the El Tigre Fault of about 1 mm/yr. Along the central segment of the El Tigre Fault, a beheaded series of alluvial fans is uplifted by pressure ridges formed within local fault strands. Cosmic ray exposure dating of these alluvial surfaces yielded a local vertical slip rate on the order of 0.3 mm/yr. The vertical and horizontal slip-rates estimated at roughly 0.3 and 1.0 mm/yr, respectively, yield a reconstructed slip-rake of about 17° for the El Tigre Fault, similar to the fault-slip vector observed in a trench on the fault plane (fault plane azimuth: N17°E, dip: 78°E, striae pitch: 14°S).

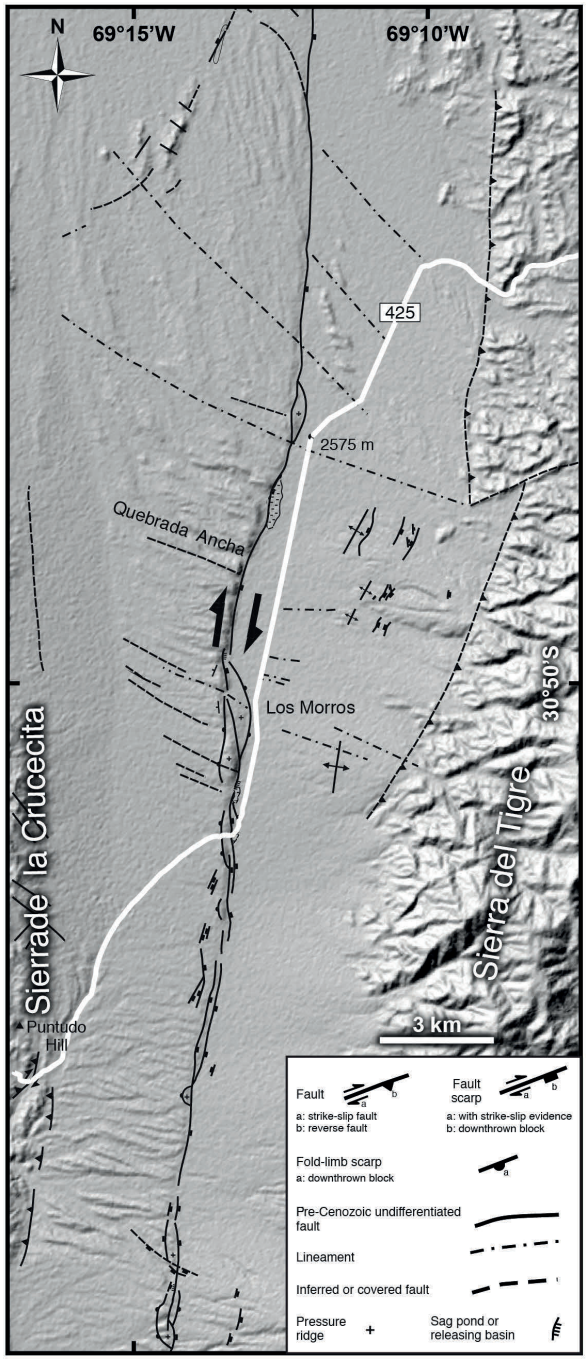

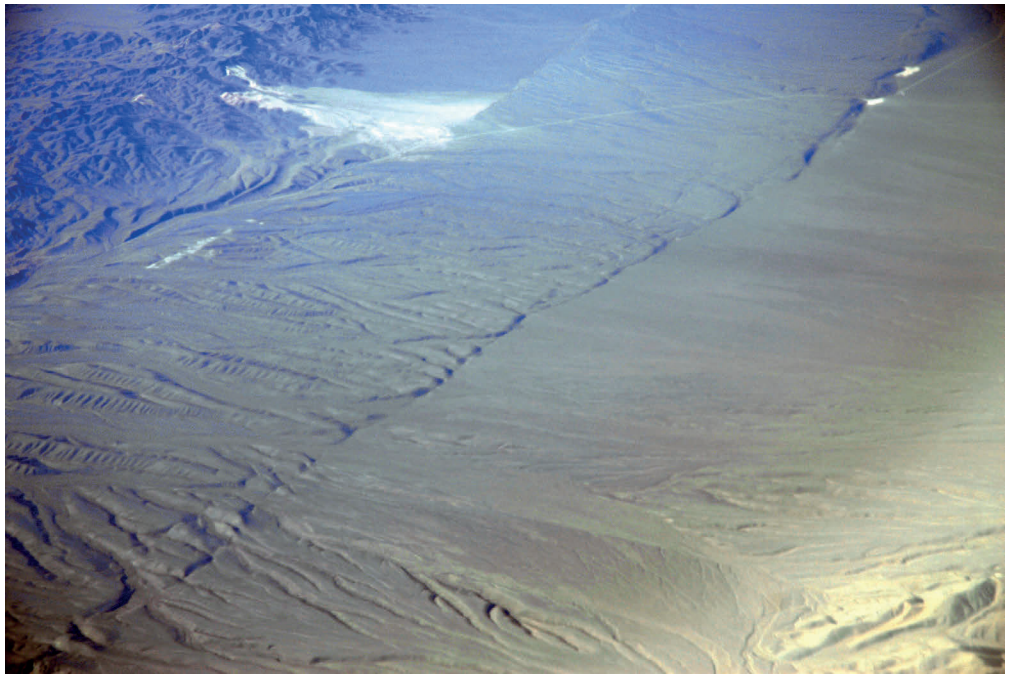

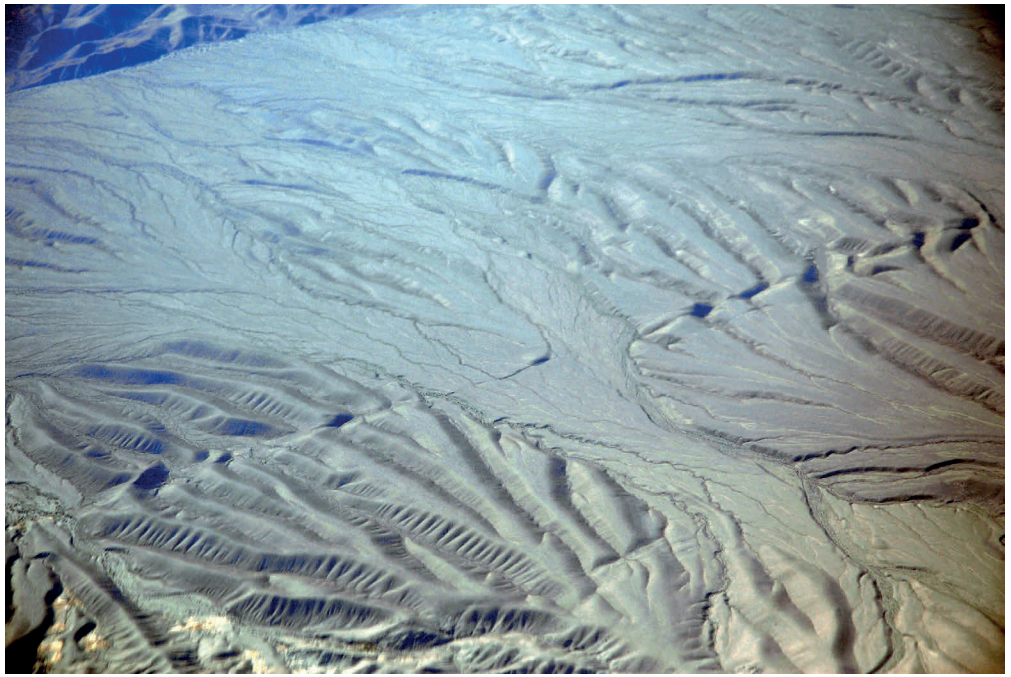

Plate 1 - (Left) Shaded relief map and superposed mayor structures of the El Tigre Fault area (after Fazzito et al., 2013). (Right) Areal photographs from the same region looking NNW. Note the sense of slip visible by offset alluvial fans and streams (photographs courtesy of Robin Lacassin, 2008). While the upper photograph shows the junction of the road with the fault (upper right), the lower photograph is from an area slightly off the map to the south.

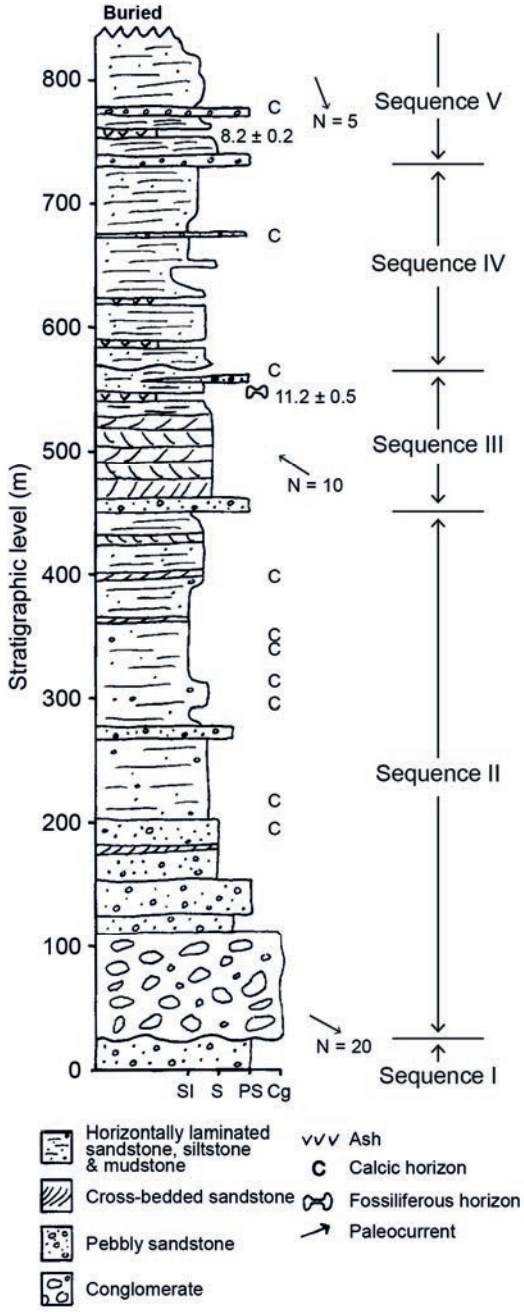

Fig. 25 - Stratigraphic section NW of Rodeo. Paleocurrent measurements are from imbricated clasts, sandstones foresets, and flute marks: Number of measurements indicated (N). Si, siltstone; S, sandstone; PS, pebbly sandstone; Cg, conglomerate (Beer et al., 1990).

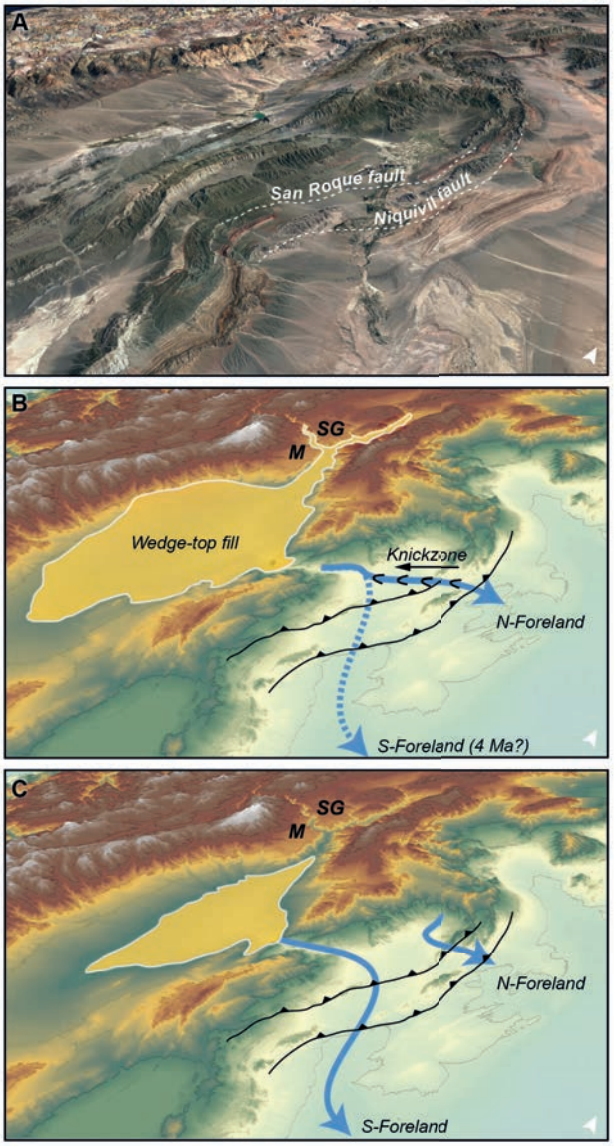

Fig. 26 - (A) Oblique view of the northern Iglesia Valley with approximate location of the San Roque and Niquivil faults. (B,C) Conceptual model for wedge-top evolution in the northern Iglesia Valley subsequent to deformation and incision of the Iglesia Group. Blue arrows show hypothesized flow direction of major drainages. The San Roque and Niquivil thrusts were active during aggradation in the Iglesia Basin following internal basin deformation and erosion. The Médano (M) and San Guillermo (SG) surface remnants are indicated in the NW sector of the DEM (Val et al., 2016).

Stop 3.3 Ordovician pillow lavas (30.214°S; 69.0626°W)

The Ordovician slope facies are represented here by the Alcaparrosa Formation. This Ordovician unit corresponds to slope and bathyal facies of the Early Paleozoic platform. These rocks host a series of olistoliths of several-hundred meters of Cambrian and Early Ordovician rocks. The olistoliths are mainly limestone blocks that were deposited by gravitational sliding from the carbonate platform located eastward. There are many of them along the platform edge of the Early Paleozoic platform.

Day 4.

Stop 4.1 (30°10'51.02"S, 69° 7'58.56"W).

To the NW of the town of Rodeo there is an outcrop of five depositional sequence members of the Iglesia group that are exposed due to intra-basinal faulting (Fig. 25). All units dip westward. The most detailed account of the sedimentological evolution of the units exposed in the greater Rodeo region has been published by Alonso (2011) and the reader is referred to that thorough study.

Here, we follow the simplified stratigraphic scheme and nomenclature developed by Beer et al. (1990), who linked surface outcrops of Tertiary units to seismic-stratigraphic units. Sequence I constitutes a pink, pebbly sandstone composed of porphyritic volcanic clasts, probably derived from the Frontal Cordillera. The basal unit of Sequence II is a dark-green boulder conglomerate, with clasts occasionally 1 m in diameter. The clasts are derived from Devonian and Carboniferous silt- and sandstones that are exposed in the Cordillera Frontal and in the Precordillera. However, clast imbrications suggest a transport from west to east. Transport from the Frontal Cordillera is furthermore supported by the

Fig. 27 - Satellite image of the Precordillera at the latitude of Rodeo and Jáchal (Google Earth).

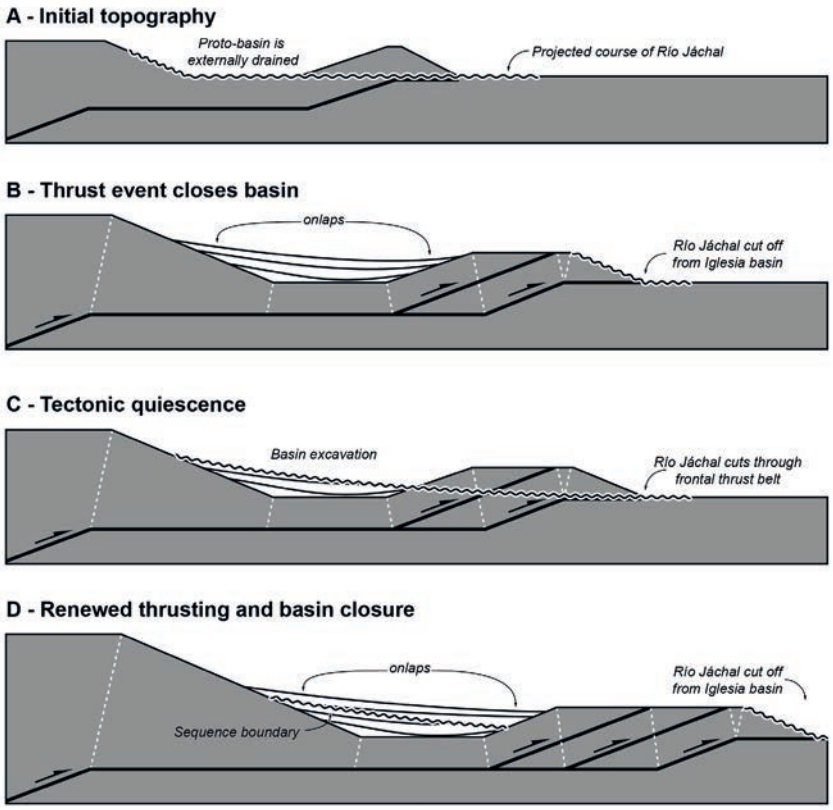

Fig. 28 - Possible scenario for sequence of events that caused severed, and ultimately internal drainage conditions in the Calingasta-Iglesia Basin due to protracted thrusting (A-B), followed by erosion and renewed aggradation during the deposition of the Iglesia Group (Beer et al., 1990). The youngest events after the deposition of the Iglesia Group are not shown.

presence of granite boulders. The basal boulder conglomerate, which is interpreted as a coarse alluvial-fan facies, is superseded by a sandy, well-sorted and partly cross-bedded facies assemblage. The former depositional environment for this sequence is associated with a sand-flat setting in the peripheral sectors of an alluvial fan. This fining-upward trend is interpreted to result from a westward migration of facies. Above this unit sequences III to V similarly document a continued fining-upward trend with evidence for pedogenic carbonate nodules. The deposition of these sequences is associated with an onlap onto Paleozoic basement, documenting the gradual filling of the Iglesia wedge-top basin. The younger sequences mainly comprise muddy facies assemblages with interbedded mudstones and fine sandstone. Lithologies include claystones and siltstones, fine-grained sandstones and occasional gypsum layers. Desiccation cracks and convolute bedding occur locally. These units are linked to deposition in an ephemeral lake environment that had developed as a result of severed drainage conditions and ultimately fluvial isolation.

Stop 4.2, Angualasto (30° 3'2.73"S, 69°10'11.69"W).

From here the northern termination of the Iglesia Basin is visible. The wedge-top basin narrows to the north and exhibits a tall-standing, more than 100-m-thick, tan to reddish coarse conglomeratic fill unit that covers all previously deposited, deformed and eroded Neogene strata of the Iglesia group. This boulder conglomerate deposit documents that subsequent to the first filling of the wedge-top basin with the Iglesia group headward erosion or downcutting of rivers at the eastern basin margin must have re-established fluvial connectivity with the foreland, which resulted in partial excavation and removal of the wedge-top sediments. Due to renewed severing of fluvial connectivity well after 4 Ma, however, this erosional episode was followed by renewed deposition of the boulder conglomerate. This second filling event may have been associated with thrusting in the Precordillera wedge during the Pliocene (Figs 26 & 28). Today, the Médano and San Guillermo conglomeratic-fill surfaces represent the vestiges of this Plio-Pleistocene(?) fill event, which in turn was followed by renewed incision during the re-establishment of fluvial connectivity with the foreland (Val et al., 2016). This sequence of events is illustrated in Figs 26 and 28.

In conclusion, the stratal geometries, fault relationships and sediment provenance indicate that the Iglesia Basin during the time of deposition of the Iglesia Group was a non-marine wedge-top basin with internal drainage conditions. The basin was bounded by the Frontal Cordillera and the evolving Precordillera thrust belt. Severed drainage conditions resulted from thrusting activity in the Precordillera and the inability of fluvial systems to downcut and maintain fluvial connectivity with the foreland. In a regional context the Iglesia basin has been passively transported above a horizontal decollement that links mid-crustal deformation beneath the Frontal Cordillera with thrusts emerging in the Precordillera fold belt (Fig. 28, A-D). While several unconformities exist within the Iglesia Group, a major unconformity was developed after the deposition of the Iglesia sequence, when these units were folded, faulted and incised, and subsequently covered by the temporal and spatial equivalents of the Médanos and San Guillermo boulder conglomerates. In places, these units were also deformed by renewed tectonic activity and incised by headward erosion of the Rio Jáchal.

Geology of the Rio Jáchal transect across the Precordillera thrust belt

The main thin-skinned thrusts of the Precordillera along the Río Jáchal are, from east to west (foreland to hinterland): the Niquivil, San Roque, Blanquitos, Blanco, Caracol East, Caracol West, and Tranca thrust plates (Fig. 29).

Stop 4.3 Niquivil thrust (30°24'11.97"S, 68°40'32.91"W).

The Niquivil thrust plate constitutes the leading edge of the thin-skinned belt at these latitudes and has been active for about the past 5 m.y. (Jordan et al., 1993, 2001). The thrust's ongoing ac-

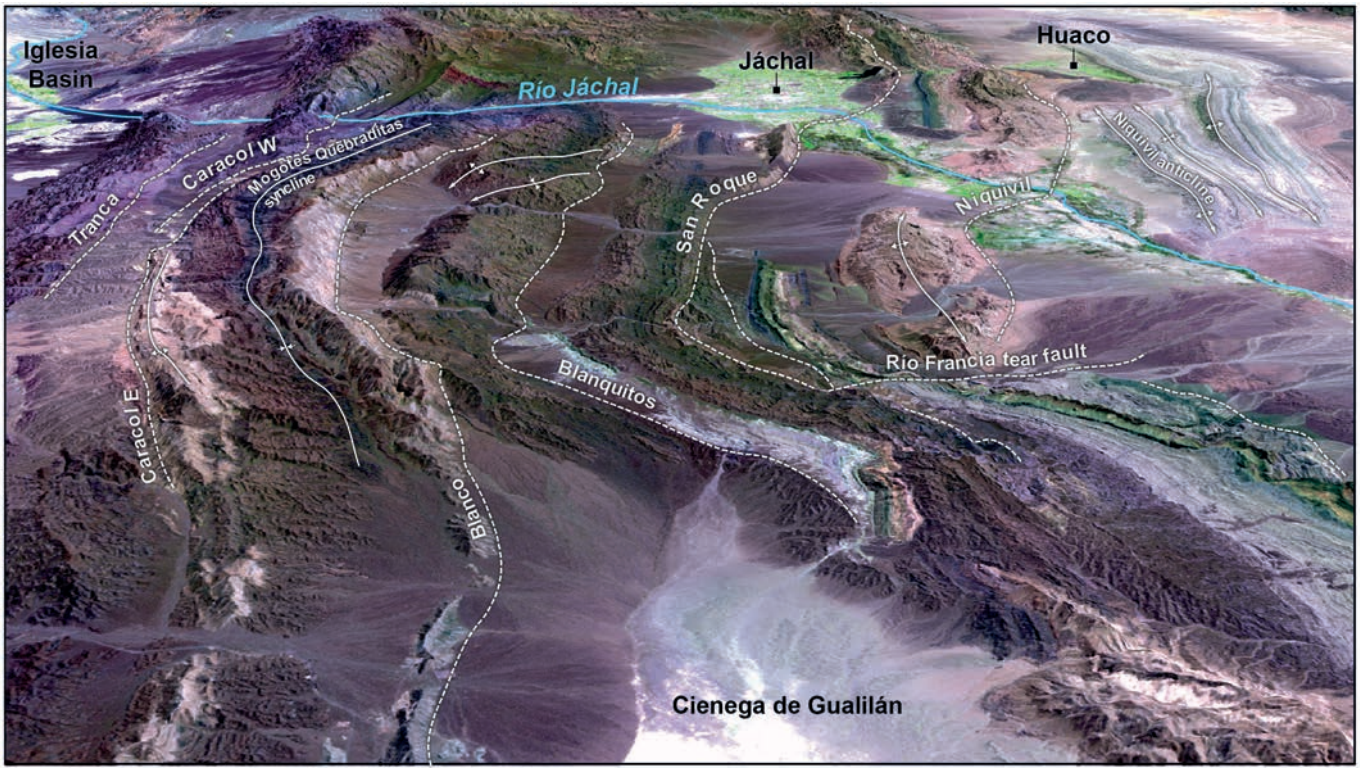

Fig. 29 - Digital elevation model of the Jachal transect visualized as a shaded relief block diagram with the Landsat enhanced thematic mapper image draped over it, looking north. Main structures of the Precordillera are shown in white.

tivity is demonstrated by a 10 to 15-m-high fault scarp where its frontal trace is crossed by the Río Jáchal at the village of Niquivil (Figs 27 and 29). To the north, the thrust dies out into the Cuesta de Huaco fault-propagation fold and to the south it terminates at the Río Francia tear fault–transfer zone. Zapata & Allmendinger (1996b) reported that the Niquivil thrust plate is cut and deformed by the thick-skinned fault coring the Niquivil anticline that is just to the east, locally reversing the vergence of the Cuesta de Huaco anticline. The base of the Niquivil thrust plate contains the thickest exposures of the Ordovician San Juan Limestone of any thrust plate in this segment of the Precordillera. The thickness of the remainder of the Paleozoic section is highly variable: at Cuesta de Huaco, no Silurian or Devonian strata are present and the Carboniferous and Permian are unconformable on the Ordovician. Due east of the town of Jáchal, thin remnants of Silurian Los Espejos and Devonian Talacasto Formations appear beneath the late Paleozoic unconformity. At the south end of the Niquivil plate, just north of the Río Francia , Silurian strata are present but the Devonian section is missing. As described in the following, the Niquivil thrust is the only one crossed by YPF seismic lines (Allmendinger et al., 1990; Zapata & Allmendinger, 1996b). Although the fault plane is not exposed anywhere, interpretation of the YPF seismic lines indicates that the 35° west-dipping thrust places Ordovician limestone over Miocene sandstone, with a stratigraphic throw of 12 to 15 km.

Stop 4.4 San Roque thrust (30°15'46.78"S, 68°41'34.55"W).

The thrust trace of the San Roque plate is at least 120 km long; it probably extends from the Guandacol area in the north (outside the map area) to the Cienega de Gualilán in the south. It was active from 10 or 9 Ma to 3 or 2 Ma (Jordan et al., 1993, 2001). The fault has a significant lateral ramp just west of the village of Niquivil: to the north, the fault is within the San Juan Limestone but to the south it steps upsection to within the Silurian Los Espejos Formation. Both north and south of the hanging-wall lateral ramp, the footwall strata are Miocene sandstones. There is a duplex at the base of the thrust plate, 10 km south of the lateral ramp, and a thin sliver of Ordovician limestone is present at the base of the plate. The San Roque fault and its hanging wall experience an 80° bend and appear to have ~200 m of separation across the Río Francia tear fault, which dies out into the San Roque plate. This suggests that at least some movement on the Niquivil thrust postdates the San Roque thrust. The San Roque plate contains a thinner section of San Juan Limestone than the Niquivil plate. North of the Río Jáchal, the rest of the lower Paleozoic section is missing and the upper Paleozoic directly overlies the limestone. To the south, a thicker Silurian and Devonian section overlie the limestone, with a thin upper Paleozoic sequence unconformably overlying the Devonian. On the western flank of the San Roque range proper, small thrusts and tight folds thicken the Silurian and Devonian section with minor involvement of the Carboniferous. Folding of the Devonian section is also prevalent farther south.

Stop 4.5 Blanquitos thrust (30°11'51.36"S, 68°49'7.55"W).

The Blanquitos plate records a brief period of activity between 11.5 and 9.5 Ma (Jordan et al., 1993, 2001). Its surface trace is <50-km-long and along most of that length Devonian strata are at the base of the upper plate. At 30.37°S, there is a lateral ramp and the thrust cuts downsection northward to include a thin sliver of San Juan Limestone at the base of the upper plate, with Miocene sandstone in the lower plate. The Cerro Bayo anticline generated by this lateral ramp propagates across the entire upper plate and appears to plunge beneath the Blanco thrust to the west. Less than 10 km north from where the limestone first appears at the base of the upper plate, it disappears in a north-plunging anticline. South of the lateral ramp, 1800–2700 m of Devonian Punta Negra Formation are overlain directly by a thin sequence of Cenozoic foreland basin strata, including a distinctive eolian cross-bedded sandstone, which overlies a redbed with a tuff dated as 21.6 ± 0.8 Ma, found through much of the region (Jordan et al., 1993; Milana,

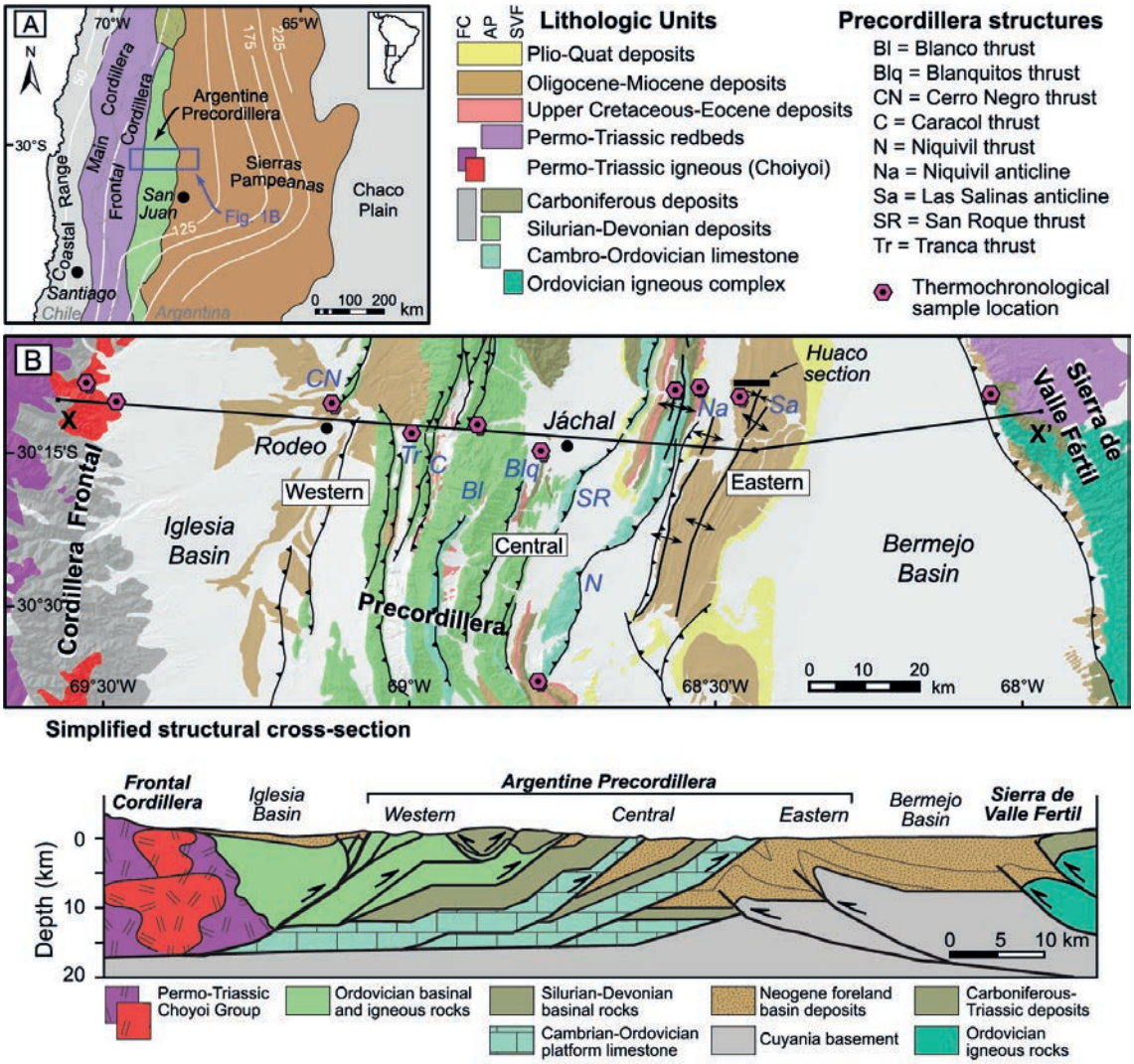

Fig. 30 - (A) Tectonic setting of the Argentine Precordillera and adjacent provinces in the southern Central Andes. White lines denote depth in km to the Wadati-Benioff zone (Cahill & Isacks, 1992). (B) Geologic map of the study area in the Precordillera with Cenozoic thrust faults and thermochronology sample locations. Black bar labeled Huaco section denotes location of detrital geochronology sample suite. Fault nomenclature modified after Jordan et al. (2001). (C) Geology and cross-section. From Fosdick et al. (2015).

1993). To the north of the lateral ramp and Cerro Bayo anticline, the Silurian and Devonian strata form a broad expanse of folds at multiple wavelengths, including outcrop-scale kink folds exposed between Jáchal and Rodeo in the Iglesia Basin.

Stop 4.6 Blanco thrust (30°12'24.41"S, 68°52'8.18"W).

The Blanco thrust was active from 13 to 9 Ma, overlapping activity on the Blanquitos thrust (Jordan et al., 1993, 2001). Although the Blanco thrust dies out at ~30.3°S, it is one of most important thrust faults in the central Precordillera and can be traced south to the Río San Juan for a total length of ~120 km. Throughout most of that trace length, San Juan Limestone is found at the base of the plate. Between the Cienega de Gualilán and the Río Jáchal, the Blanco plate contains a tight syncline in Silurian and Devonian strata. On both limbs of the syncline, dips are steep, ranging from 40° to 80°. It has been suggested that the youngest motion on the Blanco thrust is out of sequence and postdates the tilting of the strata in the Blanquitos plate. At the northern end of the Blanco plate, the Ordovician limestone and overlying Silurian and Devonian sequence are deformed into an overturned fault-propagation fold. The forelimb of this fold is complexly imbricated with the limestone thrust over the Silurian–Devonian, which is in turn thrust over the Cenozoic strata of the Blanco valley. The Blanco fault ramps into the Devonian in the hanging wall and continues for another 8–10 km northward before dying out completely into an anticline separating two large synclines. The exposures of the Silurian and Devonian along the Río Jáchal belong to the combined upper plate of the Blanquitos and Blanco thrusts.

Stop 4.7 Eastern Caracol thrust (30°13'35.08"S, 68°55'52.59"W).

The E-Caracol Thrust tracks the western limb of the Mogotes Quebraditas syncline. On the eastern side of the Caracol Valley, thin, highly deformed slivers of San Juan Limestone crop out along the base of the thrust plate. Farther south in the Cordón del Peñon (see attached geological map) more extensive outcrops of limestone and overlying Silurian rocks are tightly folded into anti- and synclines with W-vergence. The upper plate of E-Caracol thrust is also the upper plate of the Blanco thrust, and the tight syncline between them suggests that E-Caracol is a back thrust off the Blanco thrust.

Stop 4.8 La Tranca valley I (30°12'50.68"S, 69° 0'45.51"W).

Undeformed Holocene lacustrine facies in the footwall of the Tranca thrust. In the immediate vicinity of the Trancas fault and the road to Jachal there are up to 30-m-thick fluvio-lacustrine unites that are unconformable with respect to all other units in

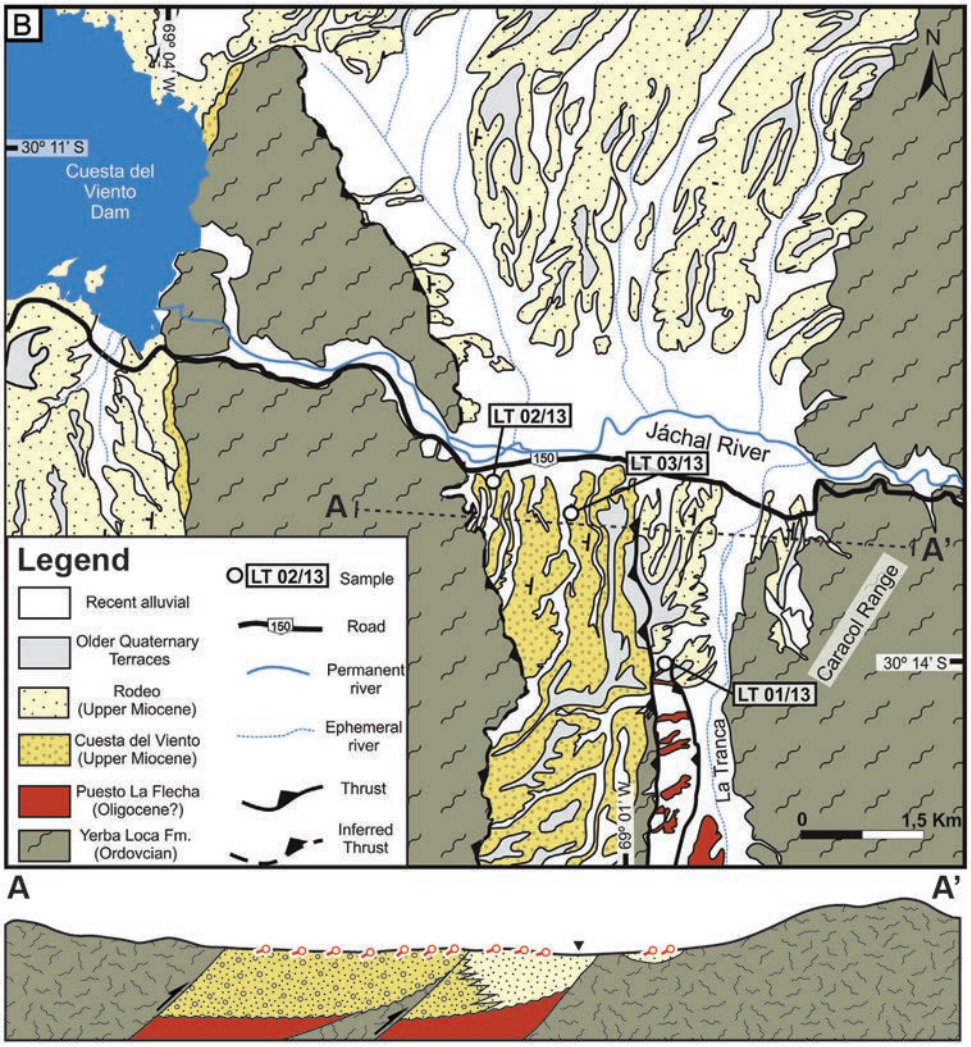

Fig. 31 - Detailed geologic map and cross section of the La Tranca valley. Radiometric dating of detrital zircons (U-Pb) for LT02/13 and LT03/13 revealed maximum depositional ages of 8.3 ± 0.9 Ma and 11.4 ± 0.5 Ma, respectively. From Suriano et al. (2017).

the area. The greyish fluvio-lacustrine strata document an episode of temporary impoundment of the Rio Jáchal. 14C-dated layers at the base and toward the top provide an age of 8930 ± 50 BP and 6,497 ± 45 BP, respectively (Colombo et al., 2005). Unlike other regions in the E Andes with landslide-related lacustrine sediments, the lacustrine units in the Tranca valley have been interpreted to be related to increased sedimentation and progradation of alluvial-fan units that ultimately caused a temporary lake.

Stop 4.9 La Tranca valley II - Western Caracol thrust

The W-Caracol (30°13'1.70"S, 68°58'4.11"W) and Tranca thrusts (30°12'55.04"S, 69° 2'6.09"W) farther west appear to be a single en échelon system that carries the western deep-water facies of the Ordovician in its upper plate. The W-Caracol thrust dies out southward and the Tranca thrust dies out northward at the Río Jáchal with an overlap of ~22 km immediately S of the river. Along the Río Jáchal, a few highly deformed slivers of limestone are imbricated in the Yerba Loca Fm., but near the Cuesta del Viento (see attached geological map) the Ordovician strata are tightly deformed into pre-Andean west-verging overturned folds associated with mafic and ultramafic igneous rocks. The Tranca thrust had activity prior to 19 Ma, and the W-Caracol possibly had activity in the same time frame. Both members of the en échelon system display younger deformation; in the case of the Tranca thrust, it is a structure that placed ca. 21 Ma redbeds over the Chestnut Conglomerate of Jordan et al. (1993; 2001), and for the W-Caracol thrust, the outcrops near Río Jáchal are thrust over mid-Miocene eolian beds. Thus, initial motion on the Tranca and W-Caracol thrusts, which carry Ordovician Yerba Loca Formation in their upper plates, occurred ~6–7 m.y. earlier than at the other thrusts in this segment of the Precordillera.

Day 5.

Structural setting of the Sierras Pampeanas

The transition between the Precordillera and the Sierras Pampeans broken-foreland basement uplifts between San Juan and Mendoza is probably the most seismically active region in Argentina. Indeed, many small to moderate (M<6.4) and several large (M>6.4) earthquakes have occurred during the last century, most notably the destructive Ms = 7.4, 1944 San Juan earthquake (Alvarado & Beck, 2006) and Mw = 7.4, 1977, Caucete earthquake (Kadinsky-Cade et al., 1985) events. This seismic activity is produced by a number of active crustal faults and may result from the reactivation of suture zones between Paleozoic terranes (Smalley et al., 1993; Alvarado et al., 2005) and other types of anisotropies. From the comparison of both present-day and Neogene-Quaternary deformation structures and fault kinematics, the Andean back-arc of western Argentina can be regarded as a foreland region that accommodates oblique convergence, where deformation is partitioned between strike-slip and thrust faulting, localized along the E-verging, thin-skinned Precordillera and the predominantly W-verging, thick-skinned Sierras Pampeanas basement blocks (Fig. 32), respectively (Siame et al., 2005).

The unifying characteristics of the Sierras Pampeanas province are high-angle reverse fault-bounded mountain blocks that consist of Precambrian to early Paleozoic basement rocks. Separated from each other by tectonic depressions that are filled with Tertiary and Quaternary sediments, the sometimes more than

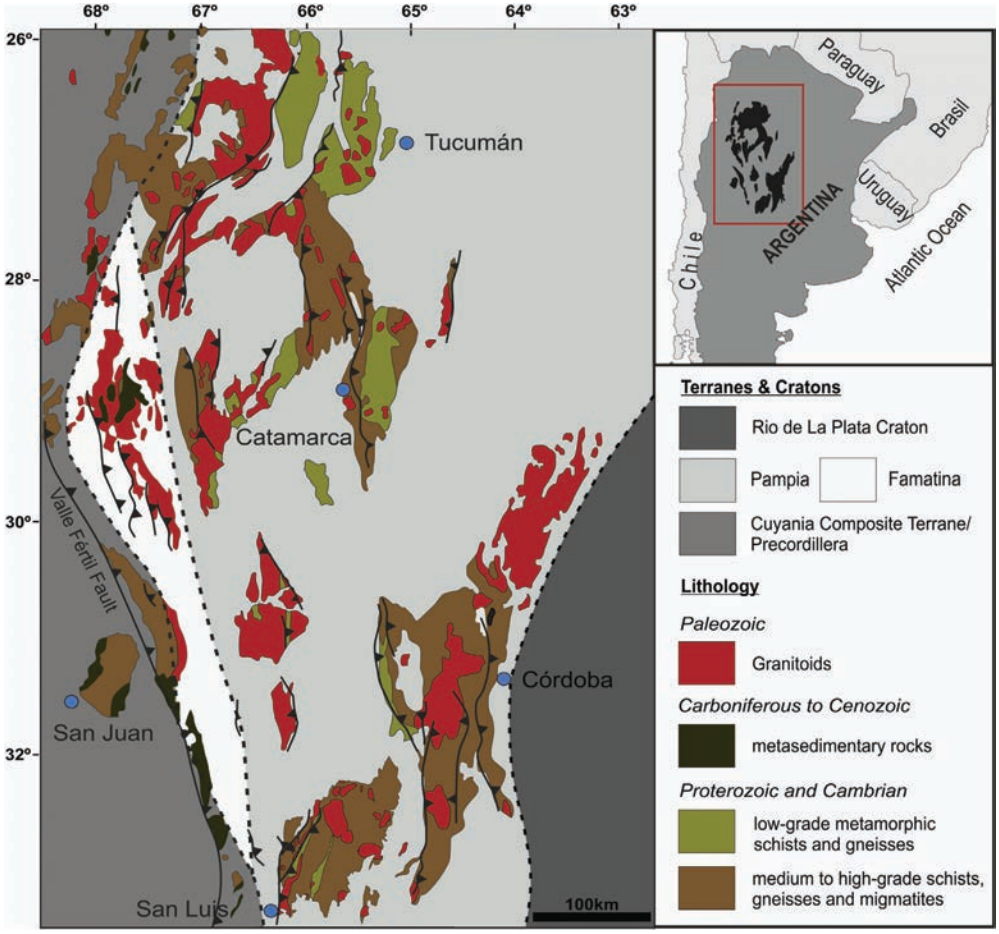

Fig. 32 - Simplified geological map of the Sierras Pampeanas. Dashed lines indicate inferred position of Precambrian to Paleozoic terrane boundaries. Also indicated are the individual Pampean basement-block uplifts and associated bounding faults. Major fault vergence based on González Bonorino (1950) and Jordan & Allmendinger (1986). From Bense et al. (2013).

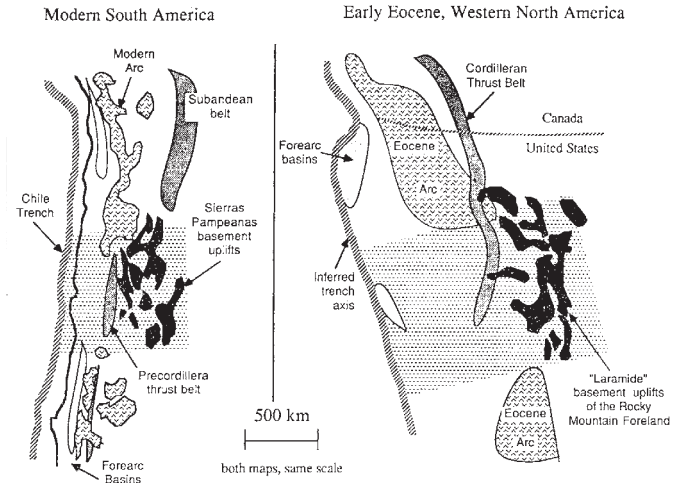

Fig. 33 - Location of Sierras Pampeanas (Rocky Mountain Foreland Ranges) and their setting in a map of active (early Cenozoic) tectonic features of Central Andes (North American Cordillera). The region of flat subduction is shown by dashed pattern; areas to north and south have a steeper dipping subducted Nazca (Farallon) plate beneath them. (Names in parentheses refer to right hand side of diagram.) After Jordan et al. (1983a).

5000-m-high ranges protrude out of the low-relief of the Argentine Pampa and define a 450-km-wide amagmatic belt of Laramide-type uplifts, whose tops or flanks expose a smooth polycyclic peneplain. As such, these ranges are very similar to the Eocene Laramide uplifts of the western US (Fig. 33). Active deformation in the Sierras Pampeanas province is associated with the subduction of the flat-slab segment of the Nazca Plate, which subducts nearly horizontally beneath the South American lithosphere for about 300 km at a depth of approximately 100 km (Jordan et al., 1983; Cahill and Isacks 1992; Smalley et al., 1993). In the area that will be visited by STRATEGY, the flat-slab geometry is attributed to the subduction of the Juan Fernandez Ridge below the South American margin (Pilger 1981), and expressed at the magmatic arc by a change in the geochemistry properties of the Neogene volcanism and a cessation of activity roughly 10 Ma ago (Kay and Abbruzzi 1996). Enhanced plate coupling above a flat-subducting segment has long been suggested to be responsible for the regional Sierras Pampeanas basement uplifts (Jordan et al., 1983, Smalley et al. 1993). Alternatively, thermal weakness of the crust associated with eastward migration of arc magmatism has also been suggested to be responsible for the thick-skinned basement uplifts of the Sierras Pampeanas (Ramos et al., 2002).

The San Juan-Mendoza region constitutes the southwestern sector of the approximately N-S-oriented uplifts of the Sierras Pampeanas morphotectonic province, which spans the region between approximately 27°S and 33°S lat. Most of the Sierras Pampeanas blocks are asymmetric and are uplifted either on their western or eastern sides (e.g. Sierra de Maz, Sierra de Valle Fértil, Sierra de la Huerta), but range-bounding reverse faults also exist on eastern and western flanks of the ranges (Sierra de Aconquija). In other cases, the faults may not surface and the basement blocks host reverse faults that caused basement folding and regional uplift (Sierra Pie de Palo; Sierra de Quílmes). These faults may be rooted in large-scale décollements that are also linked with struc-

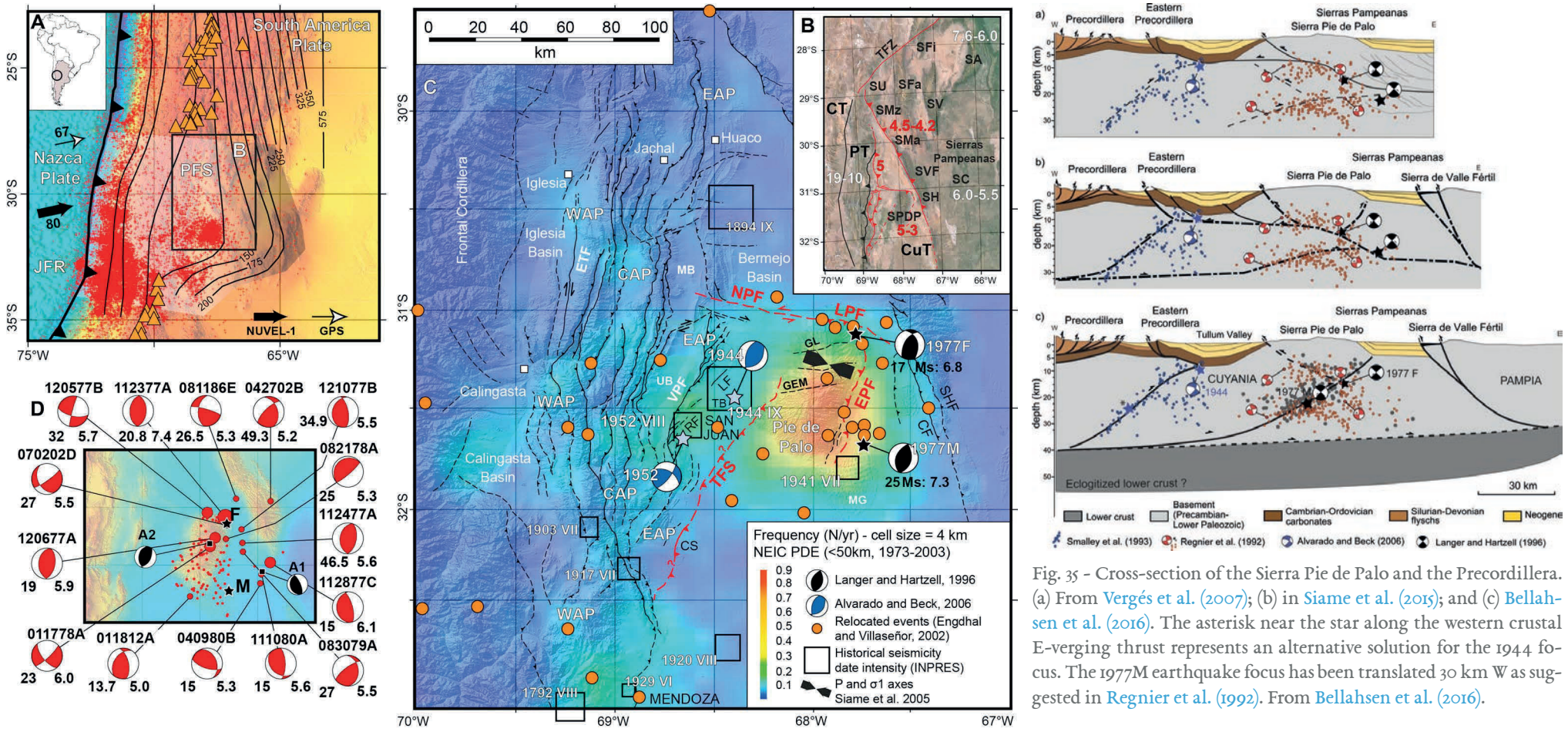

Fig. 35 - Cross-section of the Sierra Pie de Palo and the Precordillera. (a) From Vergés et al. (2007); (b) in Siame et al. (2015); and (c) Bellahsen et al. (2016). The asterisk near the star along the western crustal E-verging thrust represents an alternative solution for the 1944 focus. The 1977M earthquake focus has been translated 30 km W as suggested in Regnier et al. (1992). From Bellahsen et al. (2016).

Fig. 34 - (a) Geodynamic setting of Central Andes at 30°S. Red dots show the earthquake distribution (U.S. Geological Survey, National Earthquake Information Center; Preliminary Determination of Epicenter catalog, 1973 to 2014, depth ≤ 70 km, magnitude ≥ 4.0). Yellow solid triangles correspond to Plio-Quaternary and active volcanoes. Black and white arrows represent the relative convergence of the Nazca and South American Plates following NUVEL-1 [DeMets et al., 1990] and continuous GPS observation [Brooks et al., 2003], respectively. Numbers are given in mm/yr. Isodepth contours of the subducted Nazca Plate are shown after Cahill and Isacks [1992]. (b) Schematic regional structural map locating the Argentine Precordillera (AP) and the western Sierras Pampeanas (SP). White and red numbers (given in Ma) refer to inception of deformation [Jordan et al., 1993; Zapata and Allmendinger, 1996; Ramos et al., 2002]. (c) Structural regional map of AP and SP from SPOT and Landsat image analysis (modified after Siame et al. [2005]). Structures bounding the Sierra Pie de Palo (SPDP) are highlighted in red. Seismicity frequency grid derived from the Preliminary Determination Epicenter catalog (100 × 112, 4 km large cells). Orange solid circles show the epicenter distribution of relocated seismic events [Engdahl and Villasen ̃or, 2002]. Black squares locate historical seismic events [Instituto Nacional de Prevencòn Sísmica (INPRES), 2014]. Light blue stars locate 15 January 1944 (Mw = 7.0) and 11 June 1952 (Mw = 6.8) earthquakes with focal mechanism solutions after Alvarado and Beck [2006]. Black solid stars locate foreshore and main shocks of the Caucete 23 November 1977 (Ms = 7.4) earthquake. (d) Close-up on the seismic activity of the SPDP. Large red solid circles locate the focal mechanism solutions. Lower left number indicates the focal depth (km). Lower right number indicates the Mw value. Red dots correspond to the seismicity recorded by Régnier et al. [1992]. Solid black stars locate the foreshock and the main shock of the 23 November 1977 Caucete earthquake [Langer and Hartzell, 1996]. Black solid squares locate the two main aftershocks [Kadinsky-Cade et al., 1985]. A1 and A2 aftershocks correspond to the Harvard events 112877C and 120677A, respectively. From Siame et al. (2015).

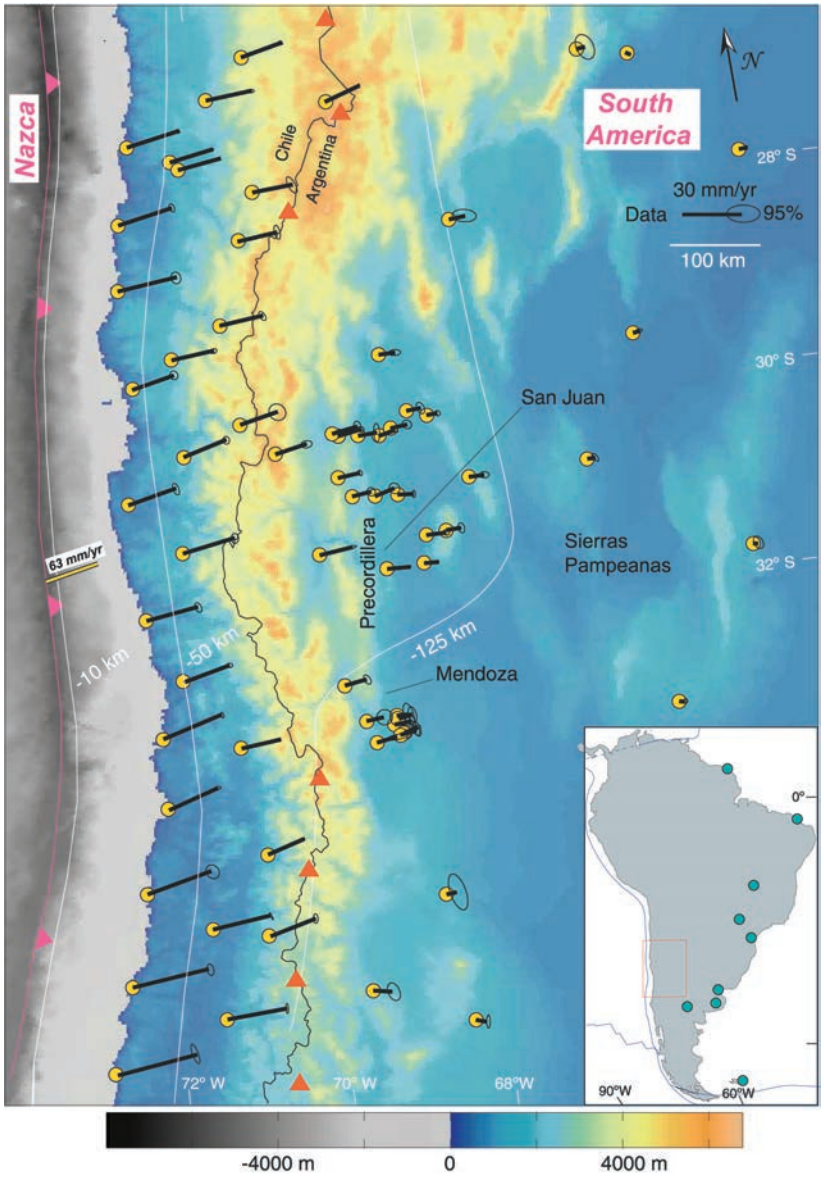

Fig. 36 - W-E GPS velocity changes across the Andes; craton-fixed reference frame exhibits velocities that are generally E-directed. Largest velocities (~35 mm/yr) are nearest the plate boundary and they decrease eastwards towards the craton; back-arc velocity vectors tend to be rotated clockwise with respect to forearc vectors. From Brooks et al. (2003).

tures that surface in other areas (Fig. 22). The region of the Sierra Pie de Palo and areas farther west may belong to such linked structures, where basement faults impinge on the gently dipping thrust faults of the Precordillera (Sierra Villicum – Chica de Zonda); similar structural relationships can be observed in the area affected by the Salinas-Berro Faults between San Juan and Mendoza; Fig. 22).

Stop 5.1 Geology of the Sierra Pie de Palo (31.30363°S, 68.16803°W)

In the broken foreland at about 31°S, the Sierra Pie de Palo appears to play a key role in the partitioning of the Plio-Quaternary deformation in the back-arc. The Sierra Pie de Palo basement range is approximately NNE-oriented, 80-km-long, and 35 to 40-km-wide; it reaches an elevation of 3162 m and constitutes an actively growing basement fold (e.g., Ramos et al., 2002) associated with pronounced seismotectonic activity (Figs 34-35). Evidence for active deformation is found along the eastern and northern flanks of the Sierra Pie de Palo as well as along the western flanks of Sierra de Valle Fértil and Sierra de la Huerta (Costa et al., 2000; Siame et al., 2002; Siame et al. 2005). With an arch-liked shape (Fig. 22), the topography of Sierra Pie de Palo is characterized by steep flanks on the eastern and northern sides and gently inclined western and southern flanks. The surface envelope of Sierra Pie de Palo corresponds to an inherited, Late Paleozoic erosional surface (Carignano et al. 1999) sculpted into Precambrian metamorphic rocks. Geologic evidence indicates that the range was covered by Late Pliocene distal synorogenic deposits derived from the Precordillera (Ramos and Vujovich 2000) and deformation associated with the growth of the range may have started between 5 and 3 Myr (Ramos et al., 2002). The eastern and western flanks of the Sierra Pie de Palo are characterized by east-dipping and west-dipping Pliocene strata, respectively, supporting the interpretation that the surface structure of Pie de Palo is characterized by a basement fold (Ramos et al., 2002). This basement structure folded the Pliocene strata and the unconformity between these strata and the basement rocks. Based on these relationships, Ramos et al. (2002) proposed that the structure of the range is controlled by a basement wedge detached at about 15-20 km depth (Fig. 35).

Drive to San Juan and Part I of the "Show & Tell Event".

Day 6.

Transition between the Sierras Pampeanas and Precordillera

The eastern sectors of the Precordillera already exhibit structural features that are determined by the involvement of high-angle reverse faults. Often these faults and their deformation characteristics are known from seismic reflection, cross-section balancing based on field observations, and seismicity (Smalley et al., 1993). While deformation is ongoing in these sectors of the transition between the fold-and-thrust belt and the reverse-faulted basement uplifts of the broken foreland, there is a pronounced

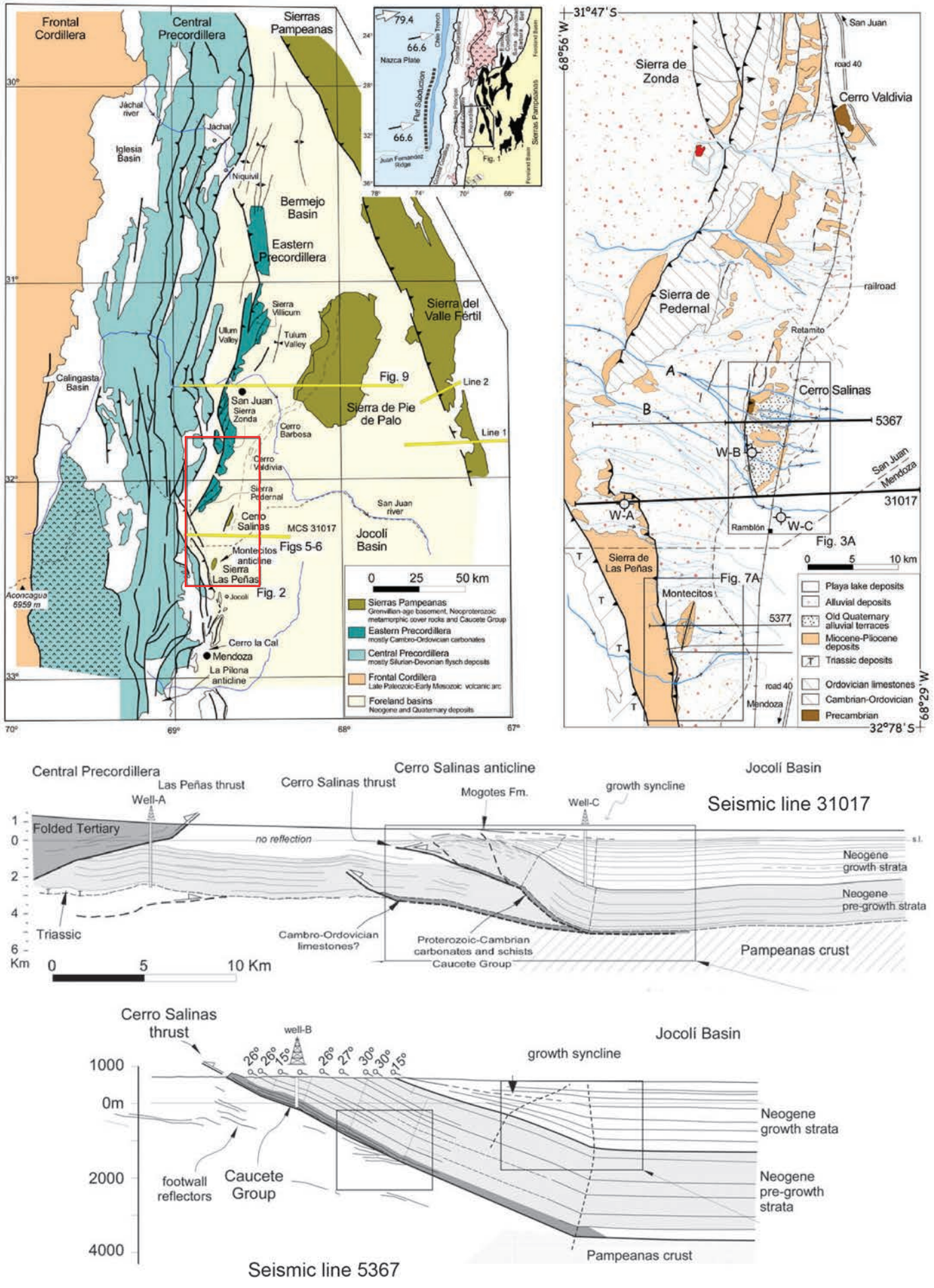

Plate 2 - (upper left) Simplified geological map. (upper right) Detailed geological map of the Cerro Salinas area. (lower figures) Structural cross sections based on seismic line interpretations. For more information see Vergés et al. (2007).

W-E gradient in deformation rates (Fig. 36) as determined by repeated GPS measurements. In this transition shortening rates of approximately 4.5mm/yr have been measured. High rates are also found in the area of the Sierra Pie de Palo and the western transition into the Precordillera. Those GPS-derived shortening estimates are thus slightly higher than the long-term geological and Quaternary rates. Moreover, north of 31°S, GPS data suggest that only 2-3mm/yr are accommodated between the western Precordillera and the Sierra de Valle Fértil, with less than 1 mm/yr within the Bermejo valley. GPS-data thus seem to confirm that most of the present-day tectonic activity is concentrated south of 31°S, in the Sierra Pie de Palo area. Despite the overall lower deformation rates in the Sierras Pampeanas there is a well-expressed topography of compressional basins and ranges that exhibit active mountain fronts. In the vicinity of the Precordillera is the NNW-oriented Bermejo Basin, which has been receiving sediments derived from the Precorillera, Fronatl Cordillera and the Sierra de Valle Fértil. The basin strata are in reverse-fault contact on the E, while the western margin of the basin is characterized by an onlap onto basement. Here, the sedimentary strata have been deformed in a thin-skinned style.

Stop 6.1 The Cerro Salinas Anticline (30.2237°S; 68.4295°W)

The Cerro Salinas Anticline is a basement backthrust similar to basement structures of the Sierras Pampeanas (see Plate 2 on page 35). This structure impinges on the easternmost Precordillera structures and it highlights the neotectonic activity in the transition between the thick-skinned and thin-skinned back-arc sectors. This structural style prevails northward along strike of the Precordillera and is responsible for the thin-skinned folding and faulting of foreland deposits between Valle Fértil and the region immediately east of Jachal (See geologic cross section in Fig. 30).

Drive to Mendoza & Part II of the "Show & Tell Event".

References

Aguirre-Urreta, M.B. and Rawson, P.F. (1997) The ammonite sequence in the Agrio Formation (Lower Cretaceous), Neuquén basin, Argentina. Geological Magazine 134(4), 449- 458.

Alvarado, P., and S. Beck (2006), Source characterization of the San Juan (Argentina) crustal earthquakes of 15 January 1944 (MW 7.0) and 11 June 1952 (MW 6.8), Earth Planet. Sci. Lett., 243(3–4), 615–631.

Astini, R.A. (1996) Las fases diastróficas del Paleozoico medio en la Precordillera del oeste argentino. XIII° Congreso Geológico Argentino y III° Congreso Exploración de Hidrocarburos, Actas V: 509-526.

Astini, R.A., Benedetto, J.L. and Vaccari, N.E. (1995) The early Paleozoic evolution of the Argentina Precordillera as a Laurentian rifted, drifted, and collided terrane: a geodynamic model. Geological Society of America,bulletin 107(3), 253-273.

Astini, R., Ramos, V.A., Benedetto, J.L., Vaccari, N.E. and Cañas, F.L. (1996) La Precordillera: un terreno exótico a Gondwana. XIII° Congreso Geológico Argentino y III° Congreso Exploración de Hidrocarburos, Actas V: 293-324.

Baldis, B., Beresi, M.S., Bordonaro, O. and Vaca, A. (1982) Síntesis evolutiva de la Precordillera Argentina. V° Congreso Geológico Latinoamericano de Geología, Actas 4: 399 445.

Baldis, B., Beresi, M.S., Bordonaro, O. and Vaca, A. (1984) The Argentine Precordillera as a key to Andean structure. Episodes 7(3), 14- 19.

Barredo SP (2004). Análisis estructural y tectosedimentario de la subcuenca de Rincón Blanco, Precordillera Occidental, provincia de San Juan. [PhD Thesis]. , Argentina. Unpublished: 325 p.

Barros, V.R., Castañeda, M., and Doyle, M., 1996, Recent precipitation trends in southern South America to the east of the Andes: An indication of a mode of climatic variability, in Rosa, L.P., and Santos, M.A., eds., Greenhouse gas emission under developing countries point of view: Rio de Janeiro, COPPE (Alberto Luiz Coimbra Institute and Graduate School of Research and Engineering), p. 41-67.

Beer JA, Allmendinger RW, Figueroa DA, Jordan TE. (1990). Seismic Stratigraphy of a Neogene Piggyback Basin, Argentina. AAPG Bull, 74, 1183-1202.

Bellahsen, N, Sebrier, M, & Siame, L. (2016). Crustal shortening at the Sierra Pie de Palo (Sierras Pampeanas, Argentina): near-surface basement folding and thrusting. Geol Mag, 153, 992-1012.

Benedetto, J.L. and Astini, R. (1993) A collisional model for the stratigraphic evolution of the Argentine Precordillera during the Early Paleozoic. Second Symposium International Géodynamique Andine ISAG 93 (Oxford), 501- 504, París.

Benedetto, J.L., Sánchez, T.M., Carrera, M.G., Brussa, E.D. and Salas, M.J. (1999) Paleontological constraints in successive paleogeographic positions of Precordillera terrane during the Early Paleozoic. In V.A. Ramos and D. Keppie (eds) Laurentia- Gondwana connections before Pangea. Geological Society of America, Special Paper 336,21-42.

Bense, FA, Löbens, S, Dunkl, I, Wemmer, K, & Siegesmund, S. (2013). Is the exhumation of the Sierras Pampeanas only related to Neogene flat-slab subduction? Implications from a multi-thermochronological approach. J S Am Earth Sci, 48, 123-144.

Bluestein, H.B., 1993, Synoptic-dynamic meteorology in midlatitudes, Volume II: Oxford, UK, Oxford University Press, 594 p.

Bodenbender, G. (1902) Contribución al conocimiento de la Precordillera de San Juan, de Mendoza y de las sierras centrales de la República Argentina. Academia Nacional de Ciencias, Boletín XVII: 203-262.

Borrello, A.V. (1969) Los geosinclinales de la Argentina. DirecciónNacional de Geología y Minería, Anales 14, 136 p.

Bond, G.C., Nickelson, P.A. and Kominz, M.A. (1984) Breakup of a supercontinent between 625 Ma and 55 Ma: new evidence and implications for continental histories. Earth and Planetary Science Letters 70,325 345.

Bookhagen, B., and M. R. Strecker (2008), Orographic barriers, high-resolution TRMM rainfall, and relief variations along the eastern Andes, Geophys. Res. Lett., 35, L06403, doi:10.1029/2007GL032011.

Borrello, A., 1963. Fremontella inopinata n. sp. del Cámbrico de Argentina. Ameghiniana, 3 (2), 51-55.

Bracaccini, O. 1946-1950. Contribución al conocimiento geológico de la Precordillera sanjuanino-mendocina. Boletín de Informaciones Petroleras 258-260-261-262- 263-264 (reprint).

Brea, M., 1997. Una nueva especie fósil del género Araucarioxylon Kraus 1870 emend. Masheshwari 1972 del Triásico de Agua de la Zorra, Uspallata, Mendoza, Argentina. Ameghiniana 34: 485-496.

Brea, M., Artabe, A., Spalletti, l., 2009. Darwin forest at Agua de la Zorra. The first in situ forest discovered in South America by Darwin in 1835. Revista de la Asociación Geológica Argentina, 64: 21-31.

Brooks, B. A., M. Bevis, R. Smalley, E. Kendrick, R. Manceda, E. Lauria, R. Maturana, and M. Araujo (2003), Crustal motion in the Southern Andes (26°–36°S): Do the Andes behave like a microplate? Geochem. Geophys. Geosyst., 4(10), 1085, doi:10.1029/2003GC000505.

Cahill, T. and Isacks, B.L. (1992) Seismicity and the shape of the subducted Nazca plate. Journal of Geophysical Research 97, 17503- 17529.

Caminos, R. (1979) Cordillera Frontal. In Turner, J.C.M.(ed.) Segundo Symposio Geología Regional Argentina, Academia Nacional de Ciencias 1, 397-454, Córdoba.

Caminos, R. (ed.) (2000) Geología Argentina. Instituto de Geología y Recursos Minerales, Anales 29, 1-796.

Carignano C. Cioccale, M. and Rabassa, J. 1999. Landscape antiquity of the Central Eastern Sierras Pampeanas (Argentina): Geomorphological evolution since Gondwanic times. Zeitschrift für Geomorphologie 118: 245-268.

Charrier, R. (1973) Interruptions of spreading and the compressive tectonic phases of Meridional Andes. Earth and Planetary Science Letters 20, 212 249, Amsterdam.

Chinn, D.S. and Isacks, B. (1983) Accurate source depths and focal mechanisms of shallow earthquakes in western South America and in the New Hebrides island arc. Tectonics 2, 529- 564.

Cortés, J.M. (1985) Vulcanitas y sedimentitas lacustres en la base del Grupo Choiyoi al sur de la estancia Tambillos, provincia de Mendoza, República Argentina. IV° Congreso Geológico Chileno, Actas I: 89-108, Antofagasta.

Cortés, J.M. (1990) Estudio geológico estructural de la Sierra de Las Peñas. Servicio Geológico Nacional (unpublished).

Cortés, J.M., (1993). El frente de corrimiento de la Cordillera Frontal y el extreme sur del valle de Uspallata, Mendoza. Actas XII Congreso geolo´gico Argentino y II Congreso de Exploración de Hidrocarburos, Mendoza, Actas III, pp. 168-178.

Cortés, J.M., Vinciguerra, P., Yamín, M., Pasini, M.M., (1999). Tectónica Cuaternaria de la Región Andina del Nuevo Cuyo (281-381 LS). In: Caminos, R. (Ed.), Geologia Argentina, Subsecretaría de Minería de la Nacion, Servicio Geológico Minero Argentino, Anales 29, pp. 760-778 (Chapter 24).

Costa, C, Machette, MN, Dart, RL, Bastias, HE, Paredes, JD, Perucca, LP, Tello, GE, Haller, KM. (2000). Map and database of Quaternary faults and folds in Argentina. U.S. Geological Survey Open-File Report 00-0108, 76p.

Costa, C. H., C. E. Gardini, H. Diederix, and J. M. Cortés (2000), The Andean orogenic front at Sierra de Las Peñas-Las Higueras, Mendoza, Argentina, J. South Am. Earth Sci., 13(3), 287–292, doi:10.1016/S0895-9811(00)00010-9.

Dalla Salda, L., Cingolani, C., and Varela, R. (1992 a) Early Paleozoic orogenic belt of the Andes in southwestern South America: Result of Laurentia-Gondwana collision?. Geology 20, 617-620.

Dalla Salda, L., Dalziel, I.W.D, Cingolani, C.A. and Varela, R. (1992 b) Did the Taconic Appalachians continue into southern South America?. Geology 20,1059-1062. .

Dalziel, I.W.D. (1991) Pacific margins of Laurentia and East-Antarctica-Australia as a conjugate rift pair: evidence and implications for an Eocambrian supercontinent. Geology 19(6), 598-601.

Dalziel, I.W.D. (1992) On the organization of American plates in the Neoproterozoic and the breakout of Laurentia. GSA Today 2(11), 240- 241.

Dalziel, I.W.D. (1993) Tectonic tracers and the origin of the proto-Andean margin. XII° Congreso Geológico Argentino y II°Congreso de Exploración de Hidrocarburos, Actas III: 367-374.

Dalziel, I.W.D. (1997) Neoproterozoic- Paleozoic geography and tectonics: review, hypothesis, environmental speculation. Geological Society of America,bulletin 109(1), 16-42.

Dalziel, I.W.D., Dalla Salda, L.H. and Gahagan, L.M. (1994) Paleozoic Laurentia- Gondwana interaction and the origin of the Appalachian-Andean mountain system. Geological Society of America,bulletin 106, 243-252.

Dalziel, I.W.D., Dalla Salda, L., Cingolani C., and Palmer, P. (1996) The Argentine Precordillera: A Laurentian terrane?. GSA Today 6(2),16-18.

Davila, FM, & Lithgow-Bertelloni, C. (2015). Dynamic uplift during slab flattening. Earth Planet Sci Lett, 425, 34-43.

Darwin, Ch. (1846) Geological observations of South America,being the third part of the Geology of the voyage of the Beagle during 1832-1836. Smith, Elder, vii+279 pp., Londres.

Di Tommaso, I.M., Fauque , L., 2005. Estimacio n del volumen de agua embalsada en paleolagos generados por endicamientos naturales en la cuenca del río Mendoza. In: Contribuciones te cnicas del Proyecto GEOSAT-AR, pp. 155e159.

Du Toit, A.L. (1927) A geological comparisson of South America with South Africa. Publications Carnegie Institute 381, 1-157.

Ereño, C. E., and J. A. J. Hoffmann (1978), El regimen pluvial en la Cordillera Central, Ser. Cuad Geogr. 5, 1-17.

Espizúa, L,E., Bengochea, J.D. and Aguado, C. (1993) Mapa de riesgo de remoción en masa en el valle del Río Mendoza. XII Congreso Geológico Argentino y II Congreso de Exploración de Hidrocarburos. Actas T° VI: 323-332. Mendoza.

Espizúa, L.E. and Bigazzi, G. (1998) Fission- track dating of the Punta de Vacas Glaciation in the Rio Mendoza Valley, Argentina. Quaternary Science Reviews 17, 755-760.

Falvey, M., and Garreaud, R., 2007, Wintertime precipitation episodes in central Chile: Associated meteorological conditions and orographic influences: Journal of Hydrometeorology, v. 8, p. 171-193, doi: 10.1175/JHM562.1.

Fauqué, L., Cortés, J.M., Folguera, A. and Etcheverría, M. (2000) Avalanchas de roca asociadas a neotectónica en el valle del río Mendoza, al sur de Uspallata. Asociación Geológica Argentina, Revista 55 (4), 419- 423.

Fauqué, L., Cortés, J.M., Folguera, A. and Etcheverría, M. (2001) Avalanchas de rocas asociadas a neotectónica. Peligrosidad geológica asociada. Servicio Geológico Minero Argentino SEGEMAR. Serie Contribuciones Técnicas. Peligrosidad Geológica, Boletín No 2, 57 pp.

Fauqué, L., Cortes, J.M., Folguera, A., Etcheverría, M., Hermanns, R., Cegarra, M., Rosas, M. and Baumann, V. (2008d) Edades de las avalanchas de rocas ubicadas en el valle del Río Mendoza aguas debajo de Uspallata. Proceedings of XVII Congreso Geológico Argentino, Jujuy, 282-283.

Fiorella, RP, Poulsen, CJ, Pillco-Zolá, RS, Barnes, JB, Tabor, CR, & Ehlers, TA. (2015). Spatiotemporal variability of modern precipitation δ18O in the central Andes and implications for paleoclimate and paleoaltimetry estimates. J Geophys Res, 120, 4630-4656.

Fazzito, SY, Cortés, JM, Rapalini, AE, & Terrizzano, CM. (2013). The geometry of the active strike-slip El Tigre Fault, Precordillera of San Juan, Central-Western Argentina: integrating resistivity surveys with structural and geomorphological data. Int J Earth Sci (Geol Rundsch), 102, 1447-1466.

Forsythe, R.D, Kent, D.V., Mpodozis, C. and Davidson, J. (1986) Paleomagnetism of Permian and Triassic Rocks, Central Chilean Andes. In McKenzie, G.D. (ed.) Gondwana Six: Structure, Tectonics, and Geophysics, American Geophysical Union, Geophysical Monographs 40, 241-252.

Fosdick, JC, Carrapa, B, & Ortíz, G. (2015). Faulting and erosion in the Argentine Precordillera during changes in subduction regime: Reconciling bedrock cooling and detrital records. Earth Planet Sci Lett, 432, 73-83.

Giambiagi, L. B. and Martinez, A. N. (2008) Permo-Triassic oblique extension in the Uspallata-Potrerillos area, western Argentina. Journal of South American Earth Sciences 26, 252-260.

Giambiagi, L. B., V. A. Ramos, E. Godoy, P. P. Alvarez and S. Orts (2003) Cenozoic deformation and tectonic style of the Andes, between 33° and 34° South Latitude. Tectonics 22(4), 1041, doi:10.1029/2001TC001354.

Giambiagi, L., Mescua, J., Folguera, A. and Martinez, A. (2010) Estructuras y cinemática de la deformación pre-andina del sector sur de la Precordillera, Mendoza, Argentina. Revista de la Asociación Geológica Argentina 66(1), 5- 20.

Giambiagi, L., Mescua, J., Bechis, F., Martínez, A. and Folguera, A. (2010) Pre- Andean deformation of the Precordillera southern sector, Southern Central Andes. Geosphere. In press.

Giambiagi, L., Mescua, J., Heredia, N., Farías, P., García Sansegundo, J., Fernández, C., Stier, S., Pérez, D., Bechis, F., Moreiras, S. M., and Lossada, A., (2014). Reactivation of Paleozoic structures during Cenozoic deformation in the Cordón del Plata and Southern Precordillera ranges (Mendoza, Argentina), J. Iber. Geol., 40, 309-320.

Godoy, E., Harrington, R., Fierstein, J. and Drake, R. (1988) El Aconcagua, parte de un volcán mioceno?. Revista Geológica de Chile 15(2),167-172.

Godoy, E., Yañez, G. and Vera, E. (1999) Inversion of an Oligocene volcano-tectonic basin and uplifting of its superimposed Miocene magmatic arc in the Chilean Central Andes: first seismic and gravity evidences. Tectonophysics 306(2), 217-336.

Gonzalez Bonorino, F. (1950) Geologic cross section of the Cordillera de Los Andes at about parallel 33°S L. (Argentina-Chile). Geological Society of America Bulletin, 61, 17-26.

Groeber, P. (1946) Observaciones geológicas a lo largo del meridiano 70°. 1. Hoja Chos Malal. Sociedad Geológica Argentina, Revista 1, 177- 208.

Handschumacher, D.W. (1976) Post Eocene plate tectonics of the Eastern Pacific. In Sutton, G.H., Manghnani, M.H. and Moberly, R.(eds) The Geophysics of the Pacific Ocean and its margins. American Geophysical Union: 117- 202.

Haselton, K., G. Hilley, and M. R. Strecker (2002), Average Pleistocene climatic patterns in the southern central Andes: Controls on mountain glaciation and paleoclimate implications, J. Geol., 110(2), 211-226, doi:10.1086/338414.

Hervé, F., Demant, A., Ramos, V.A., Pankhurst R.J. and Suárez, M. (2000) The Southern Andes. In Cordani, U.J., Milani, E.J., Thomaz Filho, A. and Campos, D.A. (eds) Tectonic evolution of South America, 31° International Geological Congress, 605-634, Río de Janeiro.

Hoffmann, J.A.J., 1992, The continental atmospheric pressure and precipitation regime of South America: Erdkunde, v. 46, p. 40-51.

Hoke, GD, Aranibar, JN, Viale, M, Araneo, DC, & Llano, C. (2013). Seasonal moisture sources and the isotopic composition of precipitation, rivers, and carbonates across the Andes at 32.5-35.5°S. Geochem Geophys Geosyst, 962-978.

Hoke, GD, Giambiagi, LB, Garzione, CN, Mahoney, JB, & Strecker, MR. (2014). Neogene paleoelevation of intermontane basins in a narrow, compressional mountain range, southern Central Andes of Argentina. Earth Planet Sci Lett, 406, 153-164.

Irigoyen, M.V., Buchan K.L., Brown, R.L. (2000): Magnetostratigraphy of Neogene Andean foreland-basin strata, lat 33°S, Mendoza Province, Argentina. Bulletin of the Geological Society of America 112, 803-816.

Isacks, B. (1988) Uplift of the Central Andean plateau and bending of the Bolivian orocline. J. Geophys. Res. 93, 3211- 3231.

Isacks, B., Jordan, T., Allmendinger, R. and Ramos, V.A. (1982) La segmentación tectónica de los Andes Centrales y su relación con la placa de Nazca subductada. V° Congreso Latinoamericano de Geología, Actas III: 587-606.

Jordan, T. and Allmendinger, R. (1986) The Sierras Pampeanas of Argentina: a modern analogue of Laramide deformation. American Journal of Science 286, 737-764, New Haven.

Jordan, T., Isacks, B., Ramos, V.A. and Allmendinger, R. (1983a) Mountain building in the Central Andes. Episodes 1983(3), 20-26.

Jordan, T., Isacks, B., Allmendinger, R., Brewer, J., Ramos, V.A. and Ando, C. (1983b) Andean tectonics related to geometry of subducted plates. Geological Society of America,bulletin 94, 341-361.

Jordan, TE, Zeitler, P, Ramos, VA, & Gleadow, A. (1989). Thermochronometric data on the development of the basement peneplain in the Sierras Pampeanas, Argentina. J S Am Earth Sci, 2, 207-222.

Jordan, TE, Allmendinger, RW, Damanti, J.F., Drake, R.E. (1993). Chronology of motion in a complete thrust belt: the Precordillera, 30-31°S, Andes Mountains. J. Geol., 101, 135-156.

Jordan, TE, Schlunegger, F, & Cardozo, N. (2001). Unsteady and spatially variable evolution of the Neogene Andean Bermejo foreland basin, Argentina. J S Am Earth Sci, 14, 775-798.

Kadinsky-Cade, K., R. Reilinger, and B. Isacks (1985), Surface deformation associated with the November 23, 1977, Caucete, Argentina, earthquake sequence, J. Geophys. Res., 90(B14), 12,691–12,700.

Kay, SM, & Abbruzzi, JM. (1996). Magmatic evidence for Neogene lithospheric evolution of the central Andean "flat-slab" between 30°S and 32°S. Tectonophysics, 259, 15-28.

Kay, SM, & Mpodozis, C. (2002). Magmatism as a probe to the Neogene shallowing of the Nazca plate beneath the modern Chilean flat-slab. J S Am Earth Sci, 15, 39-57.

Kay, S.M., Maksaev, V., Moscoso, R., Mpodozis, C. and Nasi, C. (1987) Probing the evolving Andean lithosphere: Mid-late Tertiary magmatism in Chile (29°-30°30'S) over the modern zone of subhorizon-

tal subduction. Journal Geophysical Research 92 (B7), 6173- 6189.

Kay, S.M., Ramos, V.A., Mpodozis, C. and Sruoga, P. (1989) Late Paleozoic to Jurassic silicic magmatism at the Gondwanaland margin: analogy to the Middle Proterozoic in North America? Geology 17: 324-328.

Kay, S.M., Mpodozis, C., Ramos, V.A. and Munizaga, F. (1991) Magma source variations for mid to late Tertiary volcanic rocks erupted over a shallowing subduction zone and through a thickening crust in the Main Andean Cordillera (28-33°S). In Harmon, R.S. and Rapela, C. (eds) Andean Magmatism and its Tectonic Setting. Geological Society of America, Special Paper 265, 113-137.

Kay, S.M., Godoy, E. and Kurtz, A. (2005) Episodic arc migration, crustal thickening, subduction erosion, and magmatism in the south-central Andes. Geological Society of America,bulletin 117, 67-88.

Keidel, J. (1921) Sobre la distribución de los depósitos glaciares del Pérmico conocidos en la Argentina y su significación para la estratigrafía de la serie del Gondwana y la paleogeografía del Hemisferio Austral. Academia Nacional de Ciencias, Boletín 25, 239 368, Córdoba.

Kraemer, P.E., Escayola, M.P. and Martino, R.D. (1995) Hipótesis sobre la evolución tectónica neoproterozoica de las Sierras Pampeanas de Córdoba (30°40'- 32°40'), Argentina. Asociación Geológica Argentina, Revista 50(1-4), 47-59.

Levi, B. and Aguirre, L. (1981) Ensialic spreading subsidence in the Mesozoic and Paleogene Andes of Central Chile. Journal of geological Society of London 138,75 81.

Levi, B., Aguirre, L. and Nystrom, J.O. (1982) Metamorphic gradients in burial metamorphosed vesicular lavas: comparison of basalt and spilite in Cretaceous basic flows. Contributions to Mineralogy and Petrology 80, 49-58.

Liebmann, B, & Allured, D. (2005). Daily precipitation grids for South America. Bull. Amer. Meteor. Soc., 86, 1567-1570, doi: 10.1175/BAMS-86-11-1567.

Llambías, E. and Sato, A.M. (1990) El batolito de Colangüil (29-31° S), Cordillera Frontal de Argentina: estructura y marco tectónico. Revista Geológica de Chile 17, 89- 108.

Lo Forte, G. (1992) Evolución paleogeográfica del Mesozoico marino en la región del Aconcagua. Universidad de . PhD Thesis (Unpublished). 348 pp. .

Lo Forte, G. (1999) Los depósitos jurásicos de la Alta Cordillera de Mendoza. Geología de la Región del Aconcagua. Provincias de San Juan y Mendoza. Anales Nro 24. Subsecretaría de Minería de la Nación. Dirección Nacional del Servicio Geológico. Chapter 6: 139-178.

Lo Forte, G., Orti, F. and Rossell, L. (2005) Isotopic characterization of Jurassic evaporites. Aconcagua-Neuquen basin. Argentina. Geologica Acta (2): 155-161.

Masiokas, M., Villalba, R., Luckman, B., Le Quesne, C., and Aravena, J., 2006, Snowpack variations in the central Andes of Argentina and Chile, 1951-2005: Large-scale atmospheric influences and implications for water resources in the region: Journal of Climate, v. 19, p. 6334-6352.

Martínez, A., Rodríguez Blanco, L. and Ramos, V.A. (2006) Permotriassic magmatism of the Choiyoi Group in the Cordillera Frontal of Mendoza, Argentina: Geological variations associated with changes in paleo-Benioff zone. Backbone of the Americas Conference Abstracts, p. 60.

Milana, J.P. (1993) Estratigrafia de las eolianitas en la zona de Jachal-Huaco, Precordillera de San Juan. Rev. Asoc. Geol. Arg., 48, 283-298.

Moores, E.M. (1991) Southwest U.S.-East Antarctic (SWEAT) connection: A hypothesis. Geology 19(5), 425-428.

Moreiras, S.M. (2004) Landslide Incidence Zonification along the Rio Mendoza Valley. Mendoza, Argentina. Earth Surface Processes and Landforms, 29 (2), 255-266.

Moreiras, S.M. (2006a) Chronology of a Pleistocene rock avalanche probable linked to neotectonic, Cordon del Plata (Central Andes), Mendoza - Argentina. Quaternary International 148 (1), 138-148.

Moreiras SM (2010a) Clustering of Pleistocene rock avalanches in the Central Andes, Argentina. En: J.A. Salfity & R.A. Marquillas (eds), Cenozoic Geology of Central Andes of Argentina. Elsevier (in press).

Moreiras, SM, Hermanns, R.L, & Fauqué, L. (2015). Cosmogenic dating of rock avalanches constraining Quaternary stratigraphy and regional neotectonics in the Argentine Central Andes (32° S). Quaternary Science Reviews, 112, 45-58.

Mpodozis, C. and Kay, S.M. (1990) Late Paleozoic to Triassic evolution of the Gondwana margin: evidence from Chilean Frontal Cordilleran Batholiths (28°-33°S). Revista Geológica de Chile 17(2), 153-180.

Mpodozis, C. and Kay, S.M. (1992) Late Paleozoic to Triassic evolution of the Gondwana margin: evidence from Chilean Frontal Cordilleran Batholiths (28°-31°S). Geological Society of America,bulletin 104, 999-1014.

Mpodozis, C. and Ramos, V.A. (1990) The Andes of Chile and Argentina. In Ericksen, G.E., Cañas Pinochet, M.T. and Reinemud, J.A. (eds) Geology of the Andes and its relation to Hydrocarbon and Mineral Resources. Circumpacific Council for Energy and Mineral Resources, Earth Sciences Series 11, 59-90.

Munizaga, F. and Vicente, J.C. (1982) Acerca de la zonación plutónica y del vulcanismo miocénico en los Andes de Aconcagua (lat 32° 33°S): datos radiométricos K/Ar. Revista Geológica de Chile 16,3 21.

Pankhurst, R.J. and Rapela, C.W. (1998) The Proto-Andean margin of Gondwana. Geological Society of London, Special Publication 142: 1- 383.

Pardo, M., Monfret, T. and Comte, D. (2000) Sismotectónica y distribución de esfuerzos en la zona de subducción subhorizontal de Chile Central (30°-32°S) utilizando datos telesísmicos. IX° Congreso Geológico Chileno, Actas 2: 459-463.

Pardo, M., Comte, D. and Monfret, T. (2002) Seismotectonic and stress distribution in the central Chile Subduction zone. Journal of South American Earth Sciences 15(1),11-22.

Pardo Casas, F. and Molnar, P. (1987) Relative motion of the Nazca (Farallon) and South American Plates since Late Cretaceous time. Tectonics 6(3), 233 248.

Pérez, D. and Ramos, V.A. (1990) La actividad magmática gondwánica. Late Paleozoic of South America, IGCP Project 211, Annual Meeting of the working group, Abstracts: 89-92.

Pérez, D. J., & Ramos, V. A. (1996). Los depósitos sinorogénicos. In: Geología de la región del Aconcagua, provincias de San Juan y Mendoza. Dirección Nacional del Servicio Geológico, Anales 24(11): 317- 341.

Pilger, R.H. (1981) Plate reconstructions, aseismic ridges, and low angle subduction beneath the Andes. Geological Society of America,bulletin 92, 448 456.

Pilger, R.H. (1984) Cenozoic plate kinematics, subduction and magmatism: South American Andes. Journal geological Society of London 141,793 802.

Polanski, J. (1970) Carbónico y Pérmico de la Argentina. Editorial Eudeba, 216pp..

Poma, S., Litvak, V., Koukharshy, M., Maisonnave, B y Quenardelle, S., 2009. Darwin´s observation in South America: What did he find at Agua de la Zorra, Mendoza province?. Revista de la Asociación Geológica Argentina, 64: 13-20.

Price, R.A. (1981) The Cordilleran foreland thrust and fold belt in the Southern Canadian Rocky Mountain. In McClay, F.R. and Price, N.J. (eds) Nap and Thrust tectonics. Geological Society of London, Spec. Publication 9, 427-448.

Ramos, V.A. (1985 a) El Mesozoico de la Alta Cordillera de Mendoza: facies y desarrollo estratigráfico, Argentina. IV° Congreso Geológico Chileno, Actas 1(1): 492 513, Antofagasta.

Ramos, V.A. (1985 b) El Mesozoico de la Alta Cordillera de Mendoza: reconstrucción tectónica de sus facies, Argentina. IV° Congreso Geológico Chileno, Actas 1(2): 104 118, Antofagasta.

Ramos, V.A. (1988 a) The Tectonics of the Central Andes; 30° to 33°S latitude. In Clark, S. and Burchfiel, D. (eds.) Processes in Continental Lithospheric Deformation, Geological Society America, Special Paper 218, 31-54.

Ramos, V.A. (1988 b) Tectonics of the Late Proterozoic - Early Paleozoic: a collisional history of Southern South America. Episodes 11(3), 168-174.

Ramos, V.A. (1993) Interpretacióntectónica. In V.A. Ramos (ed.) Geología y Recursos Naturales de Mendoza. XII° Congreso Geológico Argentino y II° Congreso de Exploración de Hidrocarburos (Mendoza), Relatorio I(19): 257-266.

Ramos, V.A. (1999) Plate tectonic setting of the Andean Cordillera. Episodes 22(3), 183- 190.

Ramos, V.A. (2004) Cuyania, an exotic block to Gondwana: Review of a historical success and the present problems. Gondwana Research 7(4), 1009-1026.

Ramos, VA. (2008). The Basement of the Central Andes: The Arequipa and Related Terranes. Annu Rev Earth Planet Sci, 36, 289-324.

Ramos, V.A. and Kay, S.M. (1991) Triassic rifting and associated basalts in the Cuyo basin, central Argentina. In Harmon, R. and Rapela, C. (eds) Andean magmatism and its tectonic setting. Geological Society of America, Special Paper 265, 79-91.

Ramos, V.A. and Yrigoyen, M.R. (1987) Geología de la región del Aconcagua, provincia de Mendoza. X° Congreso Geológico Argentino, Actas 4: 267-271, Tucumán.

Ramos, V. and G. Vujovich 2000. Hoja Geológica San Juan, escala 1:250.000. Servicio Geológico Minero Argentino, Boletín 245, 82 p., Buenos Aires.

Ramos, V. A., E. O. Cristallini, and D. J. Pérez (2002), The Pampean flatslab of the Central Andes, J. South Am. Earth Sci., 15(1), 59–78.

Ramos, VA, & Folguera, A. (2009). Andean flat-slab subduction through time. GSL Special Publications, 327, 31.

Ramos, V.A., Jordan, T.E., Allmendinger, R.W., Kay, S.M., Cortés, J.M. and Palma, M.A. (1984) Chilenia: un terreno alóctono en la evolución paleozoica de los Andes Centrales. IX° Congreso Geológico Argentino, Actas 2: 84 106.

Ramos, V.A., Jordan, T.E., Allmendinger, R.W., Mpodozis, C., Kay, S.M., Cortés, J.M. and Palma, M.A. (1986) Paleozoic terranes of the Central Argentine Chilean Andes. Tectonics 5(6), 855-880.

Ramos, V.A., Munizaga, F. and Kay, S.M. (1991) El magmatismo cenozoico a los 33°S de latitud: geocronología y relaciones tectónicas. VI° Congreso Geológico Chileno, Actas I: 892- 896.

Ramos, V.A., M. Cegarra and E. Cristallini, (1996 a). Cenozoic tectonics of the High Andes of west-central Argentina, (30°- 36°S latitude). Tectonophysics 259, 185-200, Amsterdam.

Ramos, V.A., Aguirre Urreta, M.B., Alvarez, P.P., Cegarra, M., Cristallini, E.O., Kay, S.M., Lo Forte, G.L., Pereyra F. and Pérez, D., (1996 b) Geología de

la Región del Aconcagua, Provincias de San Juan y Mendoza. Dirección Nacional del Servicio Geológico, Anales 24, 1-510.

Ramos, V.A., Cristallini, E. and Pérez, D.J. (2002) The Pampean flat-slab of the Central Andes. Journal of South American Earth Sciences 15(1), 59-78.

Ramos, VA. (2008). The Basement of the Central Andes: The Arequipa and Related Terranes. Annu Rev Earth Planet Sci, 36, 289-324.

Rapalini, A.E. (1989) Estudio paleomagnético del vulcanismo permotriásico de la región andina de la República Argentina. Universidad de , Tesis doctoral (unpublished), 278 pp.

Régnier, M., Chatelain, J.-L., Smalley R., Chiu, J.- M., Isacks, B.L. and Araujo, M. 1992. Seismotectonics of Sierra Pie de Palo, a base- ment block uplift in the Andean Foreland of Argentina. Bulletin of the Seismological Society of America 82 (6): 2549-2571.

Ross, R.J. (1975) Early Paleozoic trilobites, sedimentary facies, lithospheric plates, and ocean currents. Fossil Strata 4, 307-329.

Ruskin, BG, & Jordan, TE. (2007). Climate Change Across Continental Sequence Boundaries: Paleopedology and Lithofacies of Iglesia Basin, Northwestern Argentina. Journal of Sedimentary Research, 77, 661-679.

Saavedra, N., and Foppiano, A.J., 1992, Monthly mean pressure model for central Chile: International Journal of Climatology, v. 12, p. 469-480.

Sanguinetti, A. and Cegarra, M. (1991) El volcanismo Jurásico Superior al este de Las Cuevas, Cordillera Principal de Mendoza, Argentina. VI Congreso Geologico Chileno, Actas I: 737-741.

Schiller, W. (1907) Geologische Unterschungen bei Puente del Inca (Aconcagua). Neues Jahrbuch für Mineralogie, Paläontologie und Geologie, Beilageband XXIV: 716-736, Stuttgart.

Schiller, W. (1912) La Alta Cordillera de San Juan y Mendoza y parte de la provincia de San Juan. Anales del Ministerio de Agricultura, Sección Geología, Mineralogía y Minería 7(5): 1 68.

Siame, LL, Bellier, O, Sebrier, M, & Araujo, M. (2005). Deformation partitioning in flat subduction setting: Case of the Andean foreland of western Argentina (28 S-33 S). Tectonics. doi:10.1029/2005TC001787

Siame, L.L., Sébrier, M., Bellier, O., Bourlés, D.L., Castano, J.-C. and Araujo, M. 1997b. Geometry, segmentation and displacement rates of the El Tigre fault, San Juan Province (Argentina) from SPOT image analysis and 10Be datings. Annales Tectonicae 1-2: 3-26.

Siame, LL, Bourlès, DL, Sébrier, M, Bellier, O, Castano, JC, Araujo, M, Perez, M, Raisbeck, GM, & Yiou, F. (1997). Cosmogenic dating ranging from 20 to 700 ka of a series of alluvial fan surfaces affected by the El Tigre fault, Argentina. Geol, 25, 975-978.

Siame, LL, Bellier, O, & Sebrier, M. (2006). Active tectonics in the Argentine Precordillera and western Sierras Pampeanas. Revista de la Asociación Geológica Argentina, 61, 604-619.

Siame, LL, Sébrier, M, Bellier, O, Bourlès, D, Costa, C, Ahumada, EA, Gardini, CE, & Cisneros, H. (2015). Active basement uplift of Sierra Pie de Palo (Northwestern Argentina): Rates and inception from 10Be cosmogenic nuclide concentrations. Tectonics, 34, 1129–1153.

Smalley, R., J. Pujol, M. Regnier, J. M. Chiu, J. L. Chatelain, B. L. Isacks, M. Araujo, and N. Puebla (1993), Basement seismicity beneath the Andean Precordillera thin-skinned thrust belt and implications for crustal and lithospheric behavior, Tectonics, 12(1), 63–76.

Smith, R. B., and J. P. Evans (2007), Orographic precipitation and water vapor fractionation over the southern Andes, J. Hydrometeorol., 8(1), 3-19, doi:10.1175/JHM555.1.

Somoza, R. (1998). Updated Nazca (Farallon)-South America relative motions during the last 40 my: implications for mountain building in the Central Andean region. J S Am Earth Sci, 11, 211-215.

Spalletti, C., Fanning, M. and Rapella, C.W. (2008) Dating the Triassic continental rift in the southern Andes: the Potrerillos Formation, Cuyo Basin, Argentina. Geologica Acta (6): 3: 267-283.

Spalletti, L., Morel, E., Artabe, A., Zavattieri, A. and Ganuza, D. (2005) Estratigrafía, facies y paleoflora de la sucesión triásica de Potrerillos, Mendoza, República Argentina. Revista Geológica de Chile, 32, 249- 272.

Stappenbeck, R. (1910) La Precordillera de San Juan y Mendoza. Anales Ministerio Agricultura de la Nación, Sección Geología 4(3), 1-187.

Stelzner, A. (1873) Uber die argentinische Cordillere zw. 31° und 33° S. Beitrage Neues Jarhbuch Mineralogie Geologie Paläontologie: 726 744, Stuttgart.

Stelzner, A. (1885) Beitrage zur Geologie und Palaontologie der Argentinischen Republik. I. Geologischen Theil. Ed. von Fischer, Cassel.

Stern, L. A., and P. M. Blisniuk (2002), Stable isotope composition of precipitation across the southern Patagonian Andes, J. Geophys. Res., 107(D23), 4667, doi:10.1029/ 2002JD002509.

Stipanicic, P.N. & Marsicano, C.A. 2002: Tri asico. In L exico estra- tigr afico de la Argentina. Volumen VIII. Asociaci on Geol ogica Argentina, Serie B (Did actica y Complementaria) 26, 370 pp. , Argentina.

Suriano, J, Mardonez, D, Mahoney, JB, & Mescua, JF. (2017). Uplift sequence of the Andes at 30° S: Insights from sedimentology and U/Pb dating of synorogenic deposits. J S Am Earth Sci, 75, 11-34.

Thomas, W.A. and Astini, R.A. (1999) Simple-shear conjugate rift margins of the Argentine Precordillera and the Ouachita embayment of Laurentia. Geological Society of America,bulletin 111(7), 1069-1079.

Thomas, W.A. and Astini, R.A. (2003) Ordovician accretion of the Argentine Precordillera terrane to Gondwana: a review. Journal of South American Earth Sciences 16(1), 67-79.

Val, P, Hoke, GD, Fosdick, JC, & Wittmann, H. (2016). Reconciling tectonic shortening, sedimentation and spatial patterns of erosion from 10Be paleo-erosion rates in the Argentine Precordillera. Earth Planet Sci Lett, 450, 173-185.

Vergés, J, Ramos, VA, Meigs, A, Cristallini, EO, Bettini, FH, & Cortés, JM. (2007). Crustal wedging triggering recent deformation in the Andean thrust front between 31°S and 33°S: Sierras Pampeanas-Precordillera interaction. J Geophys Res, 112, B03S15–22.

Viale, M., and M. Nuñez (2011), Climatology of winter orographic precipitation over the subtropical central Andes and associated synoptic and regional characteristics, J. Hydrometeorol., 12(4), 481-507.

Von Huene, R., Corvalán, J., Flueh, E.R., Hinz, K., Korstgard, J., Ranero, C.R., Weinrebe, W., and the Condor scientists, (1997) Tectonic control of the subducting Juan Fernández Ridge on the Andean margin near Valparaíso, Chile. Tectonics 16(3), 474-488.

Wortel, M.J.R. (1984) Spatial and temporal variations in the Andean subudction zone. Journal of the Geological Society of London 141, 783-791.

Weaver, CE. (1931). Paleontology of the Jurassic and Cretaceous of west central Argentina. Washington, University of Washington Press.

Wherli, L. and Burckhardt, C. (1898) Rapport préliminaire sur une expédition géologique dans la Cordillère argentino- chilienne entre le 33° et 36° Latitud Sud. Museo de La Plata, Revista VIII: 373-388, La Plata.

Yañez, GA, Ranero, CR, von Huene, R, Díaz, J (2001) Magnetic anomaly interpretation across the southern central Andes (32°-34°S): the role of the Juan Fernández Ridge in the late Tertiary evolution of the margin. J. Geophys. Res. 106, 6325-6345.

Yrigoyen, M. (1976) Observaciones geológicas alrededor del Aconcagua. I°Congreso Geológico Chileno, Actas 1: 169-190.

Zapata, TR, Allmendinger, RW (1996) Growth stratal records of instantaneous and progressive limb rotation in the Precordillera thrust belt and Bermejo basin, Argentina. Tectonics, 15, 1065-1083.

MOSAIC OF GEOLOGICAL MAPS - CERRO ACONCAGUA (2369-I) AND MENDOZA (2369-II)

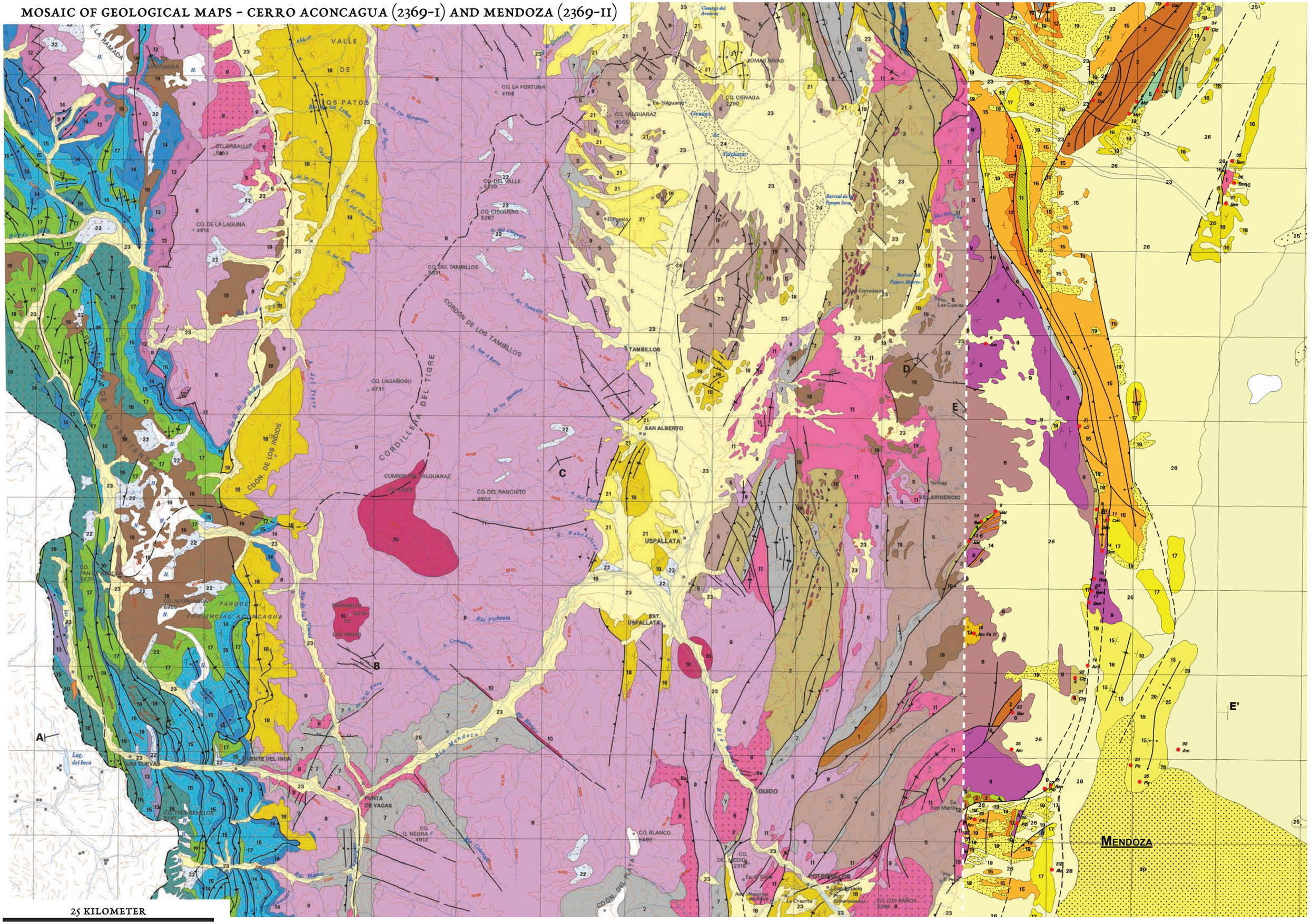

MENDOZA (2369-II)

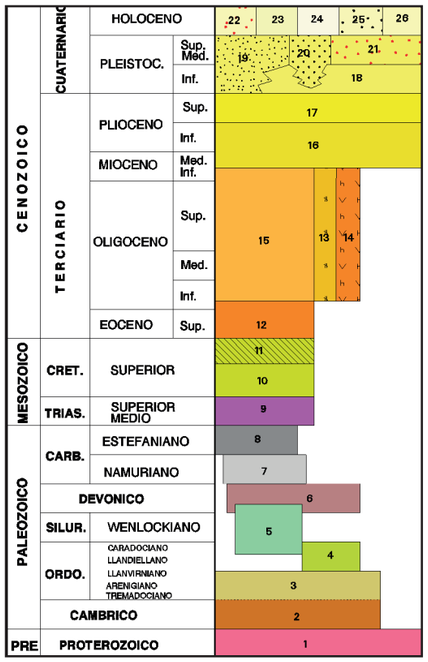

26 - DEPOSITOS COLUVIALES Y ALUVIONALES RECIENTES Y SUBRECIENTES DEL PIE DE SIERRA - Fanglomerados gruesos, gravas y arenas medianas y gruesas.
25 - DEPOSITOS EOLICOS - Arenas medianas y finas.
24 - RAMBLONES - Limos y arcillas limosas salitrosas.
23 - DEPOSITOS DE PLANICIE ALUVIAL Y ALUVIALES RECIENTES - Limos, arcillas y arenas.
22 - DEPOSITOS LACUSTRES Y DE PLAYA- Limos, arenas y aroillas.
21 - DEPOSITOS ATERRAZADOS DE VALLE FLUVIAL - Gravas gruesas, gravilla y arenas.
20 - DEPOSITOS DE CONOS ALIVIALES DEL RIO MENDOZA - Conglomerados inconsolidados, gravas gruesas, arenas, arcillas y limos.
19 - DEPOSITOS ATERRAZADOS PEDEMONTANOS - Fanglomerados, gravas polimicticas, arenas y limos.
18 - CAPAS DE "EL BORBOLLON" - Limoarcilitas, arcillas,l imos, arenas y tefras.
17 - FORMACION MOGOTES - Conglomerados, arcillas limosas, areniscas y tobas.
16 - FORMACION LOMA DE LAS TAPIAS - Conglomerados, arenas y limos.
15 - FORMACION MARIÑO - Conglomerados, arenisicas, arcillas y arcillas arenoso tobaceas.
14 - HIPABISALES LA CANOTA - Andesitas, dacitas y liparitas.
13 - PLUTONITAS E HIPABISALES LAS PEÑAS - Gabros, dioritas y piroxenitas.
12 - FORMACION DIVISADERO LARGO - Arcillitas, limolitas, areniscas y conglomerados.
11 - SEDIMENTITAS RIQUILIPONCHE - Areniscas, limolitas y yeso.
10 - FORMACION PAPAGAYOS - Conglomerados, areniscas y limolitas.
9 - GRUPO USPALLATA - Conglornerados, areniscas, arcillitas, limolitas y tobas.
8 - FORMACION JEGENES - Areniscas y grauvacas.
7 - FORMACION LEONCITO - Diamictitas, limolitas y areniscas.
6 - GRUPO VILLAVICENCIO - Grauvacas, pizarras, lutitas y conglomerados finos.
5 - FORMACION RINCONADA - Calizas, pelitas y areniscas.
4 - FORMACION EMPOZADA - Lutitas, areniscas calcarenitas y conglomerados.
3 - FORMACION SAN JUAN - Calizas, margas y chert.
2 - GRUPO MARQUESADO - Calizas, calizas dolomíticas, dolomitas, margas lutitas y chert.
1 - GRUPO CAUCETE - Mármoles y filonitas.

CERRO ACONCAGUA (2369-I)

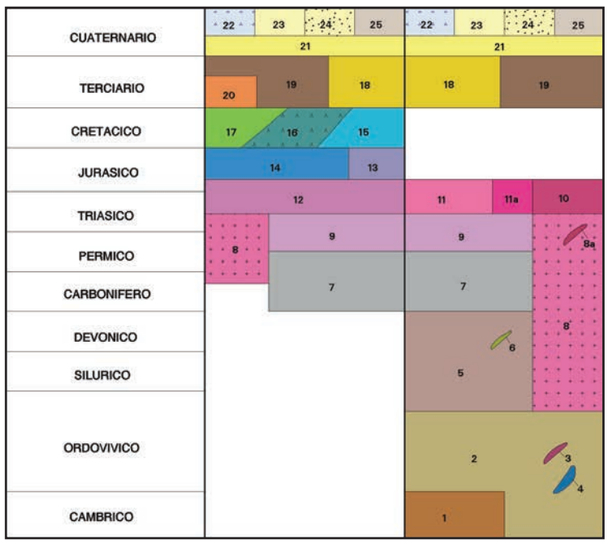

25 - Depósitos de remoción en masa - Bloques, gravas y arenas.
24 - Depósitos de playa - Limos, arcillas y evaporitas.
23 - Depósitos aluviales y coluviales - Gravas y arenas.
22 - Depósitos glaciarios - Tillitas, gravas y arenas.
21 - Depósitos pedemontanos aterrazados - Gravas, arenas y limos.
20 - Granito Matienzo - Granitoides y otros intrusivos asociados.
19 - Volcanitas miocenas - Complejo volcánicos La Ramada y Aconcagua y unidades equivalentes.
18 - Depósitos continentales - Conglomerado Santa María y otras unidades equivalentes.
17 - Formaoiones Diamante y Cristo Redentor - Conglomerados, areniscas y pelitas rojas.
16 - Formación Juncal - Rocas volcanicas y piroclásticas.
15 - Formación Tordillo y Grupo Mendoza - Areniscas rojas continentales, calizas y lutitas marinas.
14 - Formaciones Los Patillos, La Manga y Auquilco - Areniscas, lutitas, calizas y yesos.
13 - Volcanitas jurásicas - Riolitas y basaltos.
12 - Formación Rancho de Lata - Areniscas, conglomerados y tobas.
11 - Grupo Uspallata - Areniscas rojas, pelitas y conglomerados.
11a - Rocas básicas.
10 - Pórfidos riolíticos.
9 - Grupo Choiyoi - Riolitas, tobas e ignimbritas.
8 - Granitoides principalmante permotriásicos.
8a - Diques lamprofiricos.
7 - Depósitos oarboníferos - Diamictitas, grauvacas, areniscas y lutitas.
6 - Rocas básicas.
5 - Formaciones Villavicencio, Sandalio, Tontal y Grupo Ciénega del Medio - Areniscas, pizarres y pelitas.
4 - Bloques olistolíticos calcáreos en depósitos ordovícicos.
3 - Rocas básicas y ultrabásicas.
2 - Formaciones Cortaderas, Peñasco, Alojamiento y equivalentes - Metareniscas, filitas, mármores, areniscas y pelitas.
1 - Calizas Cerro Pelado.

GEOLOGICAL MAP - SAN JUAN (3169-IV)

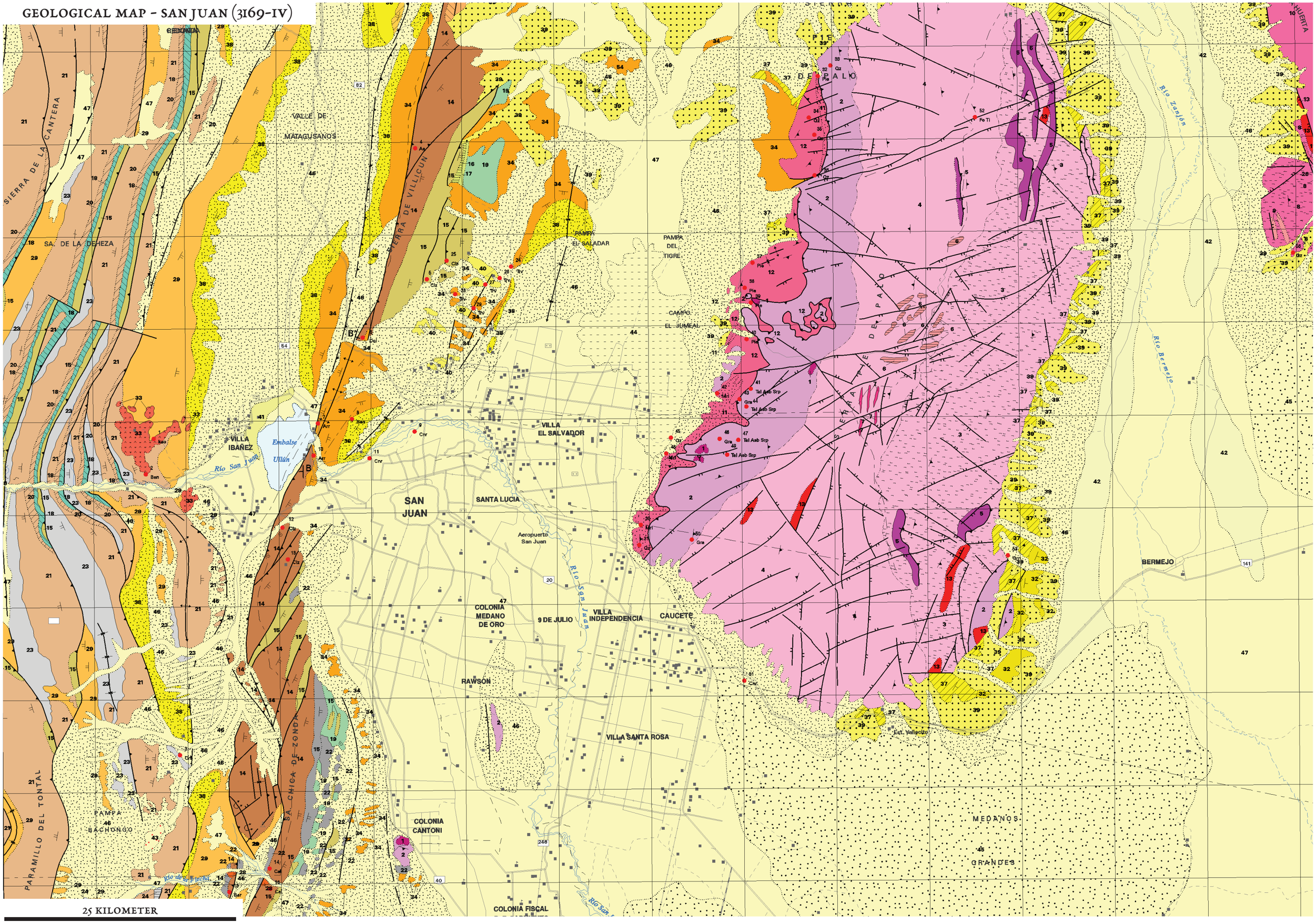

25 KILOMETER

SAN JUAN (3169-IV)

CUADRO ESTRATIGRAFICO

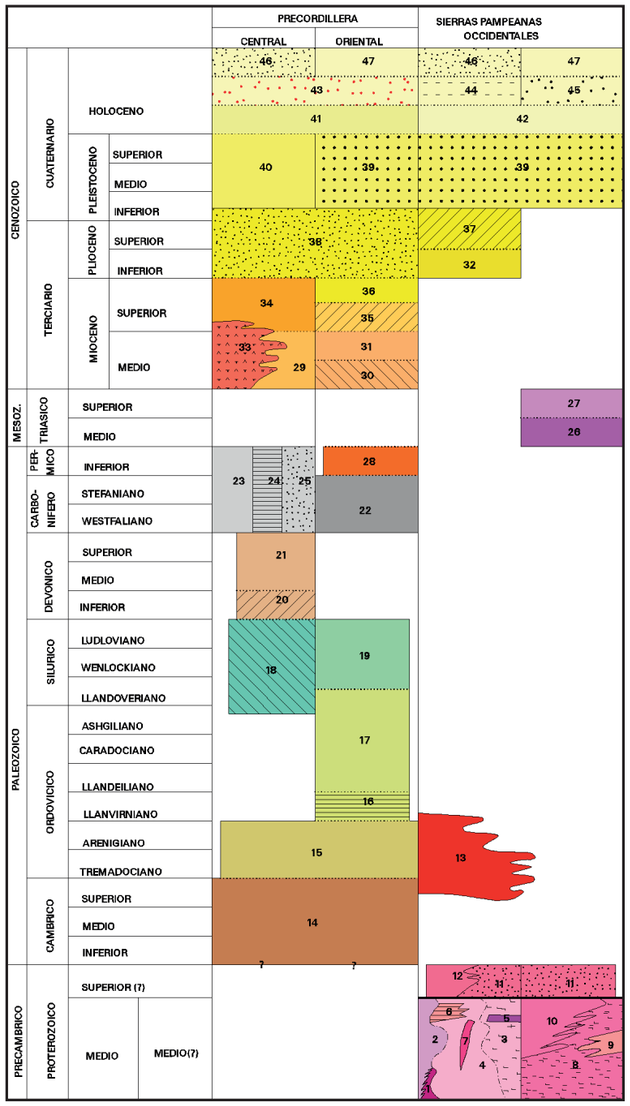

47 Depósitos aluviales. Limos,arenas y conglomerados. Planicie de inundación.
46 Depósitos coluviales. Fanglomerados, arenas, gravas y limos.
45 Depósitos eólicos. Arenas.
44 Depósitos evaporíticos. Depósitos salinos, limos y arenas finas.
43 Depósitos lacustres. Limolitas y arcillitas. Continental, lacustre.
42 Depósitos aluviales antiguos. Limos, arenas y conglomerados. Continental, planicies de inundación.
41 Formación Valentín. Fangolitas. Continental, depósitos lacustres.
40 Depósitos aterrazados y caliche. Fanglomerados con clastos calcáreos y cemento carbonático. Depósitos de travertino. Depósitos de pie de monte.
39 Depósitos aterrazados. Fanglomerados. Continental, depósitos de pie de monte.
38 Formación Mogna. Conglomerados, areniscas y sabulitas. Continental, abanicos aluviales coalescentes. Depósitos sinorogénicos de cuenca de antepais.
37 Formación Río del Camperito. Conglomerados, areniscas y limolitas. Continental, abanicos aluviales distales. Depósitos sinorogénicos de cuenca de antepais.
36 Formación Río Jachal. Areniscas, lentes de conglomerados. Continental fluvial. Depósitos sinorogénicos de cuenca de antepais.
35 Formación Quebrada del Cura. Areniscas y limolitas. Continental, fluvial; ríos meandriformes y llanuras aluviales. Depósitos sinorogénicos de cuenca de antepais.
34 Formación Loma de Las Tapias. Limolitas, areniscas y conglomerados. Continental, abanico aluvial - planicie fluvial anastomosada. Depósitos sinorogénicos de cuenca de antepais.
33 Andesitas y dacitas de Ullum. Cuerpos subvolcánicos andesíticos a dacíticos con xenolitos de basamento ígneo-metamórfico. Arco magmático.
32 Formación Nikizanga. Areniscas, limolitas y evaporitas. Continental, depósitos salíferos. Depósitos sinorogénicos de cuenca de antepais.
31 Formación El Jarillal. Areniscas y pelitas. Continental, ríos meandriformes y llanuras aluviales. Depósitos sinorogénicos de cuenca de antepais.
30 Formación Río Salado. Areniscas,tobas y tufitas con limolitas y arcillitas. Continental, fluvial, ríos meandrosos con depósitos lacustres efímeros; con aporte volcánico. Depósitos sinorogénicos de cuenca de antepais.
29 Formación Albarracín. Areniscas, limolitas, conglomerados y depósitos de flujos piroclásticos. Continental fluvial con aporte volcánico. Depósitos sinorogénicos de cuenca de antepais.
28 Traquita La Flecha. Filones capa y diques de traquitas. Ambiente de intraplaca.
27 Formación Cerrizal. Areniscas, mantos carbonosos y arcillitas. Continental fluvial, planicie de inundación distal y palustre.
26 Formación Esquina Colorada. Areniscas y conglomerados. Continental. Abanicos aluviales a facies fluviales proximales.
25 Formación Los Gauchos. Conglomerados, areniscas y subgrauvacas. Continental, glacial.
24 Formación Andapaico. Areniscas y lutitas. Continental fluvio-lacustre.
23 Formación La Deheza. Areniscas, limolitas y conglomerados. Continental fluvial, con intercalaciones marinas.
22 Formación Jejenes. Areniscas, conglomerados, pelitas y tillitas. Continental con aporte glaciario.
21 Formación Punta Negra. Grauvacas y lutitas. Abanicos submarinos de un ambiente deltaico en cuenca de antepais.
20 Formación Talacasto. Lutitas y areniscas. Ambiente marino de plataforma.
19 Formación Mogotes Negros. Limolitas, areniscas y conglomerados con olistolitos de calizas y conglomerados. Cuenca de antepais proximal.
18 Formación Tambolar. Areniscas, lutitas, margas, grauvacas.
Grupo Tucunuco: Formación La Chilca: conglomerados, lutitas, vaques y limolitas.
Formacion Los Espejos: limolitas y arenisca. Ambiente marino, somero a profundo.
Formación Rinconada: pelitas con olistolitos calcáreos y conglomerádicos.
Cuenca de antepais proximal.
17 Grupo Trapiche. Formación La Cantera: areniscas, conglomerados y pelitas. Facies marinas de mayor energía en una cuenca de antepais. Formación Don Braulio: diamictitas, conglomerados, fangolitas y areniscas. Facies marinas con un evento glaciario durante una caída del nivel del mar.
16 Formación Guaicamayo. Lutitas negras. Cuenca de antepais relativamente profunda.
15 Formación San Juan. Calizas y margas. Plataforma abierta a plataforma interna.
14 Grupo Marquesado. Formaciones La Laja, Zonda, La Flecha y La Silla. Calizas, calizas arcillosas, margas, dolomías, fangolitas calcáreas. Plataforma carbonática, cuenca interna y plataforma siliciclástica.
13 Granitoides. Tonalitas a granitos intrusivos en los Complejos Pie de Palo y Valle Fértil.
GRUPO CAUCETE
12 Cuarcita El Quemado: Cuarcitas y esquistos cuarcíticos con metamorfismo de bajo grado. Plataforma clástica-carbonática.
11 Caliza Angacos y Mármol Pan de Azúcar. Calizas y esquistos calcíferos con metamorfismo de bajo grado. Plataforma carbonática-clástica.
GRUPO VALLE FÉRTIL
10 Diques ácidos y granitoides.Faja milonítica con diques ácidos y granitoides cataclastizados.
9 Esquistos cuarzo - feldespático - moscovíticos. Rocas ígneas ácidas.
8 Gneises biotítico - granatífero - sillimaníticos y anfibolitas.Rocas sedimentarias pelíticas y arco islándico.
COMPLEJO PIE DE PALO
7 Pegmatoides. Volcanismo ácido a intermedio.
6 Esquistos cuarzo - feldespático - moscovíticos - epidóticos. Rocas ígneas ácidas.
5 Calizas cristalinas. Posible ambiente de plataforma.
4 Gneises y esquistos biotítico - moscovítico - plagioclásico-granatíferos. Rocas ígneas intermedias y sedimentarias metamorfizadas.
3 Gneises y esquistos feldespático - biotítico - granatíferos. Rocas ígneas intermedias y sedimentarias metamorfizadas.
2 Anfibolitas y esquistos anfibólicos, micáceos y grafíticos. Rocas ígneas básicas a intermedias y sedimentarias. Arcos magmáticos islándicos y fondo oceánico.
1 Rocas máficas y ultramáficas metamorfizadas. Arcos magmáticos islándicos y corteza oceánica.

mosaic of geological maps - Rodeo (3169-I) and san jose / jachal(3169-II)

25 KILOMETER

CUADRO ESTRATIGRAFICO

PRECORDILLERA

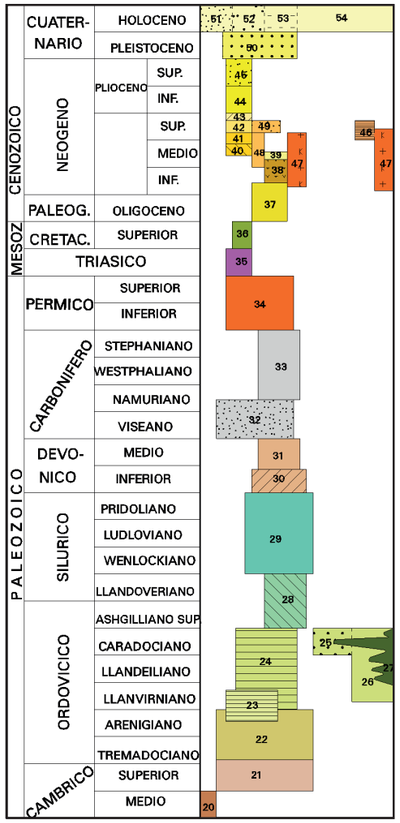

SIERRAS PAMPEANAS

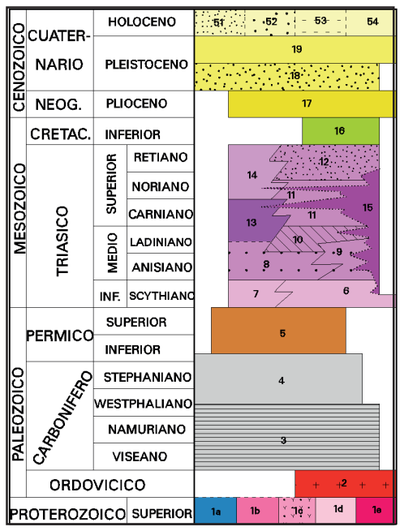

JÁCHAL (3169-11)

PRECORDILLERA

54 DEPOSITOS DE ALUVIOS ACTUALES - S?bulos,gravas,arenas muy gruesas a muy finas, limos y arcillas.
53 DEPOSITOS DE SALITRALES Y BARREALES - Limos, arcillas y arenas finas.
52 DEPOSITOS DE MEDANOS ACTUALES - Arenas finas y limos arenosos.
51 DEPOSITOS DE ABANICOS ALUVIALES ACTUALES - Fanglomerados y conglomerados inconsolidados.
50 DEPOSITOS DE ABANICOS ALUVIALES ANTIGUOS - Fanglomerados, conglomerados y areniscas gruesas parcialmente consolidadas
49 FORMACION EL CORRAL (abanico aluvial proximal) - Conglomerados y fanglomerados con escasas intercalaciones de arenisc
48 FORMACION CUCULI (fluvial anastomosado) - Areniscas, limolitas y conglomerados.
47 CUERPOS IGNEOS SUBVOLCANICOS - Dacitas y andesitas.
46 FORMACION RODEO (continental) - Conglomerados, tobas, areniscas conglomerádicas y finas, limolitas, yeso,sulfatos de magnesio y diatomitas.

GRUPO PONTON GRANDE
45 FORMACION MOGNA (fluvial anastomosado) - Conglomerados polimicticos,sabulitas, areniscas gruesas y limoarcilitas.
44 FORMACION RIO JACHAL (fluvial meandriforme) - Ritmos bandeados de areniscas finas y limolitas, con escasas intercalac
43 FORMACION QUEBRADA DEL CURA (fluvial meandriforme y lacustre) - Areniscas tobáceas y feldespáticas, limolitas y yeso.
42 FORMACION HUACHIPAMPA (abanico aluvial distal y fluvial anastomosado) - Areniscas gruesas y conglomerados finos.
41 FORMACION QUEBRADA DEL JARILLAL (fluvial entrelazado y lacustre) - Areniscas feldespáticas y pelitas.
40 FORMACION RIO SALADO (fluvial anastomosado) - Areniscas, limolitas, arcilitas y bentonitas.
39 FORMACION CAUQUENES (fluvial) - Arcilitas, limolitas, lutitas, areniscas y conglomerados.
38 FORMACION CERRO MORADO - Aglomerados y brechas volcánicas andesíticas, basaltos y andesitas.
37 FORMACION VALLECITO (e?lica y fluvial) - Areniscas muy finas a medianas, conglomerados gruesos a finos y sabulitas.

36 NECK BASALTICO - basaltos olivínicos alcalinos.
35 FORMACION CAÑON COLORADO (fluvial meandriforme) - Areniscas finas, limolitas, arcilitas, conglomerados y arcilitas be

GRUPO QUEBRADA DEL VOLCAN
34 FORMACION OJO DE AGUA (fluvial, e?lica y lacustre) - Conglomerados, areniscas finas a medias y lutitas.
33 FORMACION PANACAN (fluvial y marina) - Arcosas, arcilitas carbonosas, niveles de carbón, areniscas cuarzosas, lutitas
32 FORMACION VOLCAN (fluvial, lagunar y marina) - Conglomerados, areniscas conglomerádicas y finas, lutitas y limolitas.

GRUPO GUALILAN
31 FORMACION PUNTA NEGRA (marina) - Ritmos pulsatorios completos e incompletos de wackes y lutitas con intercalaciones d
30 FORMACION TALACASTO (marina) - Arcilitas, limolitas, lutitas, calcipelitas, areniscas y conglomerados.

GRUPO TUCUNUCO
29 FORMACION LOS ESPEJOS (marina) - Ritmos bandeados de areniscas finas y lutitas con intercalaciones de limolitas, cocu
28 FORMACION LA CHILCA (marina) - Conglomerado oligomíctico basal y ritmos bandeados de areniscas medias a gruesas y lut

27 CUERPOS IGNEOS BASICOS - Basaltos, pillow lavas, diabasas y gabros espilíticos.
26 FORMACION YERBA LOCA (marina) - Wackes, lutitas, areniscas feldesp?ticas, conglomerados y sabulitas leptometamórficas
25 FORMACION SIERRA DE LA INVERNADA (marina) - Ritmos pulsatorios de wackes o areniscas w?ckicas y lutitas con escasas i
24 FORMACION LOS AZULES (marina) - Lutitas negras graptolíticas, areniscas finas y limolitas.
23 FORMACION GUALCAMAYO (marina) - Lutitas negras graptolíticas y areniscas finas.
22 FORMACION SAN JUAN (marina) - Calizas y dolomías en parte estromatolíticas, lutitas negras y margas.
21 FORMACION SAN ROQUE (marina) - Calizas y dolomías estromatolítico-trombolíticas y chert.
20 FORMACION LA LAJA (marina) - Calizas mioríticas y lutitas.

SIERRAS PAMPEANAS

54 DEPOSITOS DE ALUVIOS ACTUALES - Arenas, gravas y limos.
53 DEPOSITOS DE SALITRALES Y BARREALES - Arcillas y limos.
52 DEPOSITOS DE MEDANOS ACTUALES - Arenas finas.
51 DEPOSITOS DE ABANICOS ALUVIALES ACTUALES - Fanglomerados y conglomerados inconsolidados.
19 FORMACION CATINZACO (Bajada aluvial) - Conglomerados gruesos pobremente consolidados.
18 FORMACION VICHIGASTA (Bajada aluvial)- Conglomerados gruesos, areniscas y limolitas.
17 FORMACION ANGOSTURAS (continental) - Limolitas, arcilitas, areniscas, tobas, conglomerados y niveles de yeso.
16 FORMACION CERRO RAJADO (bajada aluvial) - Conglomerados, areniscas medianas y limolitas.
15 FORMACION BALDECITOS - Basaltos olivínicos alcalinos.

GRUPO CHIFLON
14 FORMACION RIO CHIFLON (continental) - Limolitas, lutitas, fangolitas, areniscas finas y medianas y conglomerados.
13 FORMACION LOMAS BLANCAS (continental) - Conglomerado basal, areniscas finas, areniscas ferruginosas, limolitas, arcilitas y tobas.

GRUPO AGUA DE LA PEÑA
12 FORMACION LOS COLORADOS (fluvial entrelazado, playa lake y planicie de inundación) - Areniscas, limolitas, sabulitas, conglomerados finos y arcilitas.
11 FORMACION ISCHIGUALASTO (fluvial entrelazado y planicie de inundación) - Conglomerado basal, areniscas feldespaticas y micáceas, tobas arcillosas, sabulitas, limolitas, bancos carbonoceo y paleosuelos.
10 FORMACION LOS RASTROS (lacustre y fluvial) - Lutitas negras carbonosas, mantos de carbón y areniscas finas a medias.
9 FORMACION ISCHICHUCA (deltaica lacustre) - Lutitas negras no carbonosas y areniscas finas a gruesas.
8 FORMACION CHANARES (fluvial entrelazado, planicie de inundación y lacustre somero) - Pelitas, areniscas y niveles de paleosuelos.

7 FORMACION TARJADOS (fluvial y planicie de inundación) - Conglomerado basal,areniscas y lutitas.
6 FORMACION TALAMPAYA (fluvial y lacustre) - Conglomerados, areniscas, arcosas,limolitas y brechas intraformacionales.

GRUPO PAGANZO
5 FORMACION PATQUIA (fluvial) - Limolitas, arcosas, areniscas, tobas, fangolitas y arcilitas.
4 FORMACION TUPE (fluvial, deltaica y lacustre) - Arenisca feldespáticas, limolitas, lutitas, arcosas, y conglomerados.
3 FORMACION GUANDACOL (fluvial, deltaica y palustre) - Conglomerados, areniscas, limolitas, arcilitas y lutitas. Pelitas portadoras de clastos erráticos ('dropstones'), paleosuelos y bancos carbonosos.

2 FORMACION CERRO BLANCO - Granodioritas, tonalitas y granitos macizos a levemente foliados.

1 COMPLEJO VALLE FERTIL
1a Mármoles.
1b Anfibolitas y rocas ultramáficas.
1c Gneises granodioríticos y tonalíticos con o sin granate.
1d Gneises biotítico-granatíferos con cordierita o sillimanita.
1e Granitos sintectónicos, aplitas y pegmatitas.

RODEO (3169-1)

CUADRO ESTRATIGRAFICO

CORDILLERA FRONTAL

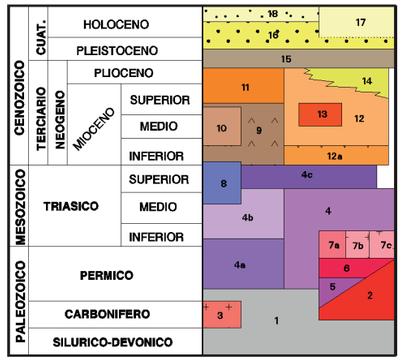

18 DEPOSITOS ALUVIALES MODERNOS
17 FORMACION TUDCUM (continental). Fanglomerados y litoarenitas
Depósitos pedemontanos antiguos y modernos
16 FORMACION LA PUENTECILLA (continental). Conglomerados, areniscas y lutitas
15 FORMACION OLIVARES. Basaltos
14 FORMACION RIO BLANCO (continental). Areniscas y conglo-merados
13 RIOLITAS
12a FORMACION VIZCACHAS. Andesitas
12 GRUPO MELCHOR. Aglomerados, ignimbritas, riolitas y riodacitas
11 FORMACION CERRO DE LAS TORTOLAS. Lavas, tobas, aglomerados e ignimbritas
10 INTRUSIVOS TERCIARIOS. Andesitas y dacitas
9 FORMACION DOÑA ANA. Andesitas, riolitas, ignimbritas y tobas
8 GRANODIORITA DE LAS VIZCACHAS. Granodioritas
7c GRANITO AGUA BLANCA. Granitos
7b GRANITO AGUA NEGRA. Granitos y granodioritas
7a GRANITO CHITA. Granitos
6 GRANITO CONCONTA. Granitos
5 GRANODIORITA ROMO. Granodioritas
4c FORMACION LAS PIRCAS. Riodacitas y dacitas
4b FORMACION LA CHILCA (continental). Calizas, riolitas, riodacitas, ignimbritas y tobas
4a FORMACION CASTAÑO (continental). Ortoconglomerados, aglomerados, tobas y andesitas
4 GRUPO CHOIYOI (continental). Tobas, aglomerados, ignimbritas y calizas
3 PLUTON LOS PATOS. Granitos y granodioritas
2 PLUTON TOCOTA. Tonalitas, granitos, granodioritas y microgranitos
1 FORMACION AGUA NEGRA (marino deltaico). Lutitas, areniscas, conglomerados y calizas.
FORMACION SAN IGNACIO (marino somero). Margas y calizas

PRECORDILLERA

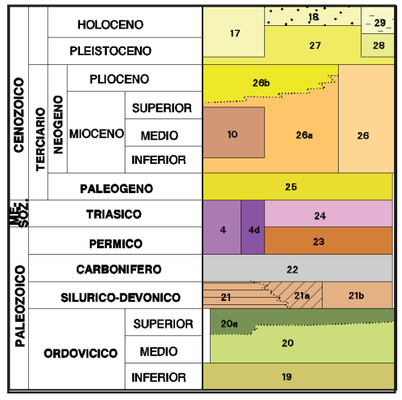

18 DEPOSITOS ALUVIALES MODERNOS
17 FORMACION TUDCUM (Continental). Fanglomerados y litoarenitas
29 DEPOSITOS DE BARREAL
28 DEPOSITOS DE DIATOMEAS (lacustre)
27 FORMACION IGLESIA. Depósitos pedemontanos. Conglomerados, gravas y arenas
26b FORMACION LAS FLORES (continental). Argilitas
10 INTRUSIVOS TERCIARIOS. Andesitas y dacitas
26a FORMACION LOMAS DEL CAMPANARIO (continental). Ignimbritas, andesitas y tobas.
26 GRUPO IGLESIA (continental).Conglomerados, areniscas, argilitas e ignimbritas
25 CONGLOMERADOS Y ARENISCAS FLUVIALES
4d INTRUSIVOS RIOLITICOS
4 GRUPO CHOIYOI (continental). Aglomerados andesíticos
24 FORMACION EL PUNTUDO (continental). Conglomerados, areniscas, calcilutitas y argilitas calc?reas y piroclastitas
23 ARCOSAS
22 FORMACION MALIMAN (mixto). Areniscas y limolitas
21b FORMACION PUNTA NEGRA (marino). Lutitas y areniscas
21a FORMACION PUNILLA (marino). Areniscas y lutitas
21 FORMACION CORRALITO (marino). Lutitas y oolitos de calizas
20a FORMACION YERBA LOCA (marino). Basaltos y pillow lavas
20 FORMACION YERBA LOCA (marino). Lutitas, areniscas y basaltos.
FORMACION LA INVERNADA (marino). Lutitas, areniscas y calizas
19 FORMACION SAN JUAN (marino). Calizas

GEOLOGICAL MAP - SAN JUAN (500K)

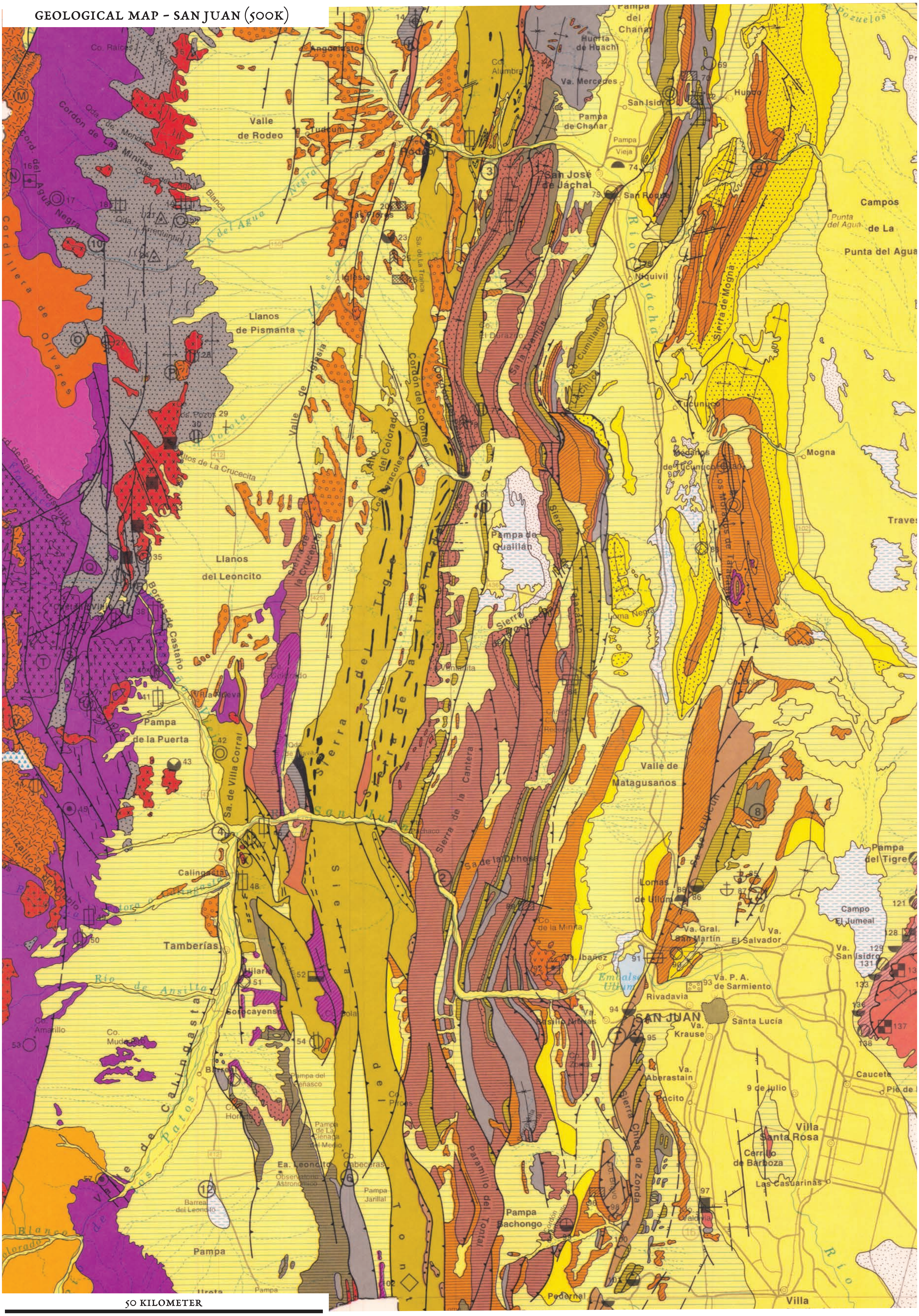

50 KILOMETER

32°30'S

69°20'W

68°50'W

32°30'S

N

W

E

S

USPALLATA CITY

Mendoza river

Cross section 1

MENDOZA

Blanco river

POTRERILLOS

33°00'S

33°00'S

Cross section 2

Mendoza river

Las Tunas river

69°20'W

Autores

Laura Giambiagi
José Mescua
Alicia Folguera
Stella Maris Moreiras
Amancay Martínez
Mariela Etcheverría
Florencia Bechis

Geología sector Barrancas:
Tomado de Chiaramonte et al. (2000)

PRECORDILLERA

- Fm. El Jagüelito
- Silúrico - Devónico sedimentitas marinas
- Intrusivos eopaleozoicos
- Cambro-Ordovícico pelitas negras
- Cambro-Ordovícico rocas carbonáticas
- Cambro-Ordovícico metasedimentitas

CORDILLERA FRONTAL

- Silúrico - Devónico rocas metamórficas
- Proterozoico - Devónico? Complejo Guarguaraz
- Proterozoico - Ordovícico rocas máficas y ultramáficas
- Proterozoico - Ordovícico rocas metamórficas

Mesozoico Temprano

- Triásico - depósitos volcaniclásticos
- Triásico - depósitos continentales
- Triásico - basaltos de rift
- Triásico Temprano - intrusivos
- Permo-Triásico- complejo gábrico
- Permo-Triásico - volcanitos

Compresión San Rafaélica

Paleozoico Tardío

- Pérmico Temprano- volcanitas
- Pérmico - intrusivos
- Carbonífero- Pérmico sedimentitas marinas

compresión Chánica

Cenozoico

- Cuaternario indiferenciado
- Fm Mesones
- Fm Mogotes
- Fm Agua de los Pozos
- Tobas Angostura
- Fm La Pilona
- Fm Mariño
- Mioceno - unidades subvolcáicas e intrusivos
- Paleógeno - depósitos continentales

- Estructuras cenozoicas
- Estructuras permo-triásicas reactivadas durante el Cenozoico
- Estructuras permo-triásicas
- Estructuras pérmicas reactivadas durante el Cenozoico
- Estructuras del Pérmico Temprano (orogenia San Rafaélica)
- Zonas de cizalla del Paleozoico Temprano (orogenia Chánica)

- falla con expresión superficial
- falla reconocida en subsuelo
- falla inferida
- anticlinal

0 5 10
km

N

SIMPLIFIED GEOLOGICAL MAP OF THE PRECORDILLERA (AFTER JUDGE, 2012)

69.25°W
69.0°W
68.75°W
68.5°W
30.25°S
30.5°S
30.75°S
A
A′
B
B′
Rodeo
Jáchal
Niquivil
Huaco
Iglesia Basin
Cuesta del Viento
Caracol West
Caracol Valley
Fig. 5
Tranca Valley
Mogotes Quebradita syncline
Cerro Bayo anticline
San Roque thrust
Blanco Valley
Blanquitos thrust
Niquivil thrust
Niquivil anticline
Fig. 7
Cuesta de Huaco anticline
Río Huaco
Las Salinas anticline
Río Jáchal
Tranca thrust
Blanco thrust
Cordón del Peñon
El Tigre Fault
Río Francia tear fault
Cerro Portezuelo Blanco
Matagusanos anticline
Mogna anticline
Cienega de Gualilán
20 km

Iglesia Basin clastic & subvolcanic igneous rocks
- Rodeo Fm.
- Iglesia Fm.
- Las Flores Fm.
- Tertiary intrusives
- Lomas del Campanario
- Iglesia Group

Quaternary
- Alluvium
- modern alluvial fans
- ancient alluvial fans
- Mogna
- Rio Jáchal
- Quebrada del Cura
- Huachipampa
- Quebrada del Jarillal
- El Corral
- Cuculi

Tertiary
- Rio Salado
- Cauquenes
- Cerro Morado
- Vallecito

Triassic
- Cañon Colorado

Permian
- Ojo de Agua
- Panacán
- Volcán

Devonian
- Punta Negra
- Talacasto

Silurian
- Los Espejos
- La Chilca

Ordovician

western facies	eastern facies
mafic igneous bodies	Los Azules
Yerba Loca	San Juan
Sierra de la Invernada	San Roque

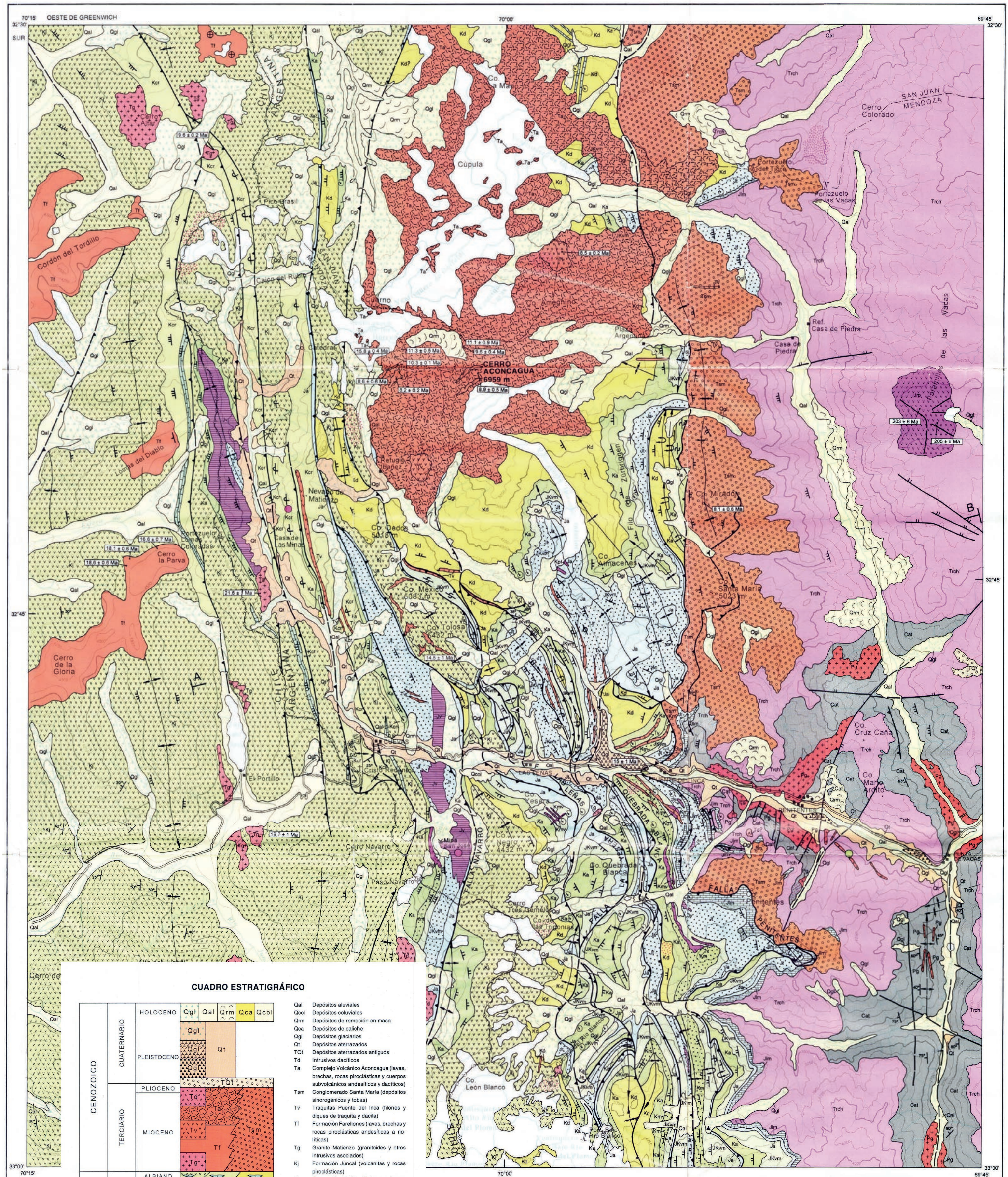

CUADRO ESTRATIGRÁFICO

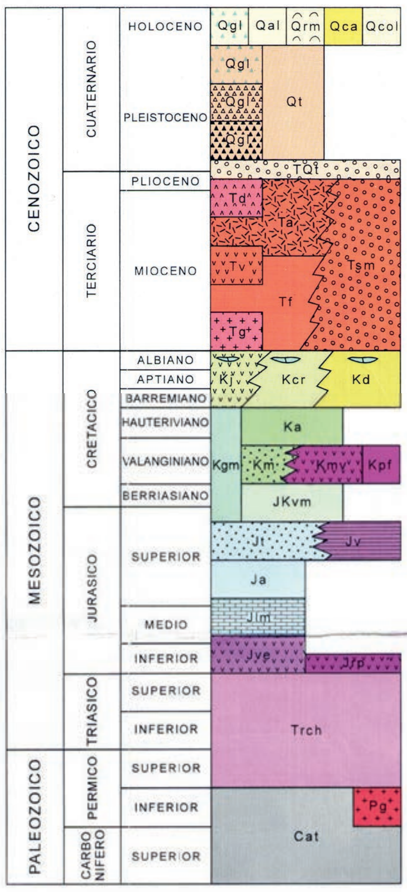

Qal	Depósitos aluviales
Qcol	Depósitos coluviales
Qrm	Depósitos de remoción en masa
Qca	Depósitos de caliche
Qgl	Depósitos glaciarios
Qt	Depósitos aterrazados
TQt	Depósitos aterrazados antiguos
Td	Intrusivos dacíticos
Ta	Complejo Volcánico Aconcagua (lavas, brechas, rocas piroclásticas y cuerpos subvolcánicos andesíticos y dacíticos)
Tsm	Conglomerado Santa María (depósitos sinorogénicos y tobas)
Tv	Traquitas Puente del Inca (filones y diques de traquita y dacita)
Tf	Formación Farellones (lavas, brechas y rocas piroclásticas andesíticas a riolíticas)
Tg	Granito Matienzo (granitoides y otros intrusivos asociados)
Kj	Formación Juncal (volcanitas y rocas piroclásticas)
Kcr	Formación Cristo Redentor (rocas piroclásticas y volcaniclásticas)
Kd	Formación Diamante (rocas epiclásticas)
Kgm	Grupo Mendoza (calizas, areniscas y lutitas verdes)
Ka	Formación Agrio (calizas y lutitas verdes)
Kmv	Volcanitas Laguna Seca (rocas piroclásticas y volcánicas)
Km	Formación Mulichinco (areniscas rojas)
Kpf	Dioritas Plaza Francia (dioritas y gabros alcalinos)
Jkvm	Formación Vaca Muerta (lutitas negras)
Jv	Volcanitas Vargas (basaltos y brechas piroclásticas)
Jt	Formación Tordillo (conglomerados y areniscas rojas)
Ja	Formación Auquilco (Yeso Principal)
Jlm	Formación La Manga (calizas marinas)
Jve	Rocas volcaniclásticas eurojurásicas
Jrp	Riolita Paramillo de Las Vacas (domo riolítico)
Trch	Grupo Choiyoi (ignimbritas y otras rocas piroclásticas)
Pg	Granito Cruz de Caña y equivalentes (granitos y granodioritas)
Cat	Formación Alto Tupungato (grauvacas y pizarras parcialmente hornfelsizadas)

REFERENCIAS GEOLÓGICAS

- Contacto
- Contacto inferido
- Corrimiento
- Corrimiento inferido
- Falla con labio bajo
- Falla inferida
- Fractura
- Anticlinal y sinclinal buzantes
- Repliegue
- Estrato inclinado (0°-10°, 10°-45°, >45°)
- Estrato con buzamiento, volcado y horizontal
- Datación radimétrica (14,5 ± 1 Ma)
- Traza de sección estructural (A)